Assimilation of Basic Xenoliths within Centre 3 Syenites of the Coldwell Alkaline Complex, Ontario

by

Derek N Nicol ©

A Thesis submitted in Partial Fulfillment of the
Requirements for the Degree of
Master of Science

Lakehead University
Thunder Bay, Ontario
Canada

April, 1990

ABSTRACT

This thesis describes the occurence, mineralogy and assimilation of basic xenoliths hosted by Centre 3 syenites. Field work was carried out in two locations, one in the vicinity of Neys/Ashburton and the other a large megaxenolith hosted by Centre 1 syenites in the vicinity of Wolf Camp Lake.

Least altered xenoliths consist of plagioclase, pyroxene. amphibole, biotite, apatite and opaque phases. With increasing assimilation this changes to a combination of plagioclase, amphibole, biotite, apatite, opaque phases, alkali feldspar, calcite, fluorite, sphene, zircon, REE phases and quartz.

Plagioclase is replaced by alkali feldspar in the form of porphyroblasts and crystals in the groundmass. Plagioclase is also decalcified to more albitic compositions along with recrystallization. Amphibole compositions extend over the same range of amphibole compositions in the host ferro-edenite syenite. The general effect of xenolith assimilation is the equilibrium of a xenolith's mineral assemblage to that of the host syenite. Assimilation processes seen at Wolf Camp Lake are similiar to those seen

at Neys/Ashburton.

Bulk rock data along with mineralogical compositional variation in clinopyroxenes, suggest a tholeiitic basalt parentage for xenoliths in both areas. Cr and Ni contents indicate an evolved nature to the parent volcanics. Data also suggest the possible existence of a second undersaturated type of volcanic xenolith present at Neys/Ashburton. Parental basalts are postulated to be coeval volcanics related to the formation of the Coldwell Complex.

Modelling by mass balance mixing calculations of contamination of host syenites indicates that contaminated ferro-edenite syenites are the result of direct assimilation of volcanic xenoliths by ferro-edenite syenite. Quartz syenites are found to be unsuitable parents to contaminated ferro-edenite syenites.

ACKNOWLEDGEMENTS

First of all, Dr. R.H. Mitchell. He is sincerely thanked for his helpfulness and guidance in my efforts to produce this thesis. Patience in revising multiple copies of chapters and correcting terrible English quickly and efficiently are also gratefully acknowledged.

I also thank Dr. J. Gittens and Dr. D. Gorman of the University of Toronto for inspiring me during undergraduate studies to continue studies in igneous petrology and mineralogy. Without them I would not have made it this far.

Thanks to all the technicians involved in the preparation of this thesis. A. Hammond and R. Viitala for preparing countless SEM discs and thin sections. S. Moogk for assistance with computer work. Al MacKenzie for invaluable assistance on the scanning electron microscope and for showing me some unbelievable duck shooting. S. Millar, geology department secretary, for always having a cheerful hello.

Fellow geology grads Bob Spark, Richard McLaughlin, Geoffery Abdallah, Barb Kowalski, David Nicol, Barb Seemayer and Mark Puumala for providing a great social atmosphere and interesting conversations, not always about geology.

Lastly, but not least of all, my family and Christina Teubner for encouragement and support through 2 years away from home and some difficult times.

A special acknowledgement goes to Ellen Siydock, my loving girlfriend and companion. Thanks for being there with me through all the good and bad times we've shared together. May we have many more with each other. Also thanks for typing the manuscript and saving me from what would be a horrific task.

TABLE OF CONTENTS

Abstract....................i
Acknowledgements....................iii
List of Figures....................viii
List of Tables....................xi
List of Plates....................xii

CHAPTER ONE INTRODUCTION

1.1 Regional Geologic Setting....................1
1.2 General Geology....................2
1.3 Lithologies....................3
1.4 Present Study: Assimilation of Basic Xenoliths
1.4.1 Object of Study....................5
1.4.2 Field Investigation....................6

CHAPTER TWO XENOLITHS OCCURRING IN CENTRE 3 AND CENTRE1 SYENITES

2.1 Macroscopic Observations
2.1.1 Neys/Ashburton - Centre 3....................7
2.1.2 Other Xenoliths....................10
2.1.3 Wolf Camp Lake - Centre 1....................10
2.2 Petrography of the Xenoliths
2.2.1 Neys/Ashburton....................12
2.2.2 Wolf Camp Lake....................17
2.3 Summary of Neys/Ashburton and Wolf Camp Lake....................20

CHAPTER THREE COMPOSITIONAL VARIATION OF AMPHIBOLE, PYROXENE AND FELDSPAR

3.1 Introduction....................22
3.2 Amphibole Compositional Variation....................22
3.2.1 Neys/Ashburton....................23
3.2.2 Wolf Camp Lake....................25
3.2.3 Discussion of Amphibole Compositional Variation....................25
3.3 Pyroxene Compositional Variation....................26

3.3.1 Neys/Ashburton....27
3.3.2 Wolf Camp Lake....28
3.3.3 Discussion of Pyroxene Compositional Variation....29
3.4 Feldspar Compositional Variation
3.4.1 Neys/Ashburton....32
3.4.2 Wolf Camp Lake....33
3.4.3 Summary of Feldspar Composition....34

CHAPTER FOUR WHOLE ROCK CHEMISTRY OF BASIC XENOLITHS

4.1 Introduction....36
4.2 Neys/Ashburton
4.2.1 Major Elements....37
4.2.2 Minor Elements....40
4.2.3 Comparison to other Keweenawan Volcanics....40
4.3 Wolf Camp Lake
4.3.1 Major Elements....42
4.3.2 Minor Elements....43
4.3.3 Comparison to other Keweenawan Volcanics....44
4.4 Comparison of Wolf Camp Lake and Neys/Ashburton....45

CHAPTER FIVE RELATIONSHIP BETWEEN XENOLITHS AND HOST SYENITES

5.1 Introduction....47
5.2 Xenolith Compositional Changes....47
5.3 Origin of Contaminated Ferro-edenite Syenite....50
5.4 Principal Component Analysis....53

SUMMARY....56

REFERENCES....57

APPENDICES
1 Methods of Microprobe Analysis
2 Amphibole Compositions for Neys/Ashburton xenoliths
3 Amphibole Compositions for Wolf Camp Lake megaxenolith
4 Amphibole Compositions for Wolf Camp Lake host syenites
5 Pyroxene Compositions for Neys/Ashburton xenoliths

6 Pyroxene Compositions for Wolf Camp Lake megaxenolith
7 Pyroxene Compositions for Wolf Camp Lake host syenites
8 Feldspar Compositions for Neys/Ashburton xenoliths
9 Feldspar Compositions for Wolf Camp Lake megaxenolith

LIST OF FIGURES

CHAPTER ONE

1.1 Tectonic setting of the Lake Superior Basin and location of the Coldwell Alkaline Complex.
1.2 Geology of the Coldwell Alkaline Complex.

CHAPTER TWO

2.1 Outcrop maps of the Neys/Ashburton study area showing distribution of rock types and xenoliths.
2.2 Wolf Camp Lake Study area.

CHAPTER THREE

3.1 Neys/Ashburton amphibole compositions.
3.2 Neys/Ashburton amphibole compositions.
3.3 Neys/Ashburton amphibole compositions.
3.4 Wolf Camp Lake amphibole compositions.
3.5 Pyroxene compositions for C2358 and C2490, Neys/Ashburton.
3.6 Pyroxene compositions for C2498, Neys/Ashburton.
3.7 Pyroxene compositions for ferro-edenite syenite and xenoliths reported by Lukosius-Sanders(1988).
3.8 Pyroxene compositions for contaminated ferro-edenite syenite, ferro-edenite syenite and xenoliths reported by Lukosius-Sanders(1988).
3.9 Pyroxene compositions for C2531A, Wolf Camp Lake.
3.10 Pyroxene compositions for C3122, Wolf Camp Lake.
3.11 Pyroxene compositions for C3123, Wolf Camp Lake.
3.12 Pyroxene compositions for C3120, Wolf Camp Lake.
3.13 Pyroxene compositions for C2515 and C2516, Wolf Camp Lake.
3.14 Pyroxene compositions for C2531A, Wolf Camp Lake.
3.15 Characterization of magmatic parentage for Neys/Ashburton xenoliths from clinopyroxene compositions.
3.16 Characterization of magmatic parentage for Wolf Camp Lake megaxenolith from clinopyroxene compositions.
3.17 Plagioclase compositions for C2358, Neys/Ashburton.

3.18 Plagioclase compositions for C2510, Neys/Ashburton.
3.19 Plagioclase compositions for C2498, Neys/Ashburton.
3.20 Plagioclase compositions for C2331, Neys/Ashburton.
3.21 Plagioclase compositions for C2490, Neys/Ashburton.
3.22 Plagioclase compositions for C2340, Neys/Ashburton.
3.23 Feldspars from host syenites Neys/Ashburton.
3.24 Plagioclase compositions for C3120, Wolf Camp Lake.
3.25 Plagioclase compositions for C3123, Wolf Camp Lake.
3.26 Plagioclase compositions for C3125, Wolf Camp Lake.
3.27 Plagioclase compositions for C2531A, Wolf Camp Lake.

CHAPTER FOUR

4.1 Variation diagrams for Neys/Ashburton xenoliths.
4.2 Streckeisen-LeMaitre rock classification plot for Neys/Ashburton xenoliths.
4.3 Variation diagrams for Wolf Camp Lake megaxenolith samples.
4.4 Streckeisen-LeMaitre rock classification plot for Wolf Camp Lake megaxenolith samples.
4.5 AFM diagram for Neys/Ashburton and Wolf Camp Lake megaxenolith.

CHAPTER FIVE

5.1 Modelling compositional changes in xenoliths with Michipicoten Island volcanic as parent.
5.2 Modelling compositional changes in xenoliths with Michipicoten Island volcanic as parent.
5.4 Modelling compositional changes in xenoliths with Keweenawan Reference suite as parent.
5.5 Modelling compositional changes in xenoliths with Keweenawan Reference suite as parent.
5.6 Mass balance mixing calculations using addition of Michipicoten Island volcanic to ferro-edenite syenite.
5.7 Mass balance mixing calculations using addition of Michipicoten Island volcanic to ferro-edenite syenite.
5.8 Mass balance mixing calculations using addition of Michipicoten Island volcanic to ferro-edenite syenite.

5.9 Mass balance mixing calculations using addition of Keweenawan volcanic to ferro-edenite syenite.
5.10 Mass balance mixing calculations using addition of Keweenawan volcanic to ferro-edenite syenite.
5.11 Mass balance mixing calculations using addition of Keweenawan volcanic to ferro-edenite syenite.
5.12 Mass balance mixing calculations using addition of Neys/Ashburton xenolith to ferro-edenite syenite.
5.13 Mass balance mixing calculations using addition of Neys/Ashburton xenolith to ferro-edenite syenite.
5.14 Mass balance mixing calculations using addition of Neys/Ashburton xenolith to ferro-edenite syenite.
5.15 Mass balance mixing calculations using addition of more assimilated Neys/Ashburton xenolith to ferro-edenite syenite.
5.16 Mass balance mixing calculations modelling quartz syenite as parent to contaminated ferro-edenite syenite.
5.17 Mass balance mixing calculations modelling quartz syenite as parent to contaminated ferro-edenite syenite.
5.18 Harker diagram for Neys/Ashburton xenoliths, ferro-edenite syenite and contaminated ferro-edenite syenite.
5.19 Principal Components Analysis scatterplot.
5.20 Principal Components Analysis scatterplot.

LIST OF TABLES

CHAPTER FOUR

4.1 Whole Rock Analyses and CIPW Norms for Neys/Ashburton Xenoliths
4.2 Minor Element Compositions for Neys/Ashburton Xenoliths
4.3 Comparison Neys/Ashburton Xenoliths to other Keweenawan Volcanics
4.4 Whole Rock Analyses and CIPW Norms for Wolf Camp Lake Megaxenolith
4.5 Minor Element Compositions for Wolf Camp Lake Megaxenolith
4.6 Comparison of Wolf Camp Lake Megaxenolith to other Keweenawan Volcanics

CHAPTER FIVE

5.1 Principal Components Analysis for Ferro-edenite Syenite, Contaminated Ferro-edenite Syenite and xenoliths from Neys/Ashburton

LIST OF PLATES

CHAPTER TWO

2.1 Xenolith-rich zone adjacent to the Little Pic River.
2.2 Xenolith-rich zone of Ashburton Lookout.
2.3 Xenoliths within contaminated ferro-edenite syenite.
2.4 Range in size and shape of the xenoliths.
2.5 Host syenite/xenolith contacts.
2.6 Relict plagioclase phenocrysts in least altered Neys/Ashburton xenoliths.
2.7 Relict clinopyroxene phenocrysts in least altered Neys/Ashburton xenolith.
2.8 Overgrowth of amphibole on relict clinopyroxene phenocryst.
2.9 Texture of least altered Neys/Ashburton xenolith.
2.10 SEM photo of opaque mass.
2.11 Coronal overgrowth of alkali feldspar on relict plagioclase phenocryst.
2.12 Alkali feldspar overgrowth on relict plagioclase phenocryst.
2.13 Alkali feldspar porphyroblastic growth in Neys/Ashburton Xenolith.
2.14 Detail of biotite ovoid.
2.15 Large biotite ovoid.
2.16 Beginning of ovoid development.
2.17 SEM photo of alkali feldspar replacement of plagioclase.
2.18 SEM photo of alkali feldspar replacement of plagioclase.
2.19 Replacement alkali feldspar with high barium content.
2.20 Recystallization of Neys/Ashburton xenolith due to assimilation.
2.21 SEM photo of zircon growth within xenoliths due to increased assimilation.
2.22 Ghosting of a xenolith.
2.23 Texture of unaltered Wolf Camp Lake xenolith.
2.24 Recrystallization of Wolf Camp Lake xenolith due to assimilation effects.
2.25 Recrystallized vesicle in Wolf Camp Lake xenolith.
2.26 Vesicle in highly assimilated Wolf Camp Lake xenolth.

Chapter 1

Introduction

1.1 Regional Geologic Setting

Located approximately 250 km east of Thunder Bay, Ontario, the Coldwell Alkaline Complex is the largest of its kind in North America and represents a manifestation of late Precambrian Keweenawan igneous activity (Mitchell and Platt, 1982). The complex is approximately circular in plan with a diameter of about 25 km. Figure 1.1 shows the location of the Coldwell Complex with respect to the major structural and tectonic features of the Lake Superior Basin.

The Coldwell Alkaline Complex intrudes an east-west trending greenstone belt within the Superior Province of the Canadian Shield. This greenstone belt is part of the Schreiber-White Lake Archean metavolcanic and metasediment terrain and consists of mafic to felsic volcanics and greywackes which are all regionally metamorphosed to greenschist and amphibolite grade. A 2 km wide contact metamorphic aureole surrounds the complex. A maximum grade of pyroxene hornfels facies is reached adjacent to the contact (Walker, 1967). The complex as a whole is the most southerly of a north-south trending group of contemperaneous alkaline

Figure 1.1 Tectonic setting of the Lake Superior Basin and location of the Coldwell Alkaline Complex.

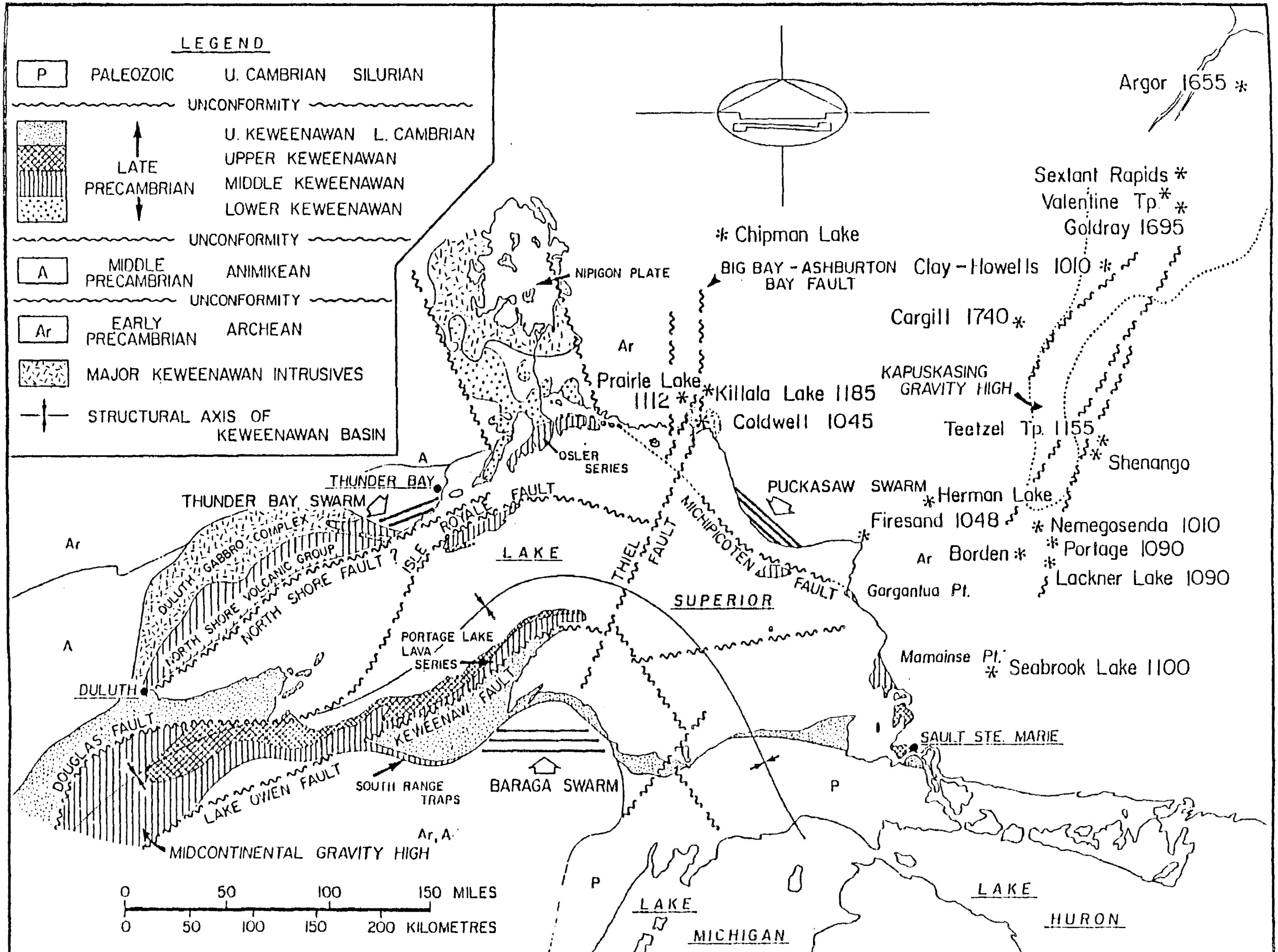

intrusions (Prairie Lake, Killala Lake, Chipman Lake) (Mitchell and Platt, 1982).

Platt and Mitchell (1982) using a seventeen point Rb-Sr isochron, reported an age of 1044.5 ± 6.2 Ma, placing the complex as Neohelikian in age. This age indicates that the Coldwell Complex was emplaced after the bulk of the Keweenawan igneous activity found in the Lake Superior Basin during the Late Precambrian.

1.2 General Geology

A summary of the geology of the complex as presented by Mitchell and Platt (1982) is shown in Figure 1.2.

A significant positive gravity anomaly over the complex suggests the infrastructure of the complex is composed of mafic rocks. Mitchell et al (1983) interpret the gravity study to suggest that the complex consists of a cap of felsic rocks, 3-5 km thick, overlying a differentiated basic intrusion consisting of a gabbro layer of peridotite and/or pyroxenite. This supports the hypothesis that at least some of the Coldwell Complex rocks are the result of the differentiation of a basic parent.

The structure of the complex is as yet poorly understood. Mitchell and

Figure 1.2 Geological map of the Coldwell Alkaline Complex.

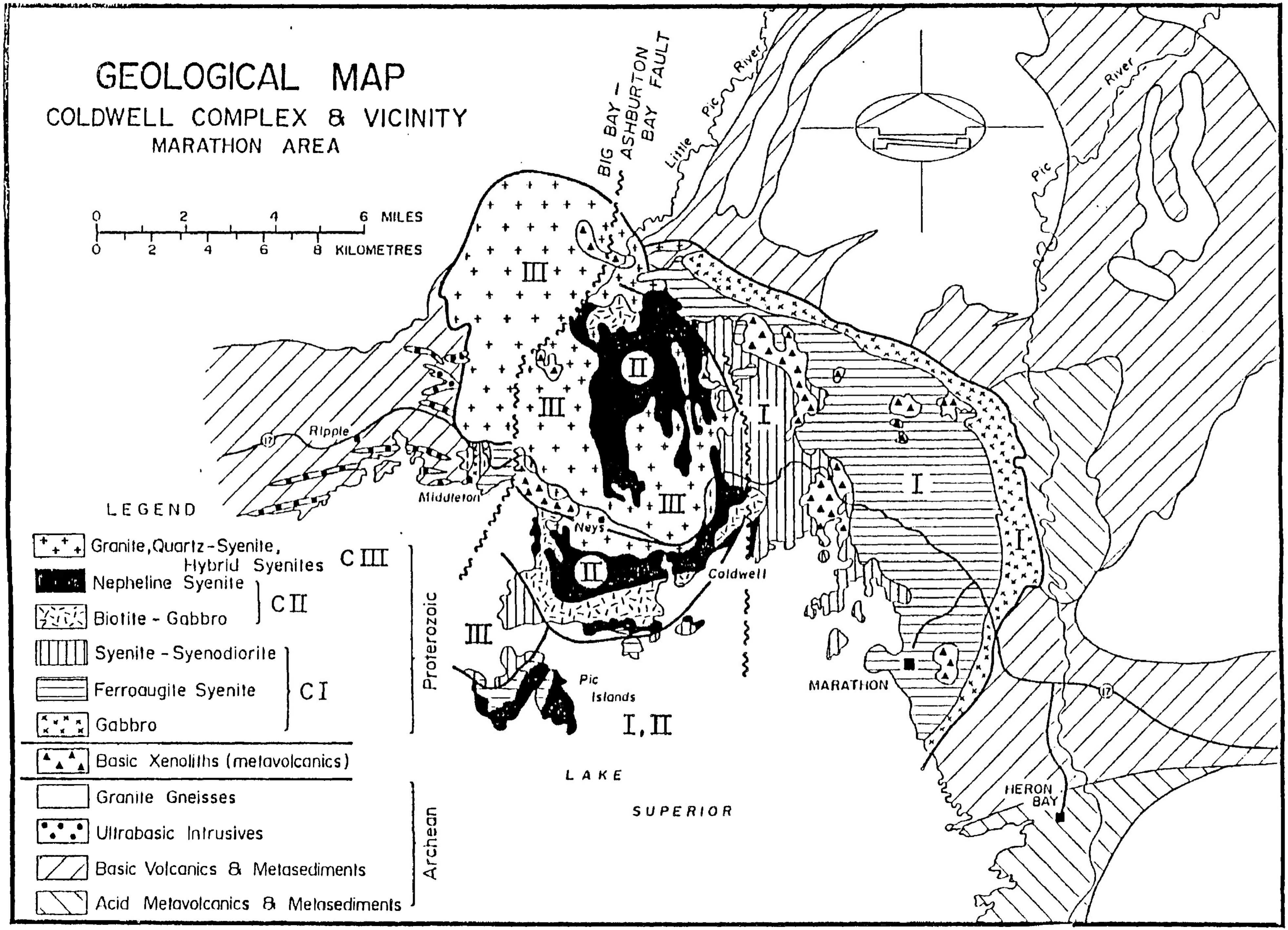

Platt (1982) propose that the original form of the intrusion has been obscured by block faulting and that several periods of magmatism were involved in its emplacement. Intrusion of magma is postulated to be related to cauldron subsidence, thereby giving the roughly circular dimensions to the body. Block faulting, breccia zones and metasomatism in the western portions of the intrusion are believed to represent an area close to the roof, whereas the absence of these features in the eastern portions indicate a deeper structural level. Many volcanic xenoliths in the central portions of the intrusion are thought to be remnants of basaltic cap rock lavas (Mitchell and Platt, 1982).

1.3 Lithologies

The Coldwell Alkaline Complex is unusual as it contains rocks of undersaturated, saturated and oversaturated character. Mitchell and Platt (1978) recognize three distinct centres of igneous activity each having a characteristic differentiation trend. Each magmatic centre is the expression of a cauldron subsidence event. The centres are, in order of intrusion;

Centre 1: saturated alkaline rocks with peralkaline residua,

Centre 2: undersaturated alkaline rocks and, Centre 3: Alkaline rocks with oversaturated residua.

Rocks of Centre 1 are the oldest in the Complex and consist of gabbro and ferro-augite syenite. The gabbro forms the border of the intrusion and has intruded the ferro-augite syenite. The petrological relationship between these two rock types is not known (Mitchell and Platt, 1978). The magma that produced the ferro-augite syenites differentiated towards extreme iron enrichment with peralkaline oversaturated residua. This has led to the formation in these rocks of the characteristic minerals; fayalite, aenigmatite, ferro-augite and ferro-richterite (Mitchell and Platt, 1978).

Centre 2 rocks consist of the earliest-formed nepheline-bearing biotite gabbro. These are followed by the intrusion of nepheline syenites which are interpreted by Mitchell and Platt (1982) as being formed by fractional crystallization of an alkali basalt parent. Associated with the rocks of Centre 2 is a swarm of lamprophyre and analcite tinguaite dikes.

The last episode of magmatic activity, Centre 3, consists of saturated and oversaturated syenites, and it is these rocks with which this thesis is mainly concerned. They are confined to the western half of the intrusion and intrude all earlier rocks. Xenoliths of comagmatic volcanics, country rock and other Centres are commonly found. A previous study by

Lukosius-Sanders (1988) has identified four main rock types in Centre 3 based upon their petrographic and mineralogical characteristics. All are alkali feldspar syenites, that are distinguished on the basis of the nature of the amphibole present. These are; magnesiohornblende syenite, ferro-edenite syenite, contaminated ferro-edenite syenite and quartz syenite. Contacts between the varieties may be sharp, gradational or undefined and the many small injections of magma have led to complex inter-relationships between all four rock types. Also present in Centre 3 are xenolith-rich areas consisting of many basaltic xenoliths in various stages of digestion, within a matrix of contaminated ferro-edenite syenite. A complete spectrum of contaminated rocks exist from uncontaminated ferro-edenite syenite through to highly contaminated ferro-edenite syenite. Study of the contamination, or assimilation, as well as determining the nature of the xenoliths is the primary objective of this thesis.

1.4 Present Study: Assimilation of Basic Xenoliths

1.4.1 Object of Study

The object of the present study is to examine xenoliths incorporated within the syenites of Centre 3, in the vicinity of Neys Lookout, in order to determine the nature of the assimilation process and the effects of assimilation on the host syenite. Methods employed include examination of samples in thin section by petrographic and scanning electron microscopy, together with whole rock analysis of xenoliths, contaminated syenites and uncontaminated syenites.

A large brecciated block of basaltic rock measuring approximately 2 km by 3 km occuring in the vicinity of Wolf Camp Lake was also examined. Host rocks to this megaxenolith belong to Centre 1. The composition and relationship to the host syenites were also investigated to determine if the processes of assimilation were similiar to those occurring in Centre 3. An attempt to determine if this xenolith is related to those occurring in Centre 3 syenites is also made.

1.4.2 Field Investigation

Detailed mapping of outcrops exposed along Trans Canada Highway #17 in the vicinity of Neys Lookout were carried out to determine relationships between the volcanic xenoliths and the contaminated syenites. Detailed sampling was undertaken for further study in the laboratory.

Traverses in the Wolf Camp Lake area were made to determine the size and boundaries of the volcanic block and samples taken to determine the composition and effects, if any, of its incorporation in Centre 1 syenites.

Chapter Two

Xenoliths occurring in Centre 1 and Centre 3 syenites

2.1 Macroscopic Observations

2.1.1 Neys/Ashburton - Centre 3

Xenoliths of country rock hornfels and other Coldwell Complex rocks are found in syenites of Centre 3, but by far the most common xenoliths found in the Neys/Ashburton study area are of volcanic origin. These were previously identified as oligoclase basalt, and Mitchell and Platt (1978, 1982) suggested that they represent a suite of coeval alkaline volcanics related to the formation of the Coldwell Complex and possibly were cap rocks to the intrusion. Figures 2.1A through 2.1J are a series of outcrop maps of the Neys/Ashburton study area showing the distribution of the xenolith types.

The volcanic xenoliths have a wide range of distribution being found also in the Western Contact Zone of the Complex (Jago, 1980) and on Pic Island (Lukosius-Sanders, 1988). The xenoliths are characteristically found only in ferro-edenite syenite and its contaminated variants in all of these areas. Inclusion of the xenoliths into the ferro-edenite syenite has led to its contamination and formation of an apparently large variety of syenite types.

The main occurence of the volcanic xenoliths is in the form of

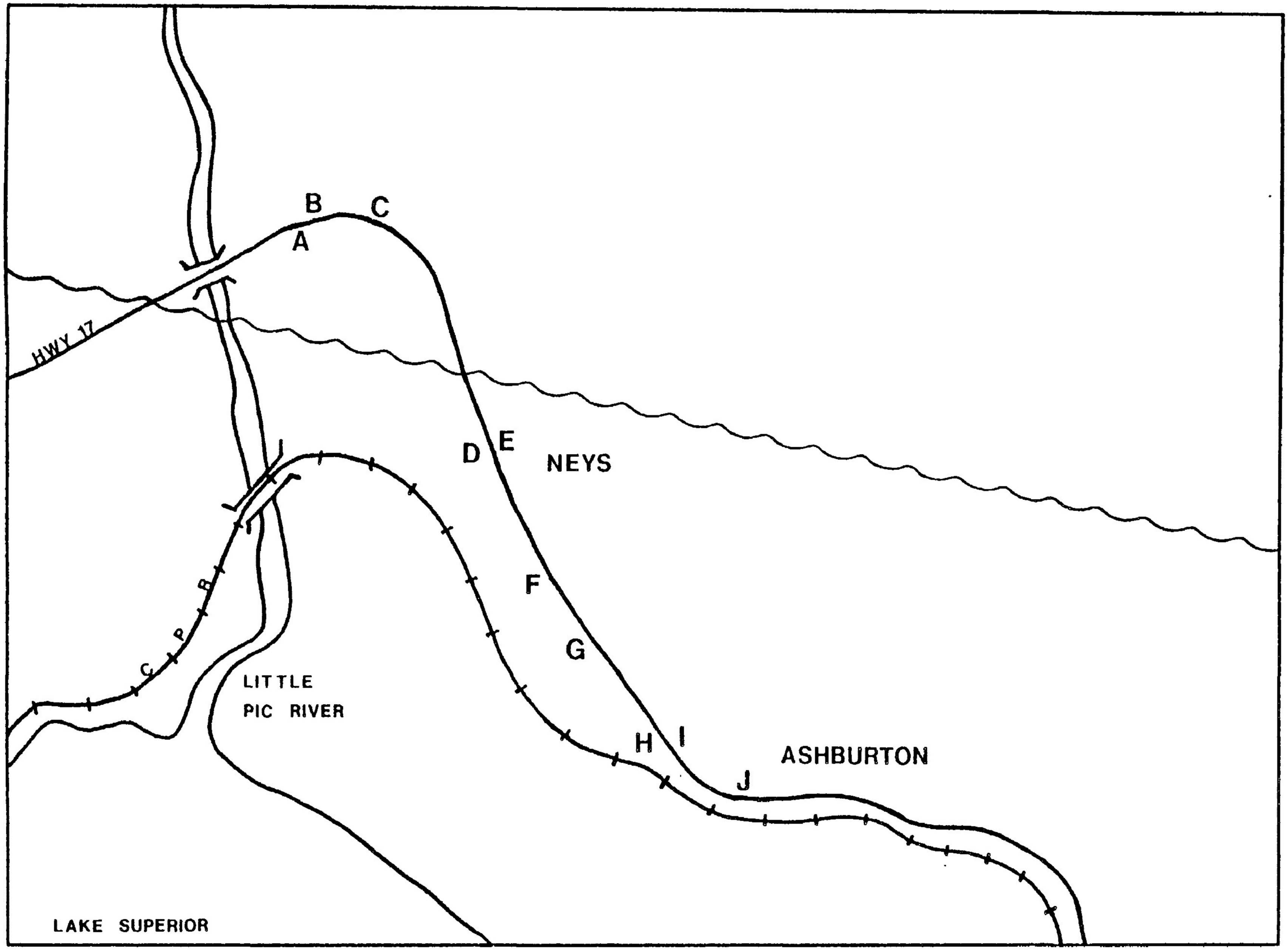

FIGURE 2.1 LOCATION OF OUTCROPS
NEYS/ASHBURTON STUDY AREA

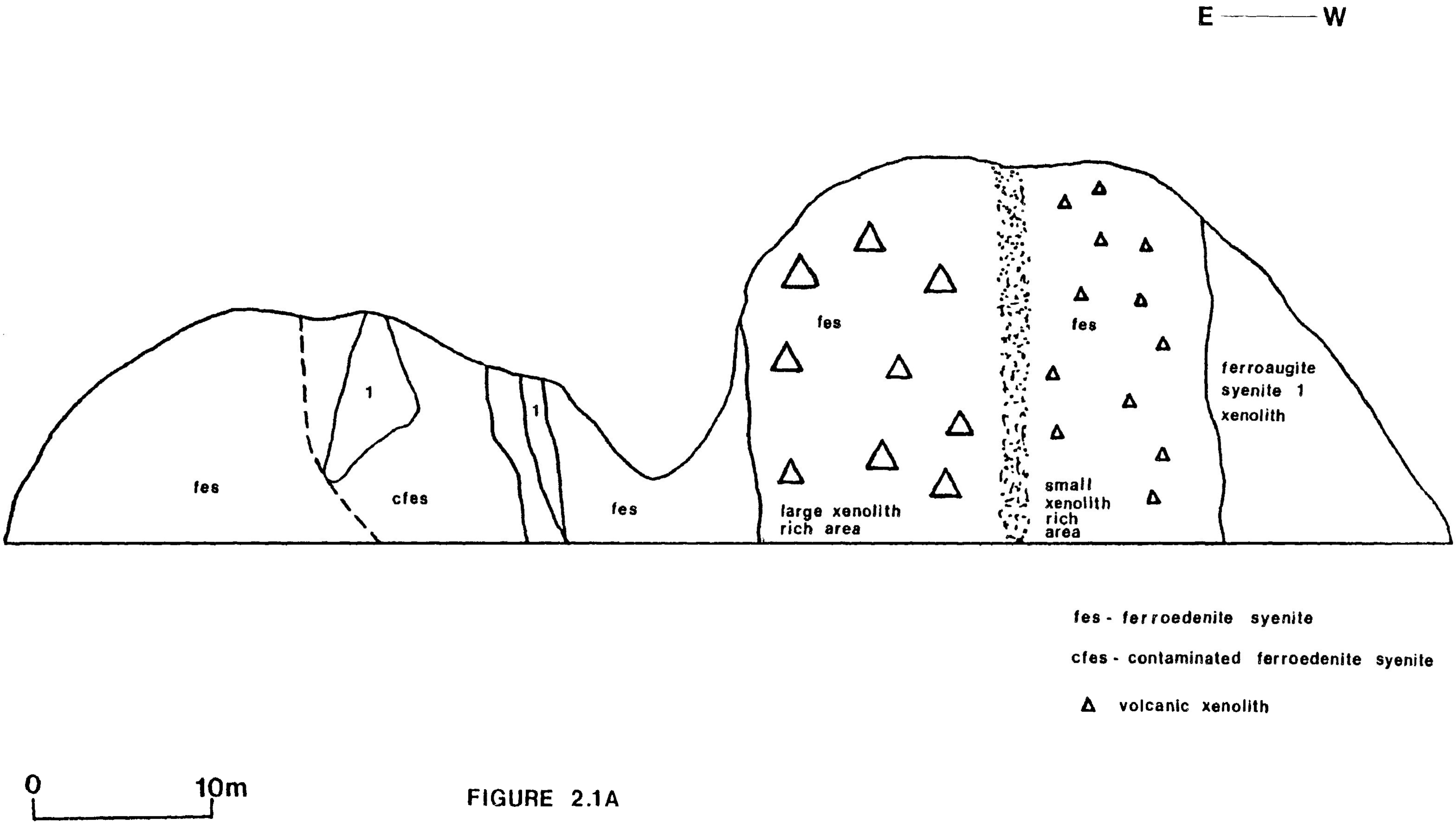
E —— W
1
1
fes
cfes
fes
fes
large xenolith
rich area
fes
small
xenolith
rich
area
ferroaugite
syenite 1
xenolith
fes - ferroedenite syenite
cfes - contaminated ferroedenite syenite
volcanic xenolith
0
10m

FIGURE 2.1A

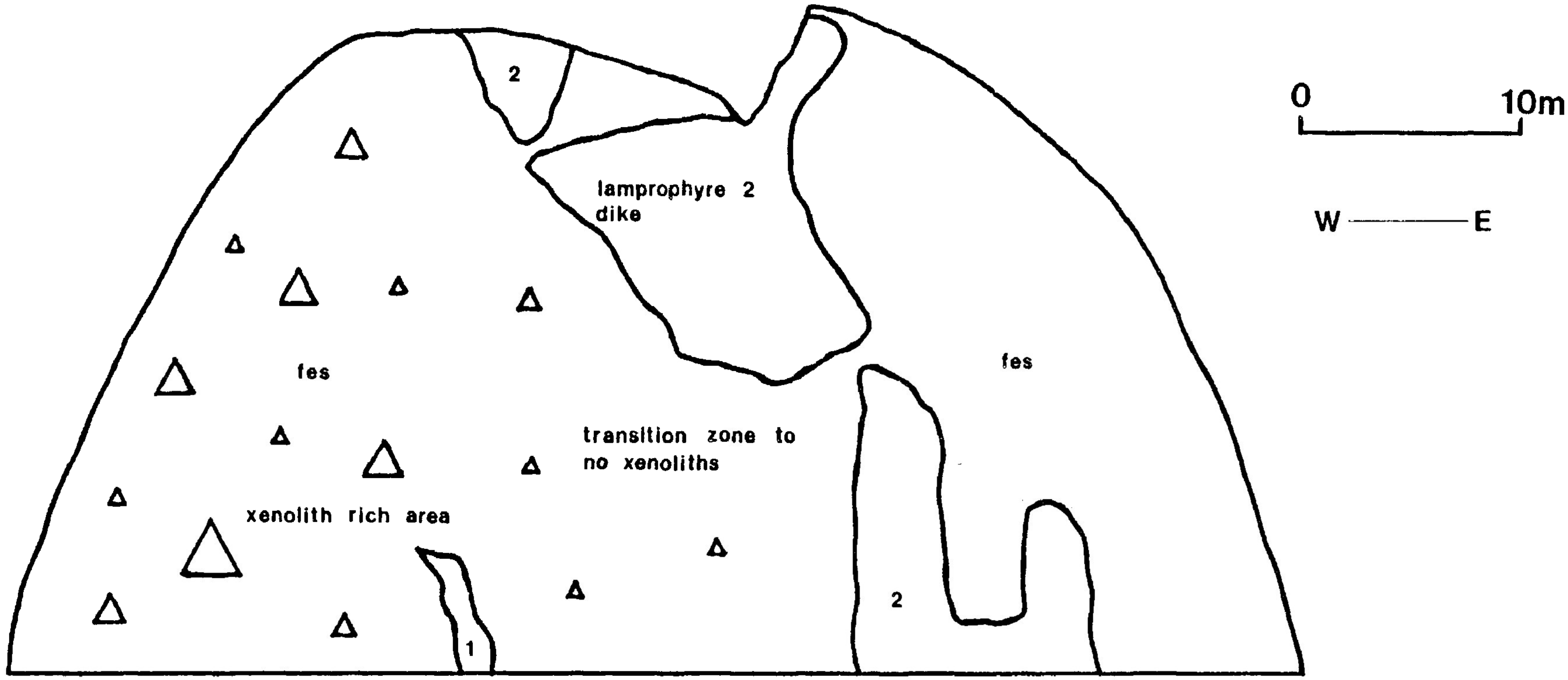

FIGURE 2.1B

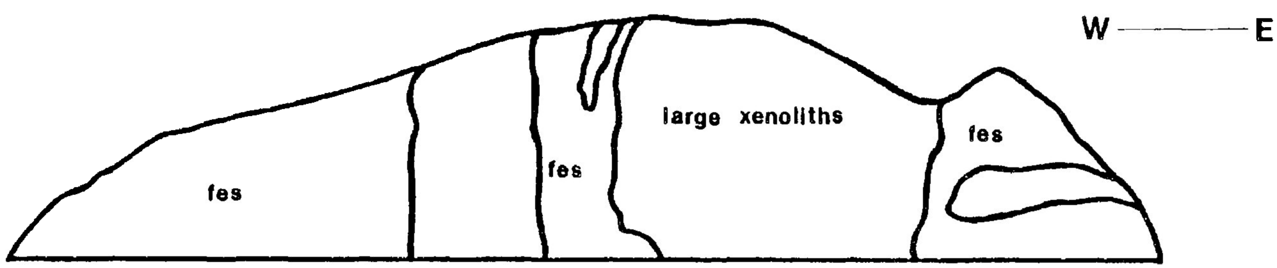

FIGURE 2.1C

0 10m

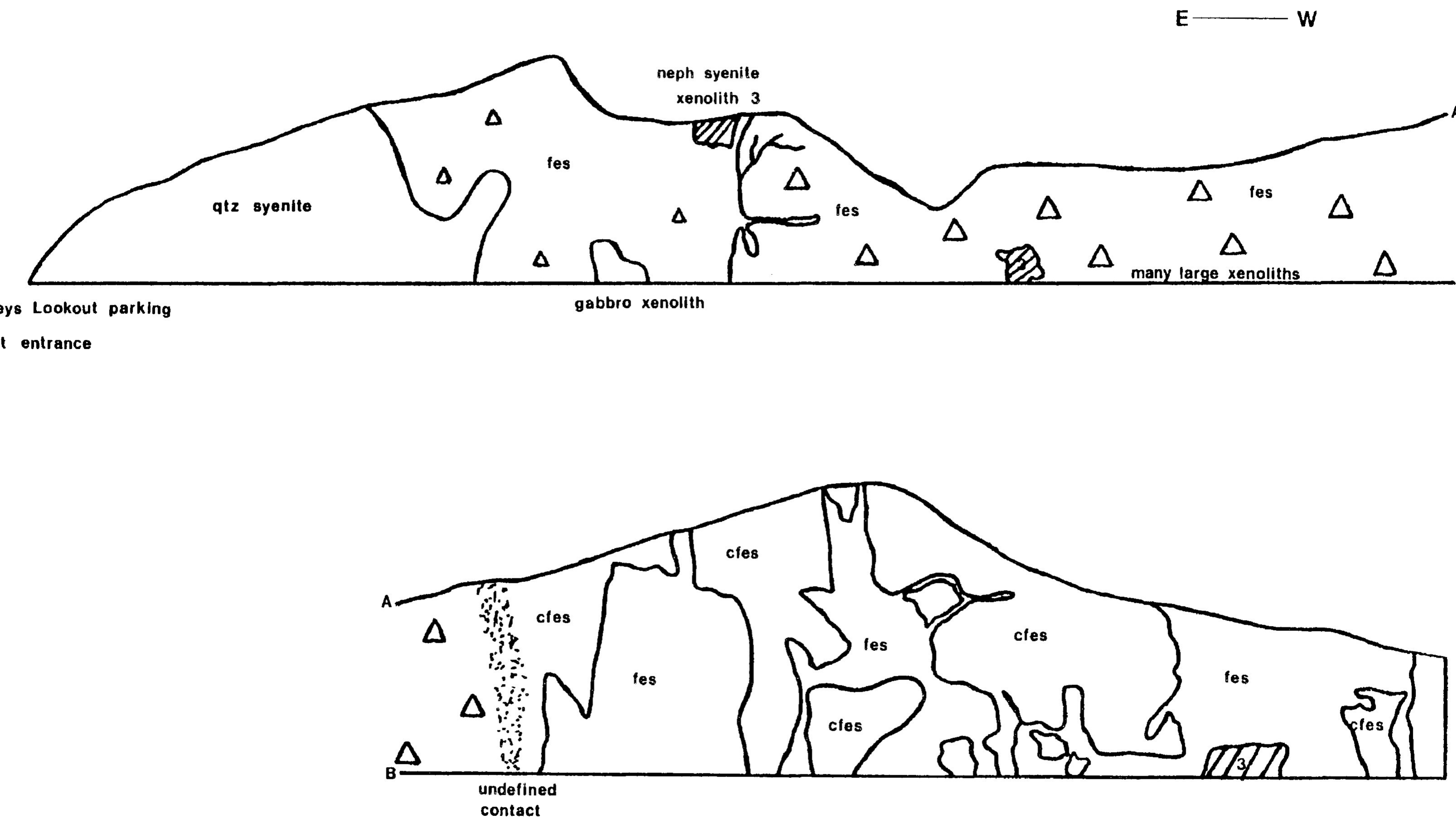

0 10m

FIGURE 2.1D

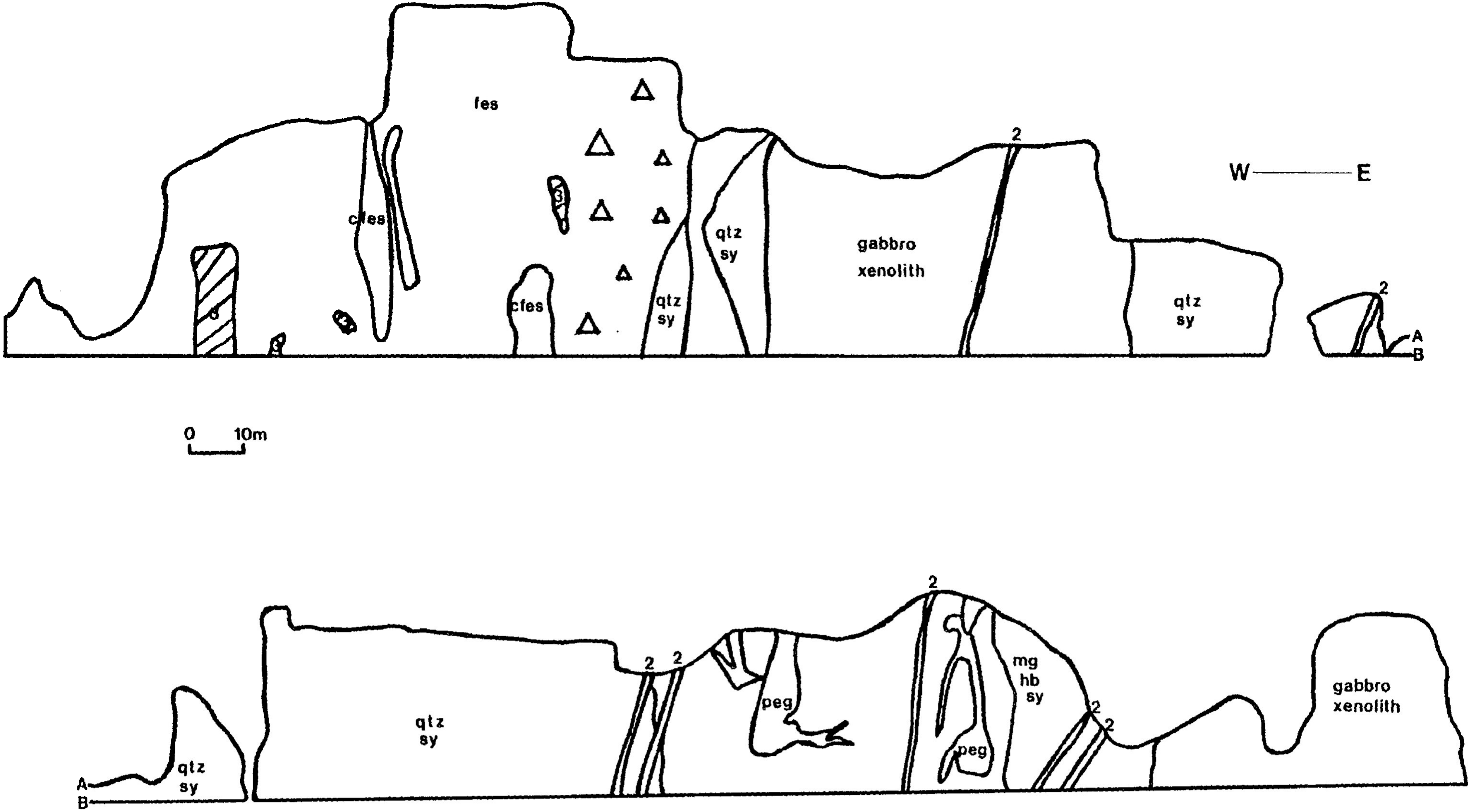
fes
cfes
cfes
qtz sy
qtz sy
gabbro xenolith
qtz sy
W — E
2
2
A
B
0 10m
qtz sy
qtz sy
2
2
peg
peg
mg hb sy
2
2
2
gabbro xenolith
A
B

FIGURE 2.1 E

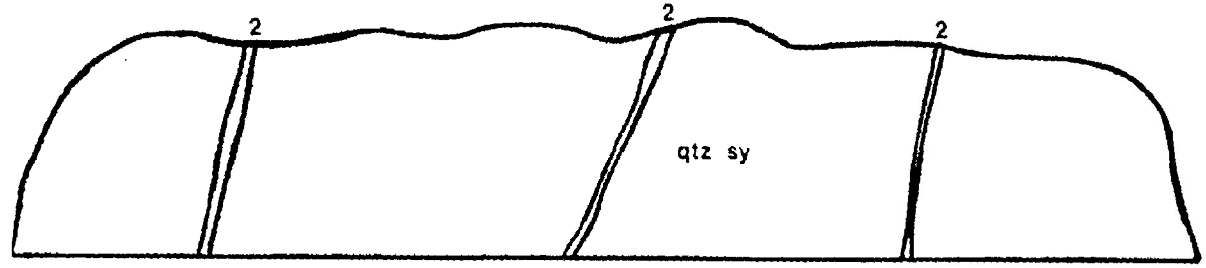

FIGURE 2.1F

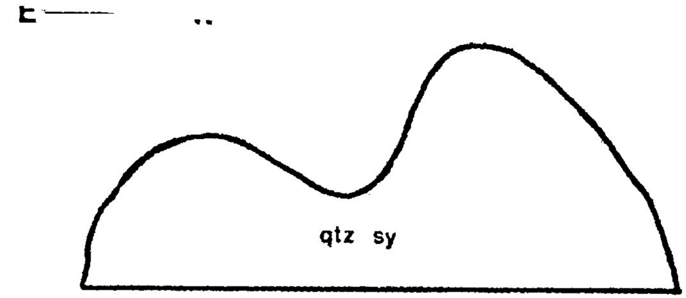

FIGURE 2.1G

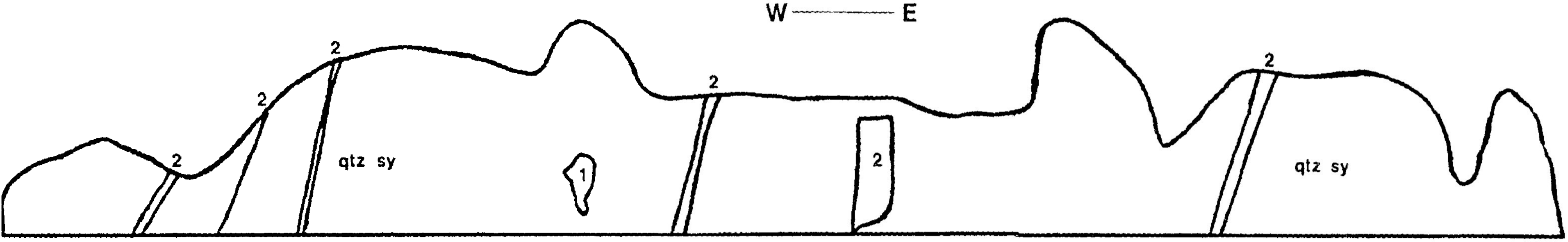

FIGURE 2.1 H

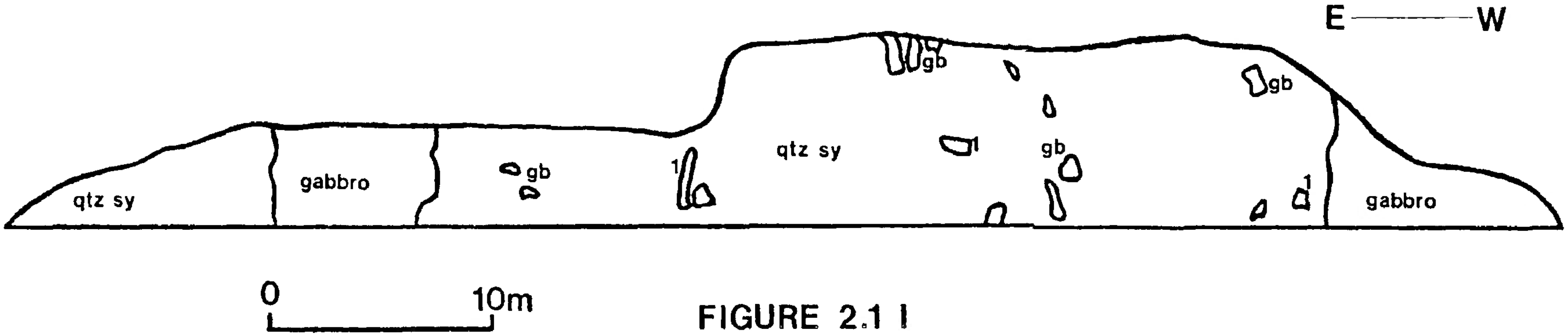

FIGURE 2.1 I

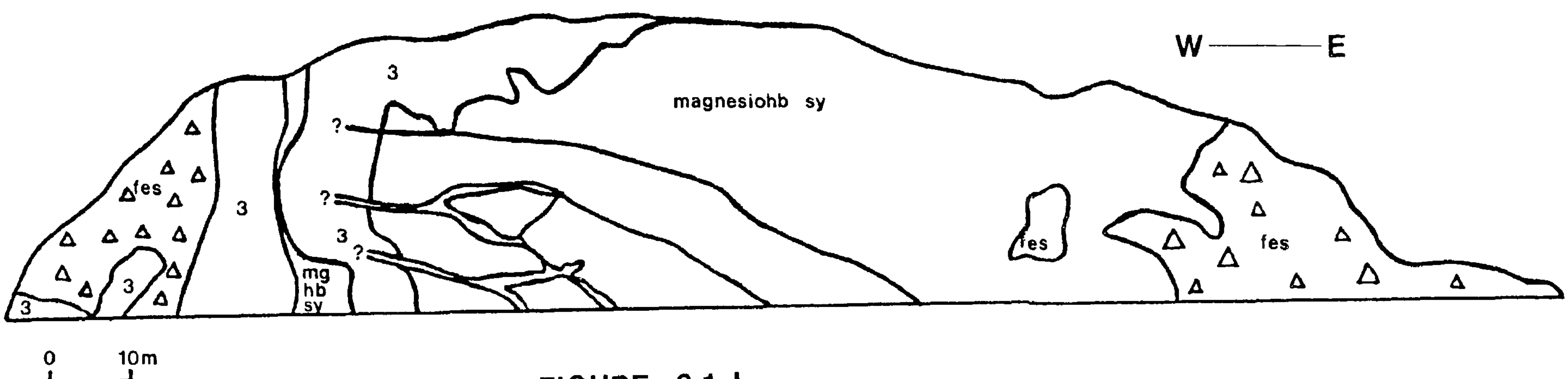

FIGURE 2.1 J

Plate 2.1 Xenolith-rich zone adjacent to the Little Pic River, Neys/Ashburton study area.

Plate 2.2 Xenolith-rich zone located at Ashburton Lookout, Neys/Ashburton study area.

xenolith-rich areas described as breccias by Lukosius-Sanders (1988). Two such xenolith-rich zones are located in the Neys/Ashburton study area, one adjacent to the Little Pic River (figure 2.1A, Plate 2.1), the other at the Ashburton Lookout (figure 2.1J, Plate 2.2). Lukosius-Sanders (1988) has identified a similiar zone on Pic Island.

Xenoliths are also found in highly-contaminated purplish ferro-edenite syenite which occurs as large masses brecciated by the intrusion of later bodies of uncontaminated ferro-edenite syenite (figure 2.1C-E, Plate 2.3).

The volcanic xenoliths are fine grained and holocrystalline ranging from aphanitic to phanerocrystalline depending on the degree of assimilation that has occurred. They are dark grey-to-black in colour, with the more resorbed specimens being less dark in colour. A wide range of sizes and shapes are seen in outcrop (Plate 2.4). The size ranges from a few millimetres to over 1 metre in diameter, and shape ranges from angular to rounded. As assimilation of any one xenolith progresses the degree of roundness increases as does grain size. Common to outcrops of xenolith-rich areas is the occurrence of a mixture of xenoliths in various stages of assimilation. Assimilation varies from nil to near complete digestion, resulting in the formation of ghost xenoliths in which it is possible only to see the remnant outline of the original clast. Such bodies are delineated by a greater

Plate 2.3 Xenoliths within highly contaminated ferro-edenite syenite. Xenoliths display development of biotite ovoids (dark spots) and porphyroblastic alkali feldspar growth (white spots).

Plate 2.4 Wide range of size and shape to volcanic xenoliths in Little Pic River xenolith-rich zone. Xenoliths are also brecciated by host syenite penetrating along fractures.

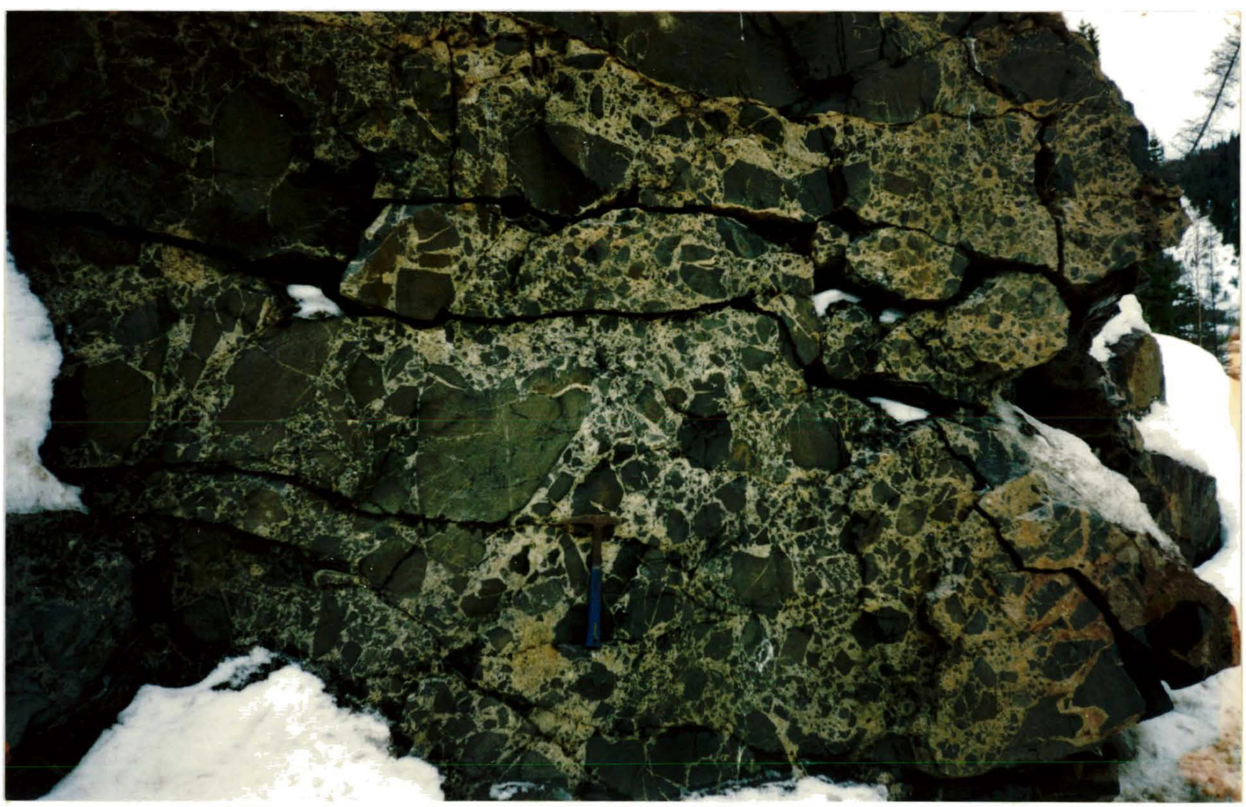

concentration of mafics in the host ferro-edenite syenite than is normally found. Unaffected xenoliths and ghost xenoliths are broken up by syenite magma that has penetrated along fractures (Plate 2.4).

Development of a porphyroblastic texture occurs concurrent with increase in grain size with progressing assimilation. This results from the formation of alkali feldspar porphyroblasts and biotite ovoids. Alkali feldspar porphyroblasts reach upto 5 mm in size and are hematized. Biotite ovoids can contribute upto 10% volume of a xenolith. The ovoids consist of biotite and amphibole and give the xenoliths a spotty, mottled appearance. On exposed surfaces preferential weathering of the ovoids occurs, resulting in the formation of a pitted surface. Xenoliths that appear to be unaffected by assimilation contain few ovoids, whereas those that are highly-altered contain many. Ovoids occur randomly within a xenolith and may straddle xenolith/host contacts. The presence of the porphyroblastic texture and ovoid development has previously been reported from the Western Contact Zone syenites by Jago (1980).

Xenolith/host contacts vary with the degree of assimilation. Those seemingly showing no assimilation have sharp contacts, whereas those which have been extensively assimilated exhibit contacts that are embayed, rounded, diffuse or undulose (Plates 2.3-2.5).

Plate 2.5 Detail of host syenite/xenolith contacts. Contacts are embayed, rounded, diffuse or undulose in assimilated samples.

Plate 2.6 Relict plagioclase phenocrysts in least altered Neys/Ashburton volcanic xenolith. Note two optically distinct amphiboles present in section, one green-to-brown the other green-to-blue green.

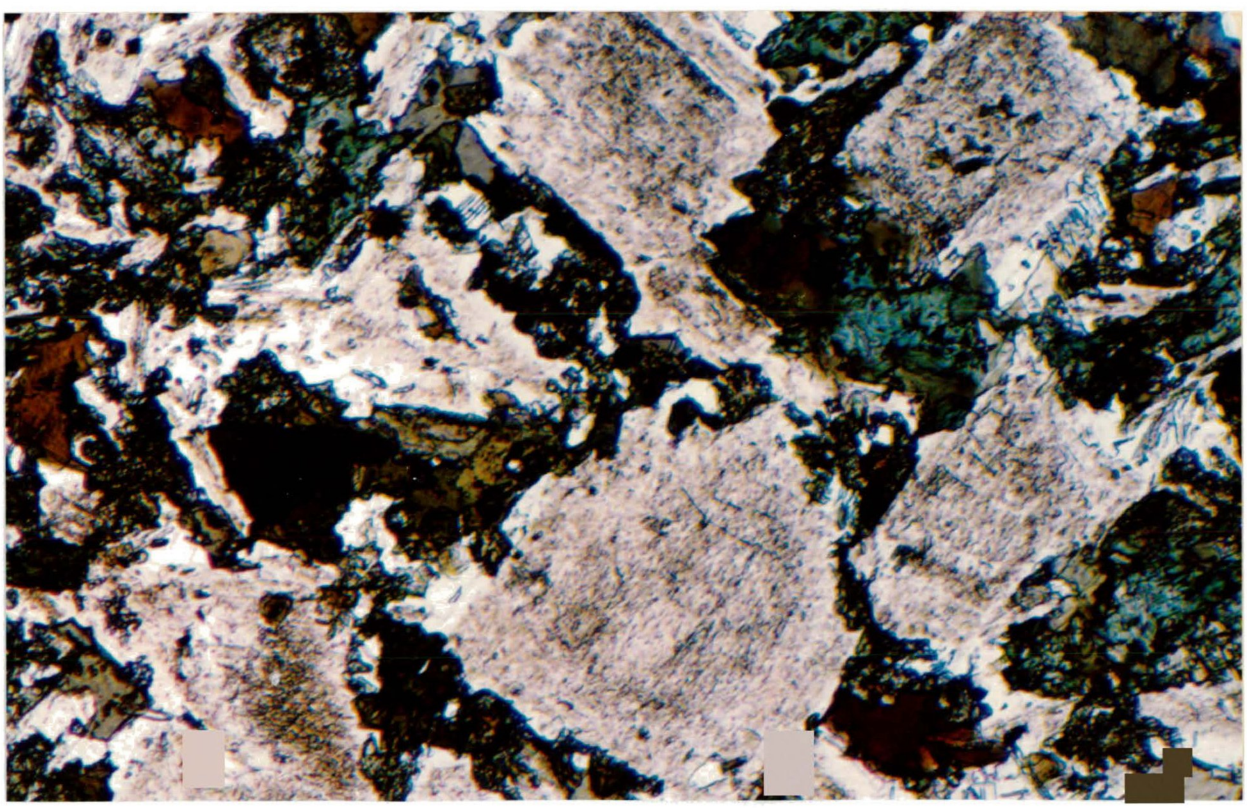

All varieties of contact type can be found in xenolith-rich areas. Xenoliths become progressively rounder as assimilation proceeds. Rarely seen is a darkening of a xenoliths rim at the contact with the host due to formation of amphibole and biotite (Plate 2.3, right of Centre).

2.1.2 Other Xenoliths

Other rock types are found as xenoliths within the Centre 3 syenites. These include metavolcanic and metasedimentary xenoliths of country rock and cognate inclusions of other Coldwell Complex rock types. The volcanic xenoliths are only found within ferro-edenite syenite and contaminated variants but the other xenoliths types can be found in all Centre 3 syenites. Cognate xenoliths include nepheline syenite, gabbro, lamprophyre and ferro-augite syenite. Xenoliths within ferro-edenite syenite are common, whereas few are found in the quartz syenite and magnesio-hornblende syenite.

2.1.3 Wolf Camp Lake - Centre 1

The megaxenolith occuring at Wolf Camp Lake forms a large block within Centre 1 at the Coldwell Complex (figure 2.2). In some portions of the block it is possible to distinguish individual lava flows of not more than a few metres thickness. Such flows are visible on the east side of Trans-Canada Highway #17 and at the southwest end of the hill which

Figure 2.2 Wolf Camp Lake study area. Large hill to south of Wolf Camp Lake comprises the bulk of the megaxenolith.

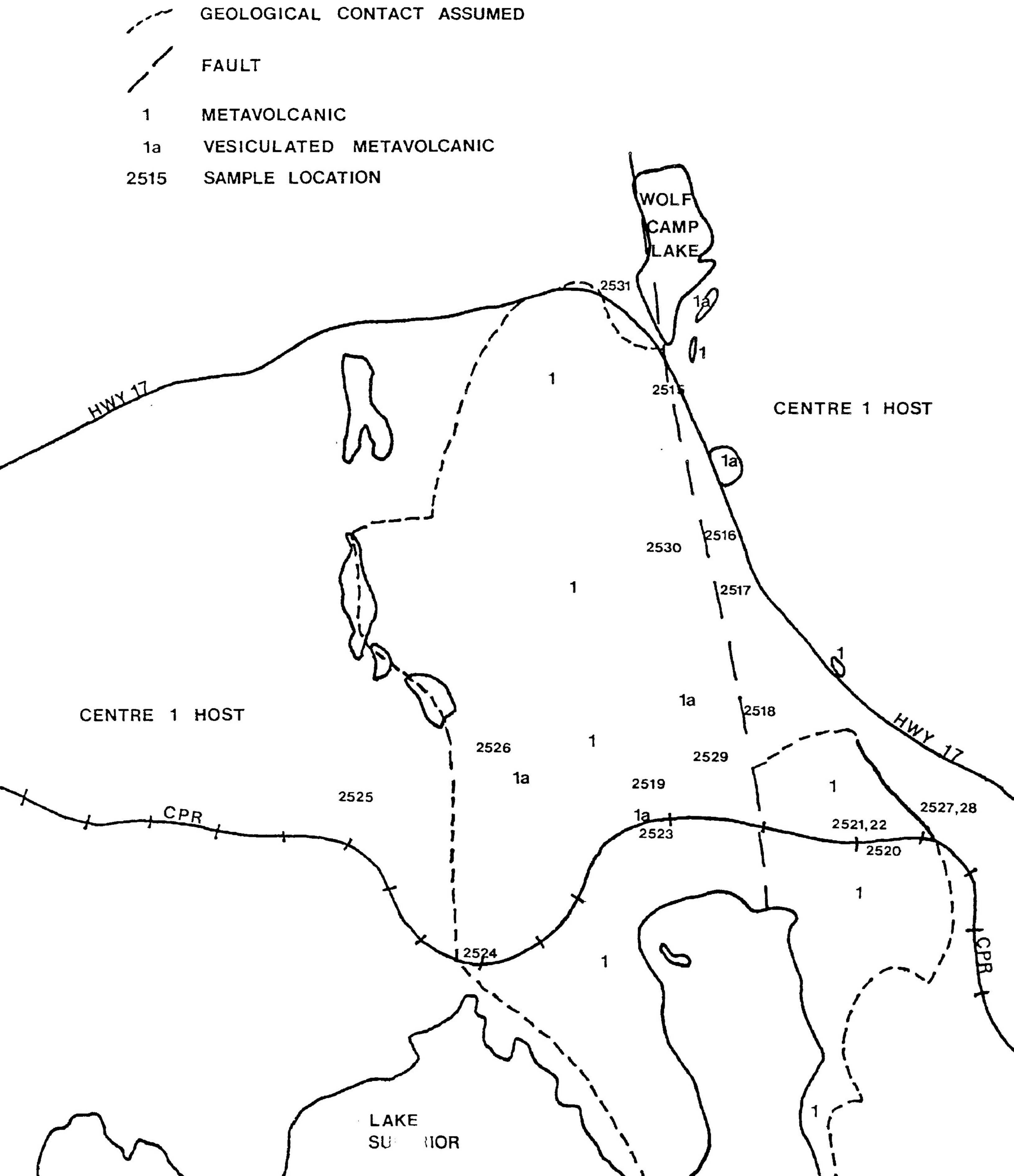

comprises the bulk of the xenolith. These flows can be distinguished from each other by the occurrence of relict flow tops that exhibit vesiculation. The outcrop of the vesicular zones is limited and tracing out of individual flows over any distance proved impossible.

The Wolf Camp Lake megaxenolith is quite different in character to those seen in the Neys/Ashburton study area. It is much finer grained and darker in colour with the overall appearance of a hornfels. Closer to the contact with the host syenites, the xenolith is slightly coarser grained, although remaining aphanitic in texture. Enlargement of grain size due to recrystallization and appearance of alkali feldspar porphyroblasts in proximity to the host contact demonstrate that portions of the block are showing the effects of assimilation in the Centre 1 syenites. Biotite ovoids are not developed.

Greenish-black, fine-grained vesicles range from 1-3 mm in size and give a spotty or mottled appearance to the weathered specimens. On highly weathered surfaces they produce a pebbly surface, as they are not as easily eroded as the matrix. Typically vesicles are too fine grained to permit characterization of their mineralogy however, in proximity to the contact with the Centre 1 host, the vesicles become coarser grained and enlarged in size (2-5x) and are seen to consist of green-black amphibole, biotite and alkali feldspar. Sulphides may or may not be present.

Contacts, when visible, between the megaxenolith and the host syenites are sharp and well-defined. On the north end of the hill, outcrops on the highway show the block to be brecciated by intruding syenite magma. The resulting fragments other than becoming coarser grained, show little effect of being incorporated within the syenite. Blocks are angular and rounded edges are absent.

2.2 Petrography of the Xenoliths

2.2.1 Neys/Ashburton

The volcanic xenoliths in the Neys/Ashburton study area consist primarily of plagioclase, amphibole and biotite with minor clinopyroxene, potassium feldspar, opaque phases and apatite. With increasing alteration due to assimilation by the host ferro-edenite syenite calcite, sphene, fluorite, zircon, thorite and rare earth carbonates appear as accessory phases.

Xenoliths that are angular in shape and show no effects of assimilation generally are porphyritic, with plagioclase and rarely clinopyroxene phenocrysts (Plates 2.6 and 2.7). Relict plagioclase phenocrysts occur mainly as lath-shaped crystals and rarer tabular zoned crystals. They are commonly highly-altered and cloudy due to the formation of hematite and

Plate 2.7 Relict clinopyroxene phenocrysts in least altered Neys/Ashburton xenolith.

Plate 2.8 Overgrowth of amphibole on relict clinopyroxene phenocryst.

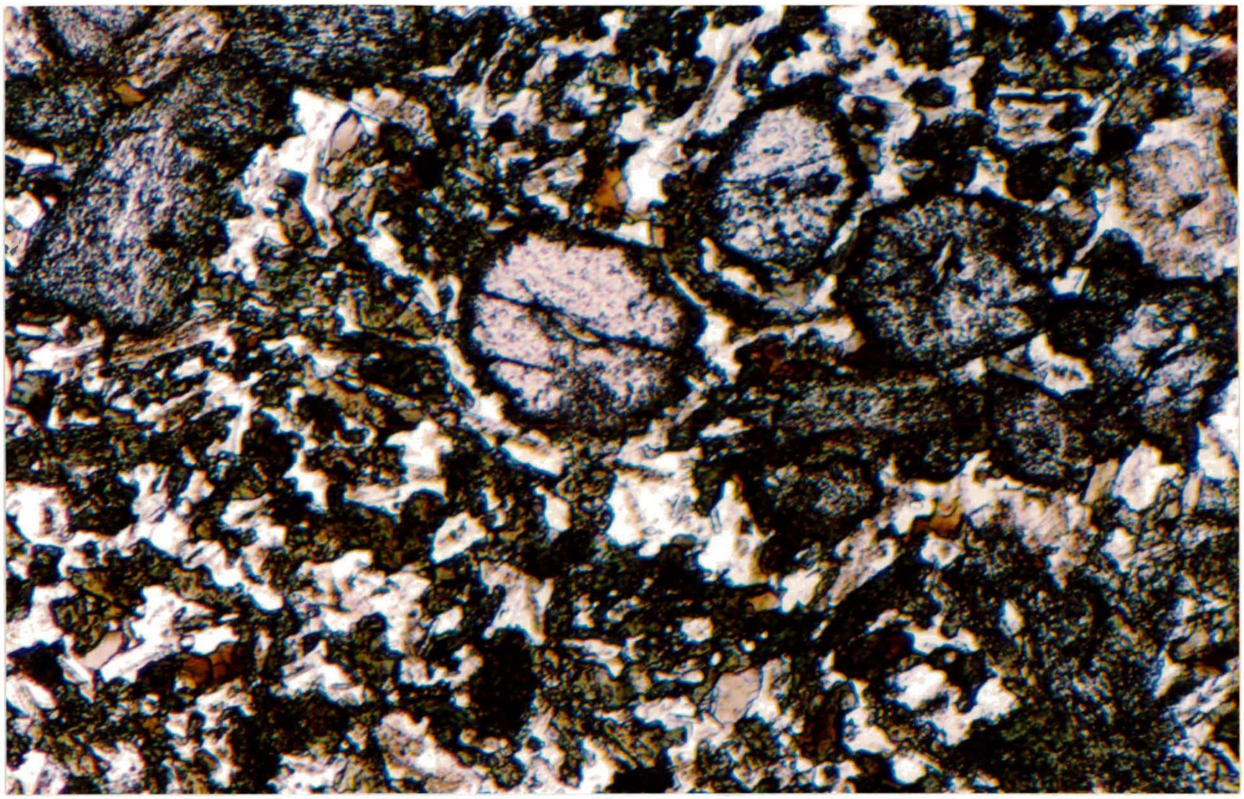

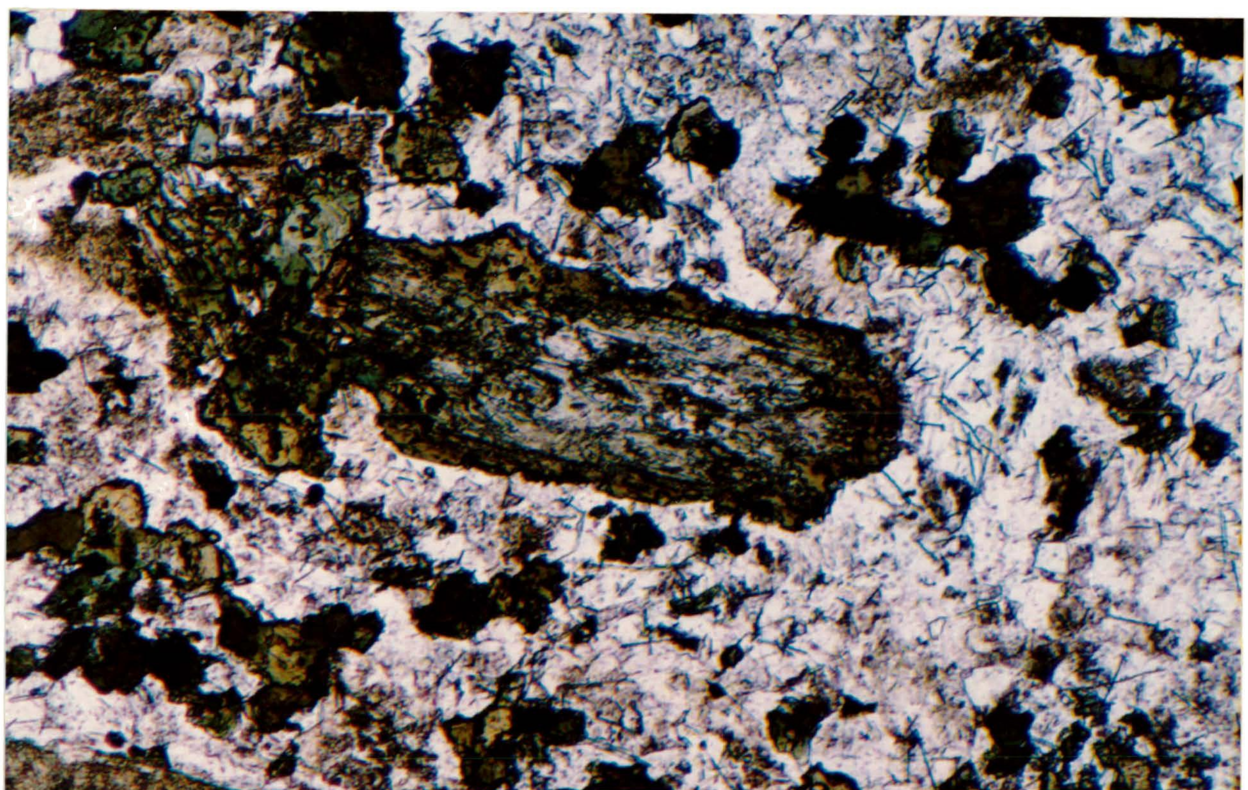

sericite/saussurite. Compositions determined using the Michel-Levy Method are in the range labradorite-bytownite. Jago (1980) reported compositions in the labradorite range and that plagioclase phenocrysts exhibited glomeroporphyrytic and interpenetrant textures. Plagioclase phenocrysts show no preferred orientation.

Relict pyroxene phenocrysts are corroded euhedral crystals that are colourless-to-pale green in colour. Slight pleochroism is exhibited by few examples. Overgrowths of amphibole (Plate 2.8) are common, as are intergrowths along cleavage traces.

Relict phenocrysts of plagioclase and clinopyroxene are set in a groundmass of corroded plagioclase laths, amphibole, biotite, opaque phases and apatite. The texture is that of a metabasalt (Plate 2.9). Groundmass plagioclase shows no preferred orientation and is highly altered to a combination of sericite/saussurite with hematite clouding. Their compositions by the Michel-Levy Method are in the range oligoclase-labradorite. Inclusions of apatite and biotite are common and strained extinction is evident.

Two optically distinct varieties of amphibole are present (Plate 2.6). The most common amphibole exhibits a pale olive green-to-dark olive green or light brown through olive green pleochroism. This amphibole occurs as

Plate 2.9 Texture of least altered Neys/Ashburton xenolith.

Plate 2.10 SEM photo of opaque mass consisting of magnetite (light gray) with exsolved ilmenite (darker gray). Such masses are common in altered xenoliths.

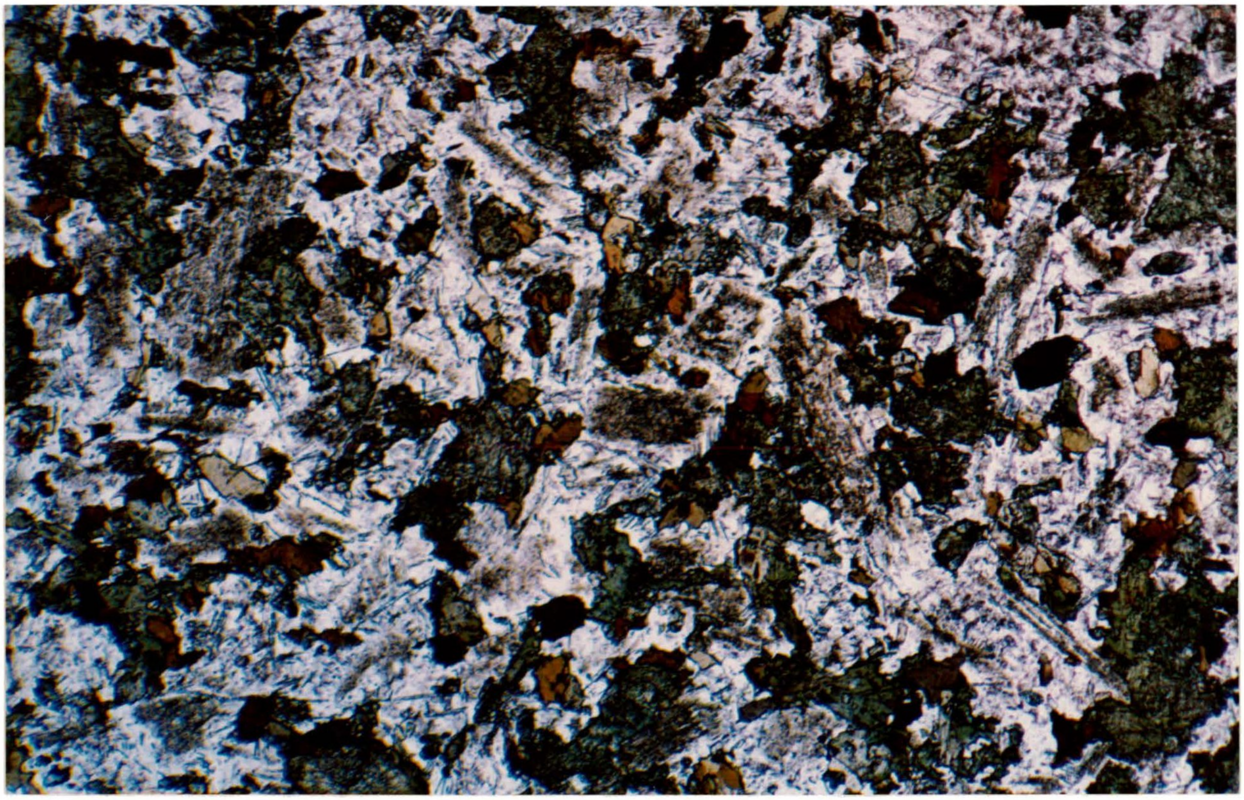


C2529
003053 25KV
75um

corroded, ragged-looking anhedral to subhedral crystals. It occurs in isolated patches with biotite or with clinopyroxene as rims and intergrowths. Replacement of this amphibole by biotite and opaques is common.

The less common amphibole exhibits light green-to-blue green pleochroism (Plate 2.6). This amphibole can be seen to be replacing the more common brown-green amphibole as diffuse patches. It also occurs within relict clinopyroxene crystals and with biotite.

Subhedral biotite is present in various proportions and is pleochroic from pale straw yellow-to-dark red brown. Commonly inclusions of radioactive phases produce radiation damage halos. Replacement of amphibole by biotite and reaction rims of biotite around opaque minerals are common.

In the majority of the least-altered specimens a small amount of clinopyroxene can be found in the groundmass. It forms small anhedral crystals exhibiting the same optical characteristics as displayed by the clinopyroxene phenocrysts. Apatite occurs as acicular needles primarily with plagioclase, but also as inclusions within amphibole and biotite. Inclusions of apatite in biotite are commonly seen to produce halos in the host. Opaque minerals are typically present as small anhedral or subhedral grains. Using EDS/SEM techniques the opaque grains were identified as pyrite, chalcopyrite, magnetite, ilmenite, sphalerite and galena. Common to the amphiboles are small sulphide blebs, consisting principally of pyrite, and lesser chalcopyrite. Larger opaque masses found with amphibole and biotite are a combination of magnetite with exsolved ilmenite (Plate 2.10). Sphalerite and galena are rare.

With increasing degrees of assimilation porphyroblastic growth of alkali feldspar occurs in the xenoliths. This feature has also been reported in the Western Contact Zone syenites by Jago (1980) and Lukosius-Sanders (1988). Growth of alkali feldspar starts with the development of coronal overgrowths on relict plagioclase phenocrysts (Plates 2.11 and 2.12) and continues until the phenocryst is completely replaced by an alkali feldspar porphyroblast. Alkali feldspar porphyroblast growth also results from the formation of alkali feldspar crystals in the xenolith matrix (Plate 2.13). The porphyroblasts may or may not show twinning (Carlsbad) and development of a perthitic texture. They commonly are corroded in appearance and altered to hematite and sericite/saussurite. Inclusions of biotite, amphibole and opaque phases are common.

Biotite ovoids consist primarily of mica and amphibole with accessory clinopyroxene, fluorite, calcite and opaque phases (Plates 2.14 and 2.15).

Plate 2.11 Coronal overgrowths of alkali feldspar on relict plagioclase phenocrysts begins development of alkali feldspar porphyroblasts.

Plate 2.12 Alkali feldspar overgrowth on relict plagioclase phenocryst.

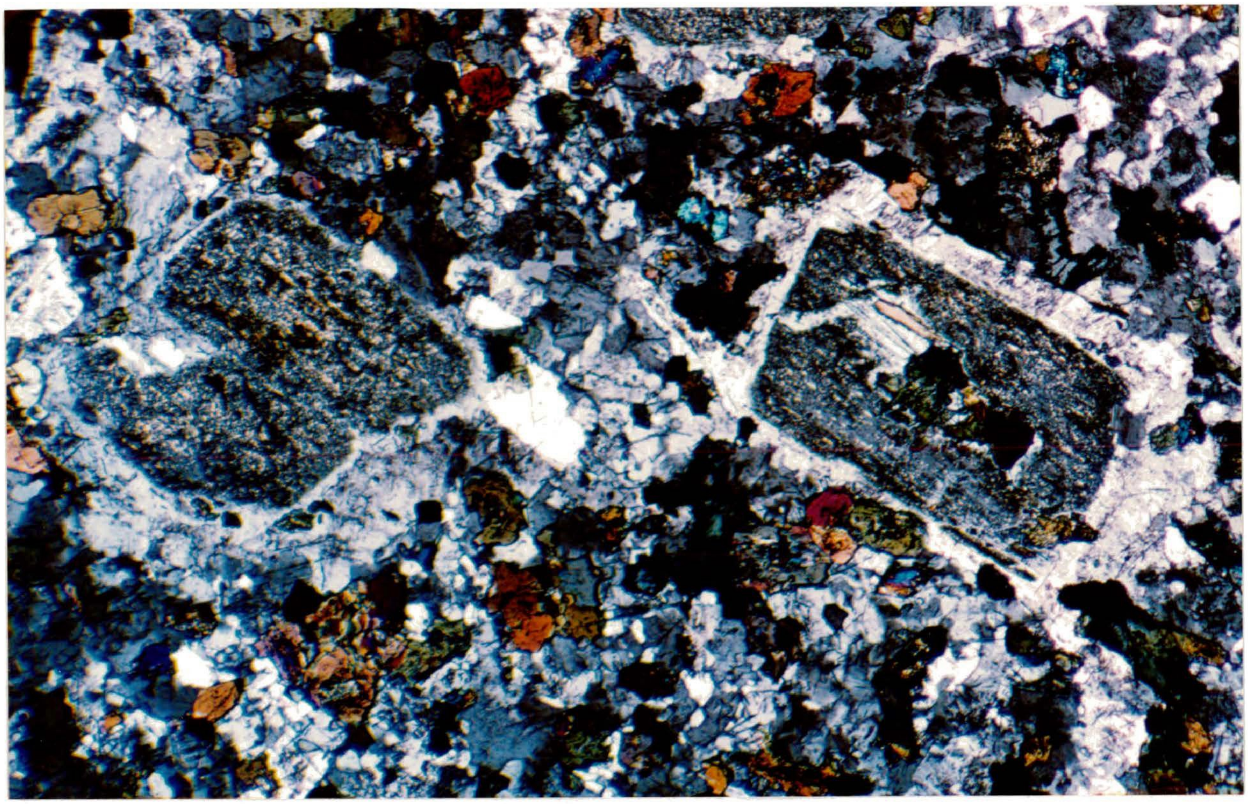

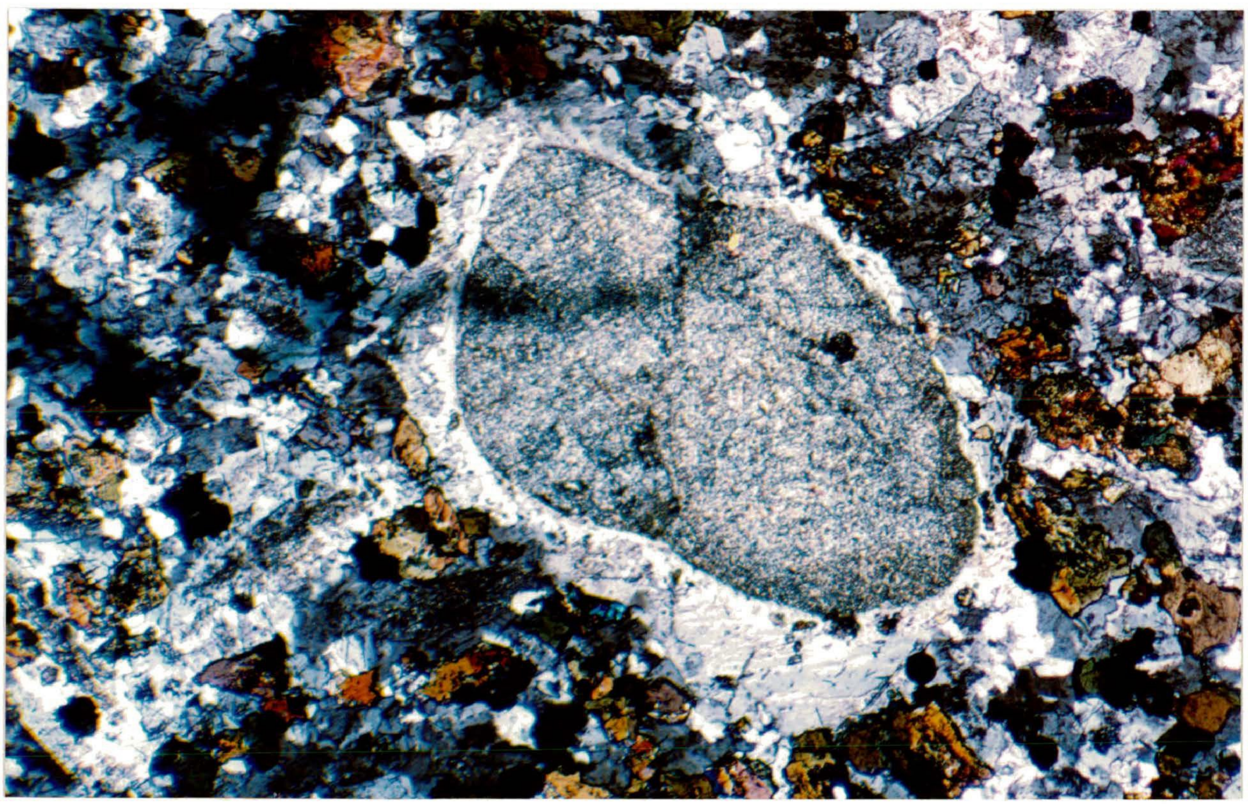

Plate 2.13 Alkali feldspar porphyroblastic growth within a Neys/Ashburton xenolith. Notice concentration of amphibole growth at the host/ xenolith contact.

Plate 2.14 Detail of biotite ovoid. Example consists mainly of subhedral biotite flakes with accessory opaques and fluorite.

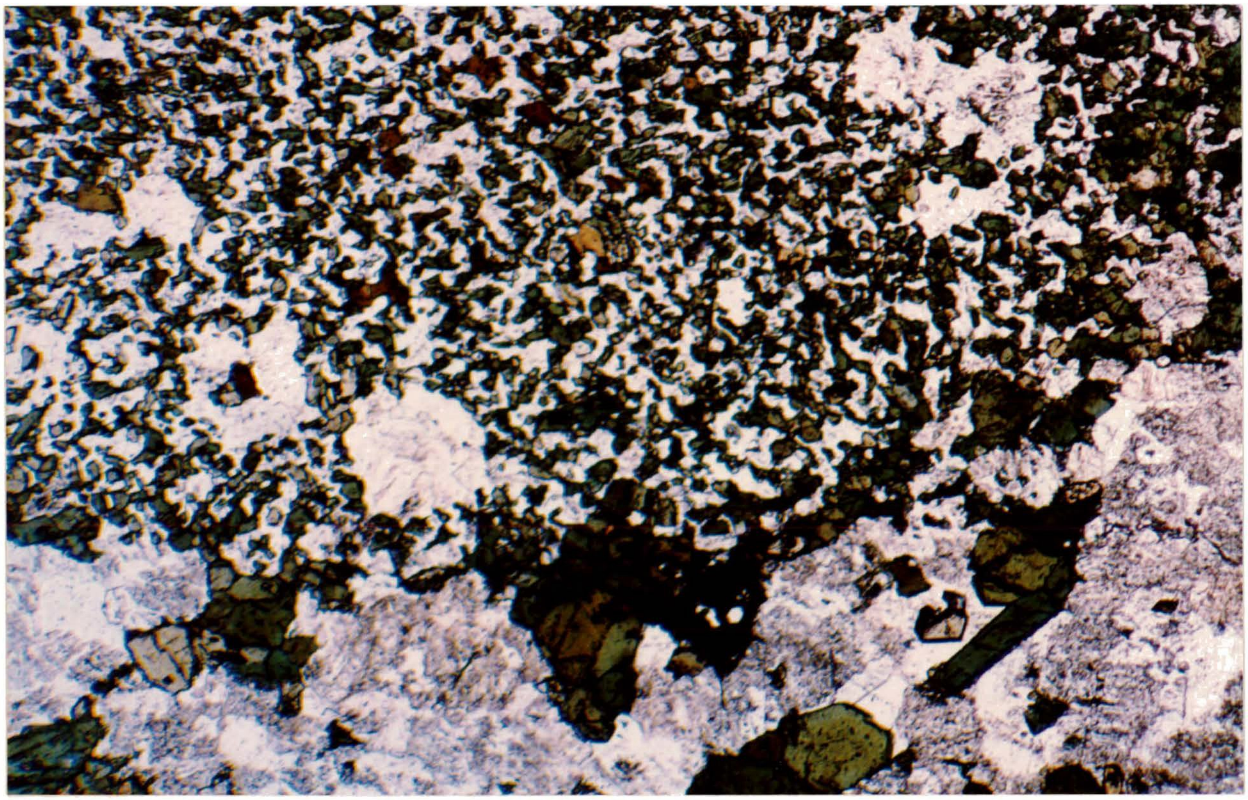

Plate 2.15 Large biotite ovoid consisting of subhedral biotite flakes and amphibole with accessory opaques. Note radiation damage halos in biotite.

Plate 2.16 Beginnings of ovoid development.

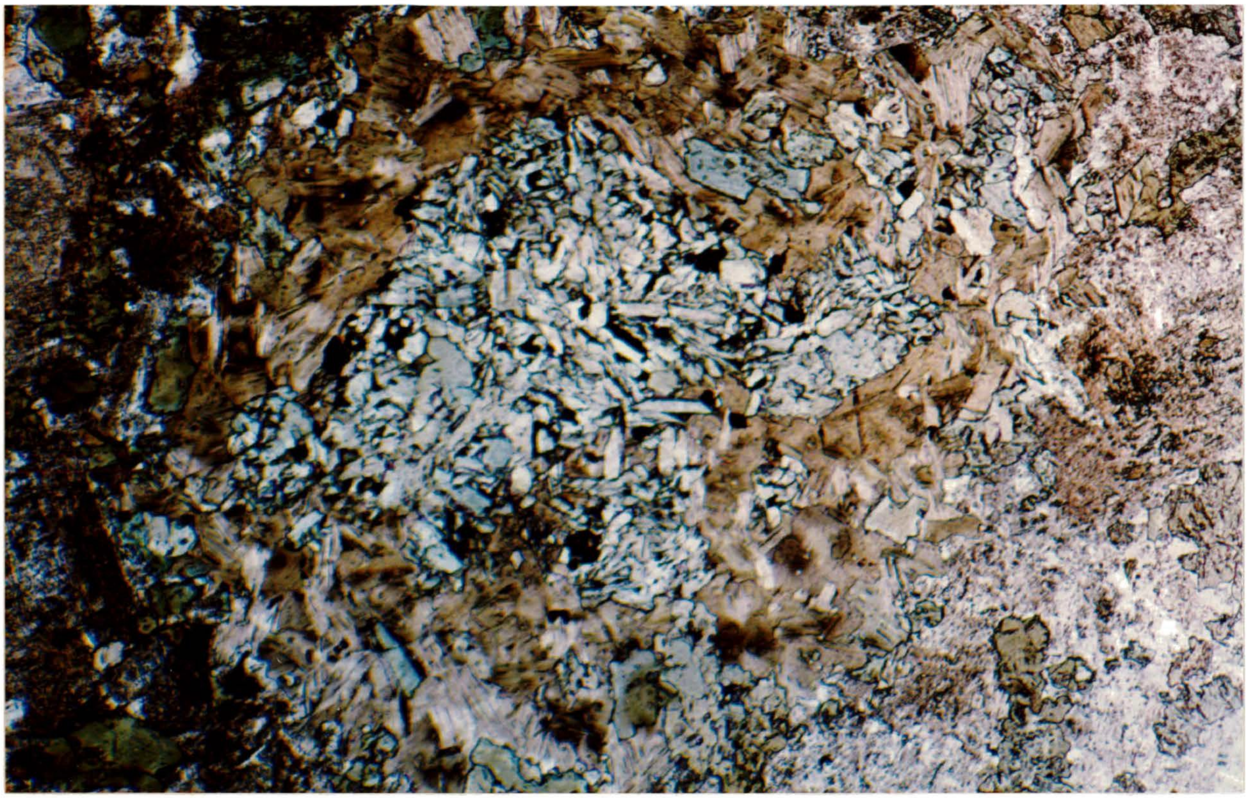

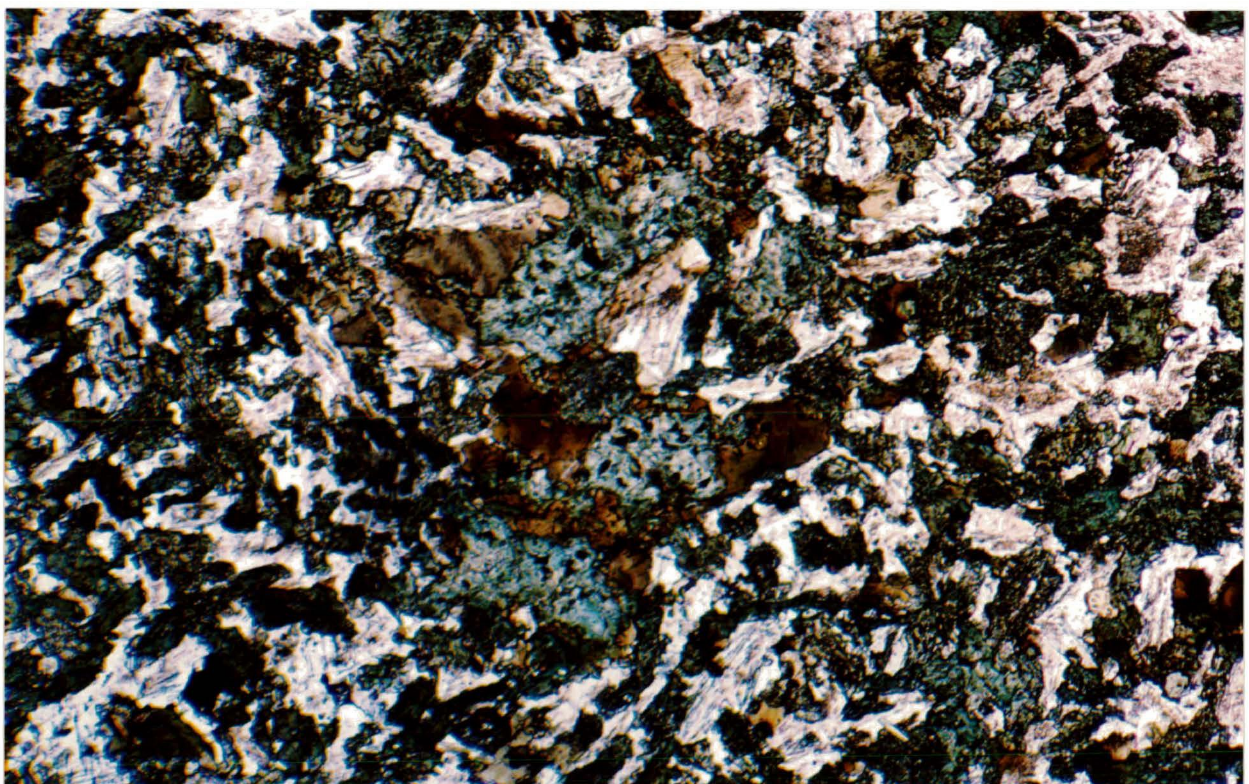

Amphibole is commonly of the blue-green variety. The appearance of the ovoid is determined primarily by biotite which occurs as randomly-oriented subhedral crystals. Biotite ovoids are roughly circular in shape and occur randomly within xenoliths or stradling the contacts between xenoliths and host ferro-edenite syenite. Biotite ovoids are also found within the contaminated host. Ovoid size increases with the degree of assimilation.

Ovoid development begins with formation of a few biotite crystals and blue-green amphibole, with or without opaque phases (Plate 2.16). As the degree of xenolith resorption increases, the ovoid grows by the addition of biotite crystals outward from the original core. In the more advanced stages of formation fluorite, opaque grains and calcite appear in the core. Development of biotite ovoids in the xenoliths appears to be a random process caused by the addition of fluids derived from the host ferro-edenite syenites.

A feature common to all volcanic xenoliths that is observable by scanning electron imagery is the replacement of plagioclase laths in the groundmass by alkali feldspar (Plates 2.17 and 2.18). Alkali feldspar formation occurs as diffuse patches within these crystals. This feldspar is rich in celsian and contains up to 6 BaO wt % (see chapter 3; Plate 2.19). Growth of alkali feldspar crystals in the groundmass occurs along with

Plates 2.17 and 2.18 SEM photos of alkali feldspar replacement and growth within plagioclase feldspar of volcanic xenoliths. Alkali feldspar shows as a lighter phase within the darker plagioclase laths.

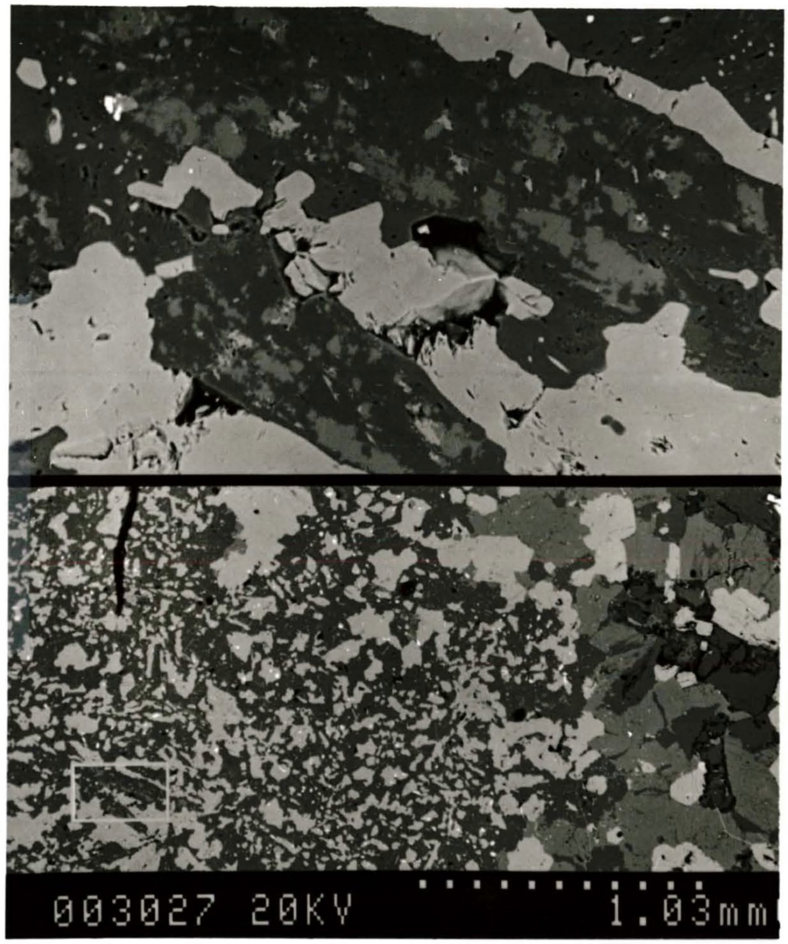
003027 20KV
1.03mm

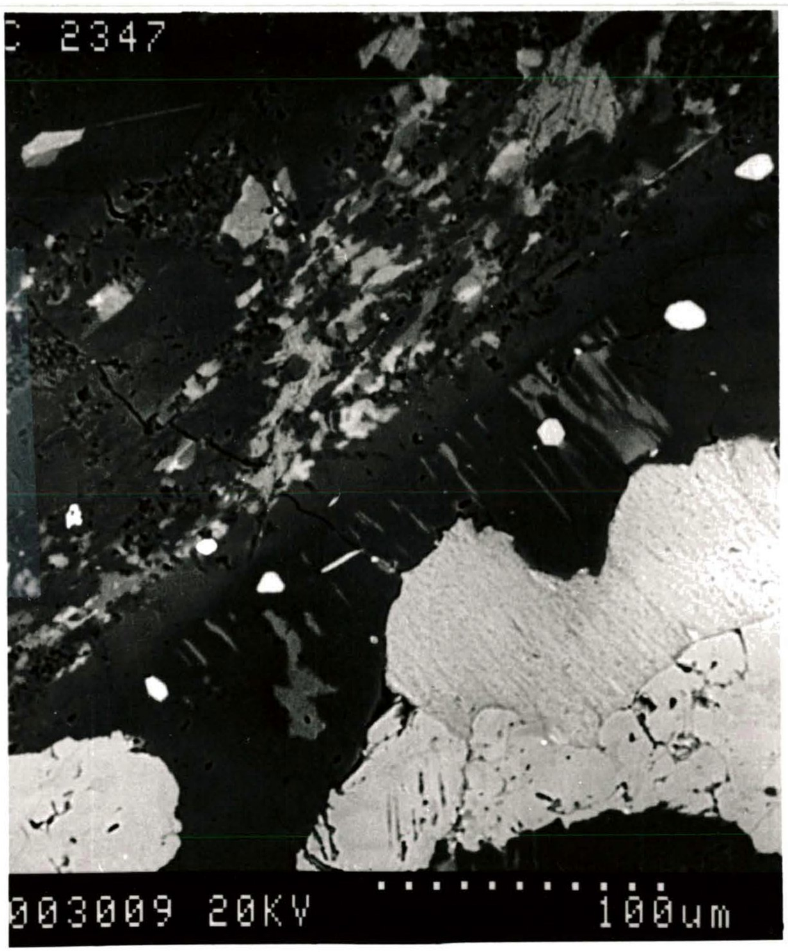
C 2347
003009 20KV
100um

Figure 2.19 Replacement alkali feldspar with high barium contents. Celsian-rich areas appear lighter in colour. Darker phase is plagioclase.

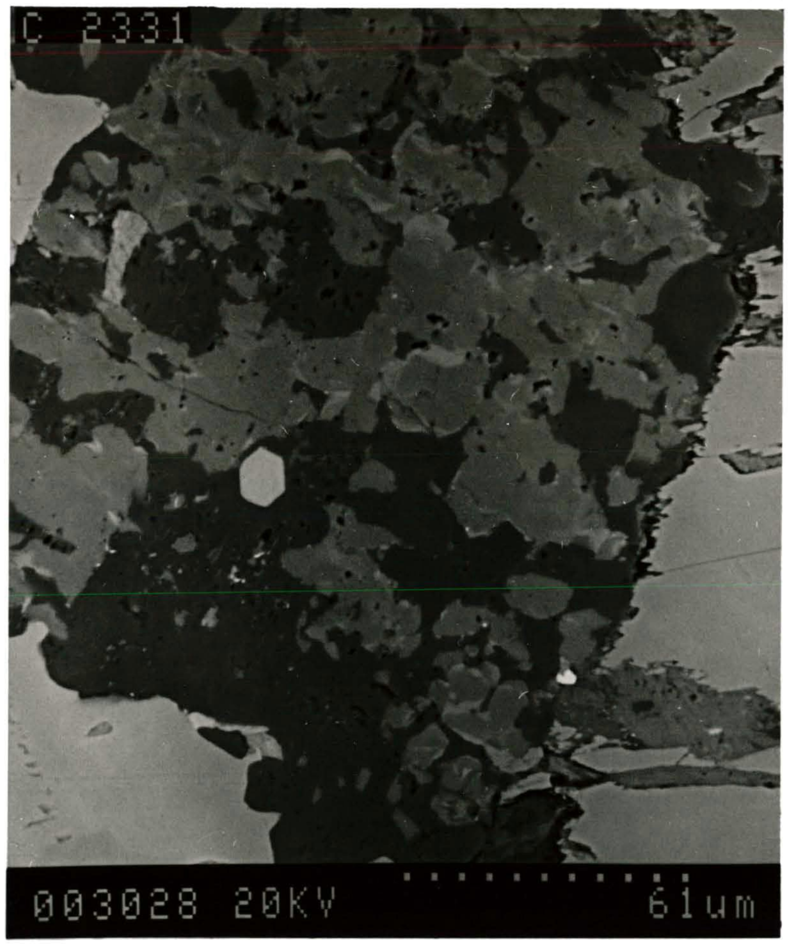
C 2331
003028 20KV
61um

plagioclase replacement.

Assimilation results in an increase in grain size and recrystallization of the groundmass (Plate 2.20). Plagioclase laths are recrystallized to produce a granular mosaic with triple point grain boundaries. Recrystallized plagioclase displays poor development of albite twinning. Fluorite, calcite and rarely quartz are present. Other phases present are anhedral zircons (Plate 2.21) that are highly altered and rare earth carbonates.

With complete assimilation the xenoliths appear as ghosts of the original volcanics from which they formed (Plate 2.22). The only evidence of their having existed are porphyroblastic alkali feldspars, biotite ovoids and increased mafic mineral content, giving the host syenite a distinct purplish colour. Assimilation results in the production of the contaminated varieties of ferro-edenite syenite.

2.2.2 Wolf Camp Lake

Typically the Wolf Camp Lake volcanics consist of plagioclase, amphibole, clinopyroxene and biotite. Minor phases are opaque minerals and apatite together with accessory sphene, calcite and fluorite. Accessory phases occur in recrystallized specimens close to syenite contacts. Olivine, or is pseudomorphs, are absent.

The volcanics are holocrystalline and aphanitic. In some cases grain size

Plate 2.20 Higher degrees of assimilation results in the recrystallization of the volcanic to coarser grain size. Plagioclase laths are recrystallized to a granular mosaic.

Plate 2.21 SEM photo of zircon growth within xenoliths with increased degree of assimilation.

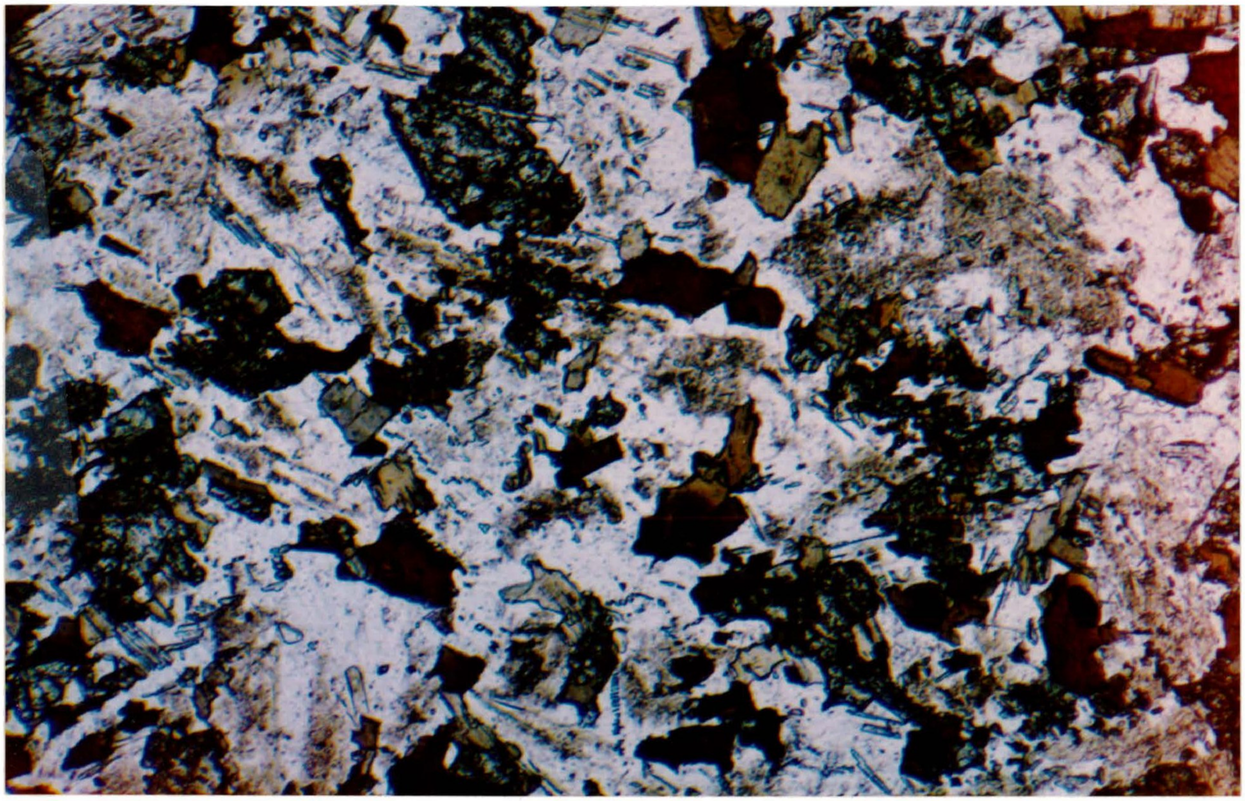

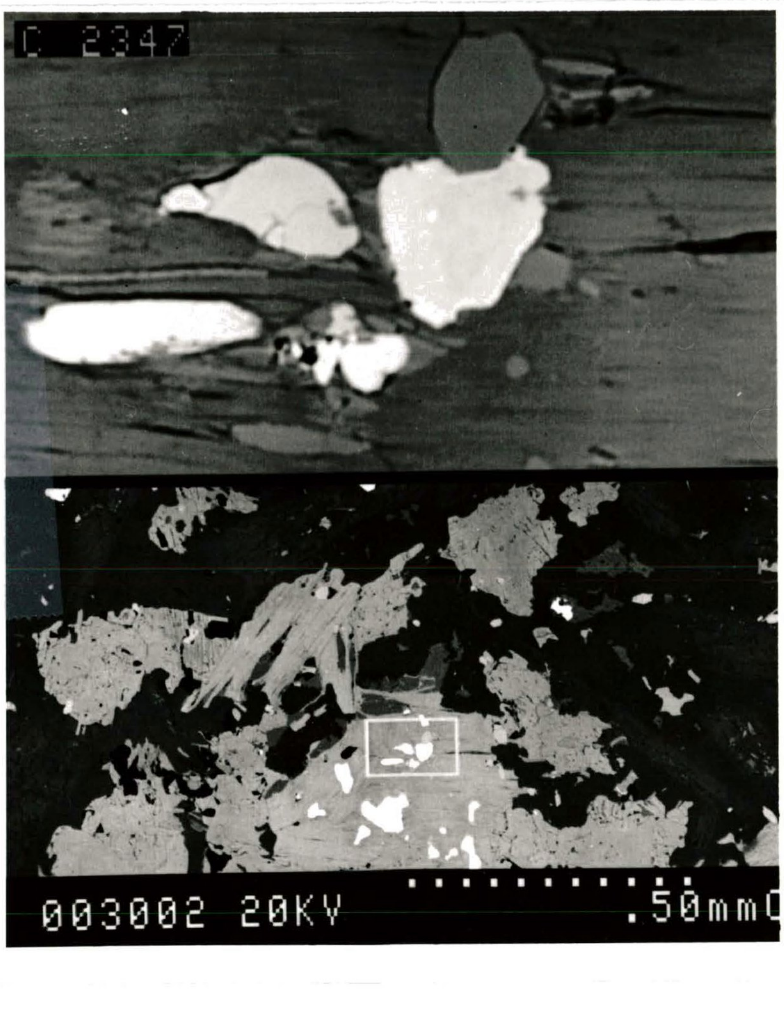
C 2347
003002 20KV
.50mm

Plate 2.22 With complete assimilation xenoliths appear as ghosts of the original volcanics from which they formed. In photo a partially assimilated xenolith is seen on the left and a ghost is seen on the right. Note coarser grain size and and decreased mafic content of ghost relative to the other xenolith.

Plate 2.23 Texture of unaltered Wolf Camp Lake xenolith of fine grained non-oriented plagioclase crystals. Texture is that of a common basalt.

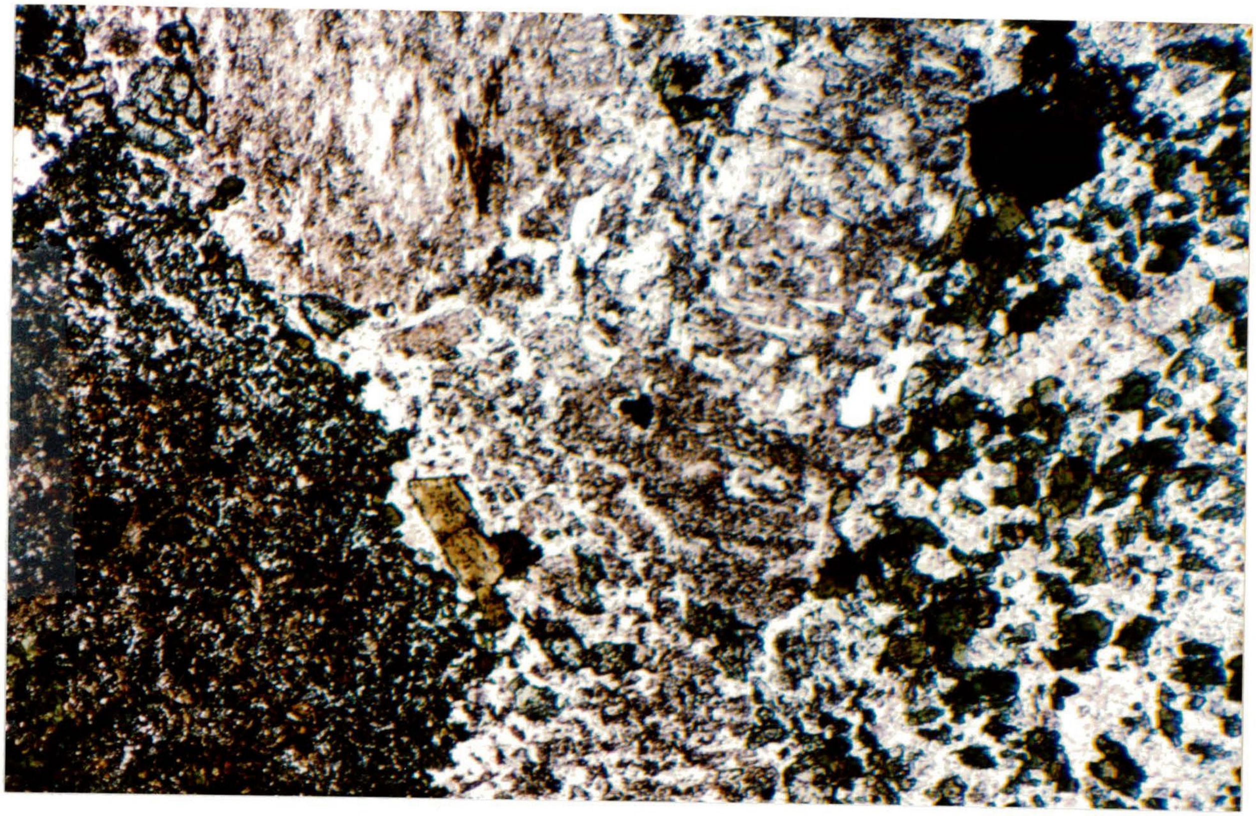

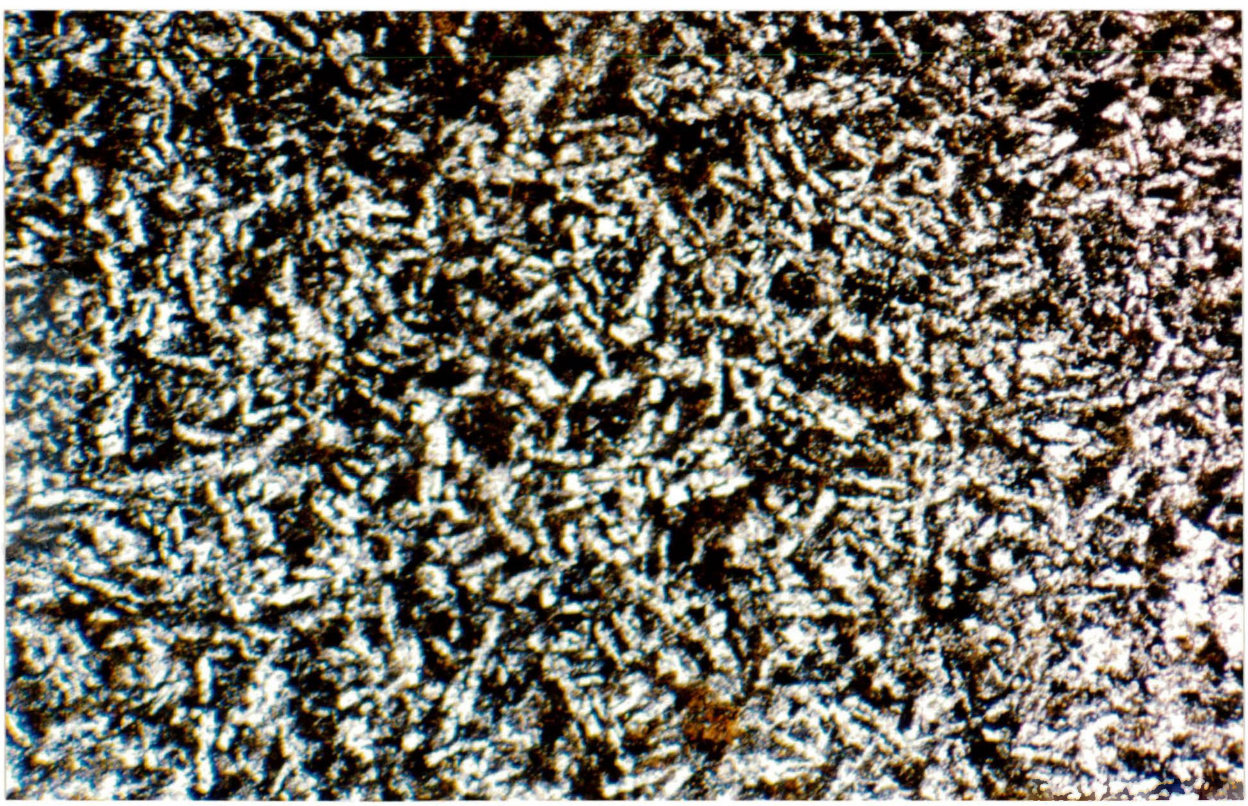

is so small that the rocks appear cryptocrystalline. Specimens closer to the contacts with the host Centre 1 syenites are recrystallized and coarser in grain size, although they remain aphanitic in character. The rocks rarely contain plagioclase and clinopyroxene phenocrysts.

Unaltered specimens display a distict volcanic texture and are similiar to common basalts (Plate 2.23). Plagioclase occurs as very small acicular laths showing no preferred orientations. Plagioclase is commonly turbid in appearance due to hematization and sericite/saussurite formation and exhibits poor development of albite twinning, precluding optical composition determination. In those areas of the megaxenolith near to or at the contact with the host syenites, plagioclase is recrystallized to a granular mosaic of crystals exhibiting poor albite twinning (Plate 2.24). Alkali feldspar forms as granular crystals in association with the recrystallized plagioclase or as porphyroblasts with inclusions of clinopyroxene and amphibole.

Amphibole occurs as ragged anhedral-to-subhedral crystals in slightly coarser grained recrystallized samples. Amphibole shows pleochroism from pale straw yellow-to-brown green, colourless or pale green-to-green and pale green-to-blue green. The blue green amphibole is less common. Inclusions of opaque minerals are common, inclusions of feldspar, biotite

Plate 2.24 Recrystallization occurs towards the host/syenite contact to a coarser grain size.

Plate 2.25 Recrystallized vesicle within Wolf Camp Lake volcanic. Granular clinopyroxene and amphibole are major constituents

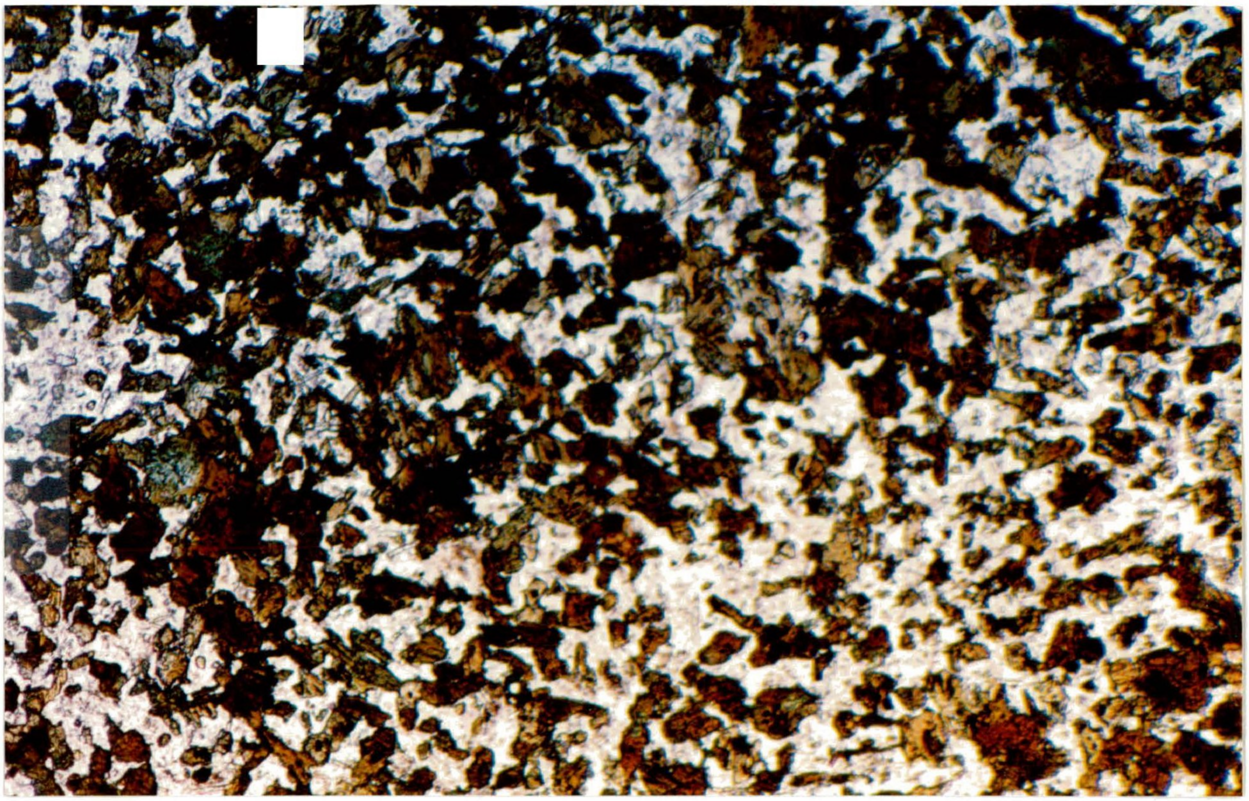

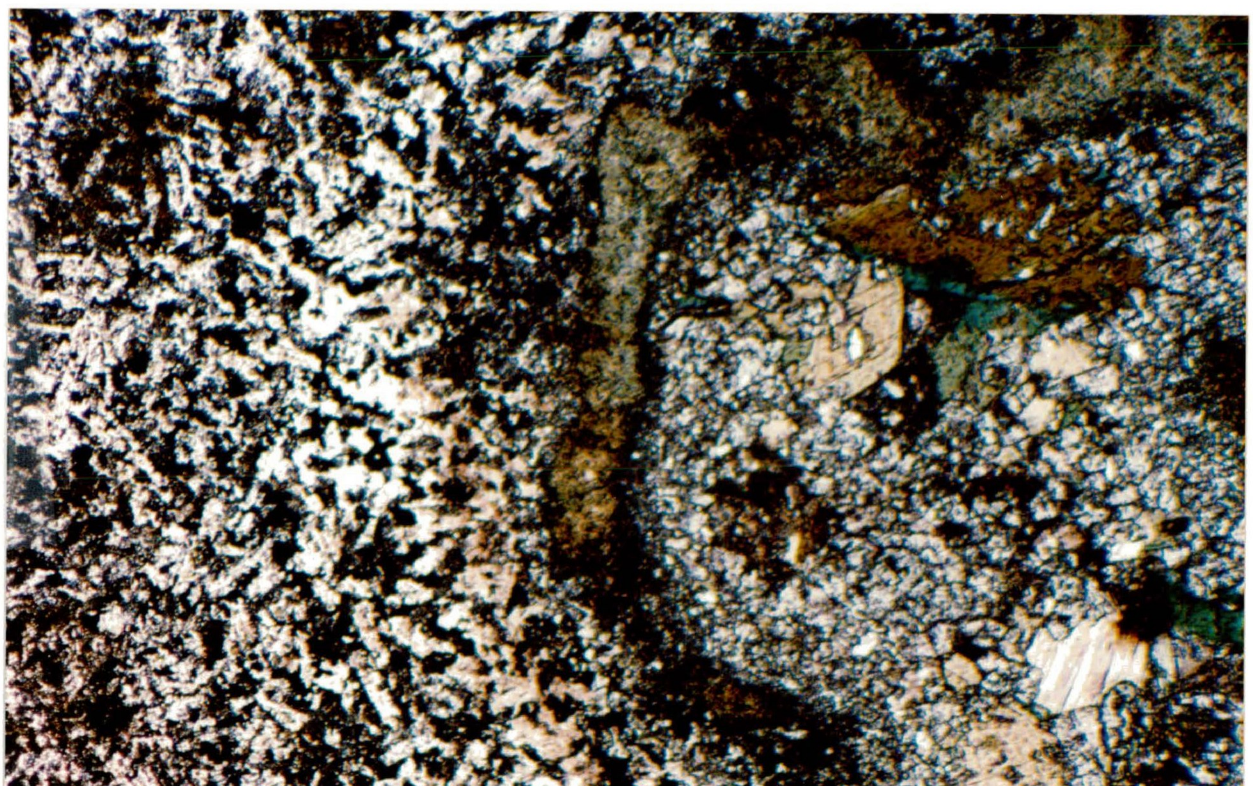

and pyroxene rare. The more common brown-green amphibole can be seen forming rims on pyroxene grains or altering to biotite. The less common blue-green amphibole occurs as zones within the brown-green amphibole.

Pyroxene occurs as isolated granular anhedral crystals or as inclusions within biotite and amphibole. It is pale green in colour and may exhibit slight pleochroism from colourless-to-pale green. Inclusions of opaque phases are commonly present.

Subhedral biotite is pleochroic pale red-brown-to-dark red-brown and pale straw yellow-to-dark red-brown. It occurs as rims to opaque grains and zones within amphibole crystals. Halos around inclusions within biotite crystals are rarely seen.

Apatite occurs as acicular needles within plagioclase and the other major minerals of the xenolith. Anhedral-to-subhedral opaque grains commonly occur as inclusions within amphibole and biotite and may have rims of sphene. They consist mainly of magnetite with exsolved ilmenite. Sulphides are rarely seen. The accessory minerals calcite, fluorite and sphene appear towards syenite contacts where recrystallization has occurred.

Vesicles are seen in few specimens from the megaxenolith and are interpreted to represent the tops of individual flows. Clinopyroxene and amphibole are major constituents (Plate 2.25). Clinopyroxene forms a core of granular crystals which are colourless-to-pale green in colour forming a core which is surrounded by a rim of amphibole. With increasing alteration the vesicles are recrystallized to a mass of randomly-oriented amphibole crystals and biotite. Accessory calcite, fluorite, sphene, opaques and rarely alkali-feldspar occur in recrystallized vesicles. Biotite-rich recrystallized vesicles resemble biotite ovoids (Plate 2.26).

Distinct changes can be seen in the megaxenolith from the interior to the contact with the host Centre 1 syenites. The block grades from a fine grained volcanic rock to a slightly-coarser grained metabasalt as the contact is approached. Pyroxene begins to dissappear as it is replaced by biotite, amphibole and opaques. Plagioclase begins to recrystallize and alkali feldspar growth and replacement of plagioclase occurs. In proximity to the contact with the host syenites plagioclase recrystallization is complete and growth of alkali feldspar, both as crystals in the groundmass and porphyroblasts, is extensive. Accessory calcite, fluorite and sphene are present. Vesicles if present are recrystallized to assemblages of amphibole, biotite and accessory phases.

2.3 Summary of Neys/Ashburton and Wolf Camp Lake

Although different in mineralogical character, the xenoliths of

Plate 2.26 Vesicle in altered xenolith close to host/syenite contact. Amphibole and biotite become more prominent with increasing assimilation. Biotite-rich recrystallized vesicles resemble biotite ovoids.

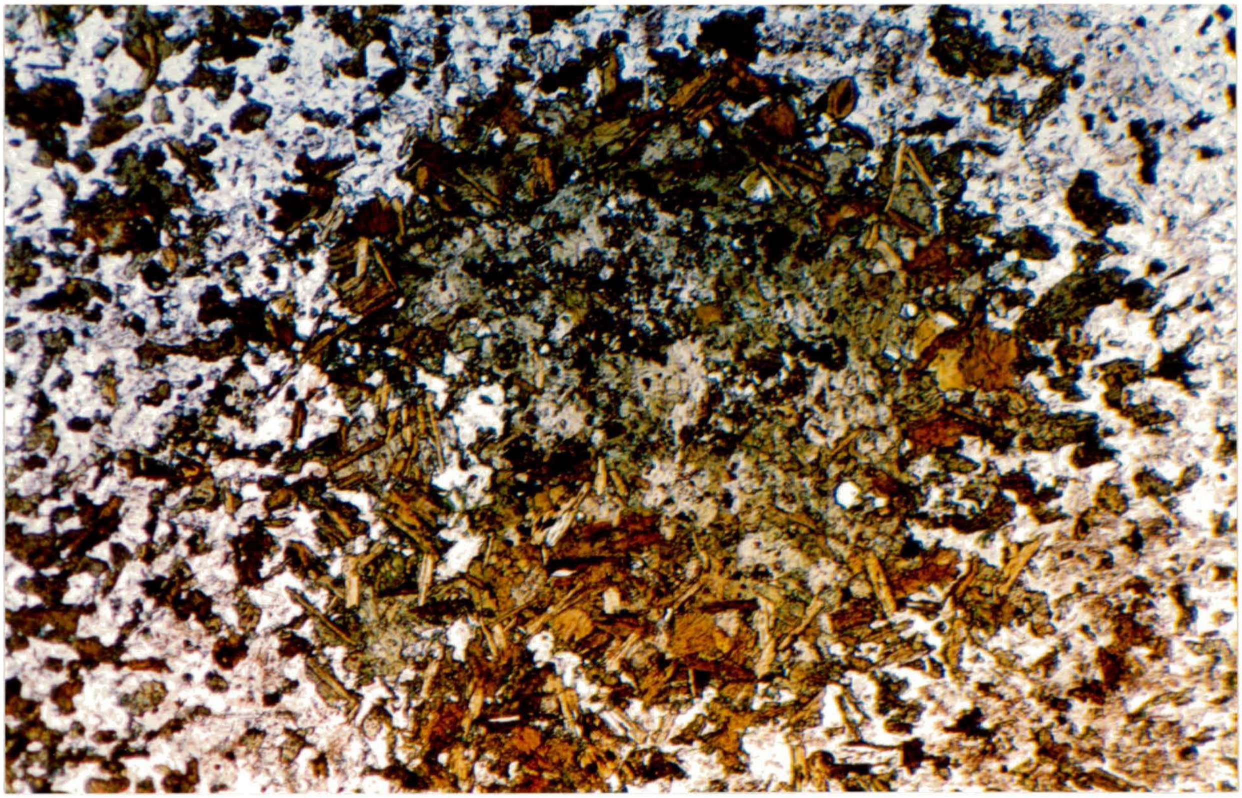

Neys/Ashburton Lookouts and the megaxenolith of Wolf Camp Lake show related effects of being immersed in their host syenitic magmas. With increasing assimilation recrystallization occurs such that plagioclase laths produce a granular mosaic of poorly albite-twinned crystals. As this recrystallization occurs, alkali feldspar forms both in the groundmass and as porphyroblasts. The porphyroblasts begin growth as rims to relict plagioclase phenocrysts. Wolf Camp Lake xenoliths however do not show the development of biotite ovoids that are prevalent in the xenoliths of Neys/Ashburton. Other similarities include the appearance of accessory calcite, fluorite and sphene with increasing assimilation and the formation of biotite. It appears the assimilation process involves the addition of alkalies, iron and volatiles into the xenoliths, the source of these materials being the host syenites.

Chapter Three

Compositional Variation of Amphibole, Pyroxene and Feldspar

3.1 Introduction

Other than the limited data reported by Lukosius-Sanders (1988), little is known of the compositional variation exhibited by amphibole, pyroxene and plagioclase within the xenoliths found in the vicinity of Neys/Ashburton Lookouts. The present study expands on this limited data base and provides new data for the Wolf Camp Lake megaxenolith.

Xenoliths studied ranged from those least-affected by assimilation to those highly-affected to obtain the best possible representation of compositional variations. Specimens were prepared as one inch diameter polished discs and analyzed using a Hitachi 570 scanning electron microscope by energy dispersive analysis. Back scattered electron imagery and x-ray energy spectra were used to identify mineral grains suitable for analysis. Five-to-ten spot analyses were made per thin section. Analytical methods are outlined in Appendix 1.

3.2 Amphibole Compositional Variation

Classification and nomenclature used for the amphiboles are those recommended by the IMA subcomittee on amphiboles (Leake, 1978). Structure formulae were calculated on the basis of 23 oxygens with cations allocated to structural sites according to the standard formula of $A_{0-1}X_2Y_5Z_8O_{22}(OH,F,Cl)_2$. Ferric iron contents were calculated on a stoichiometric basis using the method proposed by Droop (1978). A complete list of amphibole compositions is given in Appendices 2, 3 and 4.

Figures 3.1, 3.2 and 3.3 are classification diagrams for amphiboles from xenoliths in the Neys/Ashburton study area. The compositions of amphiboles found in the ferro-edenite syenite and contaminated ferro-edenite syenite (Lukosius-Sanders, 1988) are plotted for comparison. Figure 3.4 is an amphibole classification diagram for amphiboles in the Wolf Camp Lake megaxenolith with amphiboles from host syenites plotted for comparison.

3.2.1 Neys/Ashburton

All amphiboles from xenoliths in the Neys/Ashburton study area are calcic and exhibit a wide range of composition, ranging from magnesian hastingsite and ferroan pargasitic hornblende to ferro-edenite and ferro-actinolite to ferro-hornblende. In Figures 3.1 and 3.2 there occurs a cluster of points in the compositional fields of ferroan pargasitic hornblende and magnesian hastingsite respectively. From these clusters, points spread with increasing Si contents and near-constant magnesium

FIGURE 3.1 NEYS LOOKOUT / ASHBURTON AMPHIBOLE COMPOSITIONS

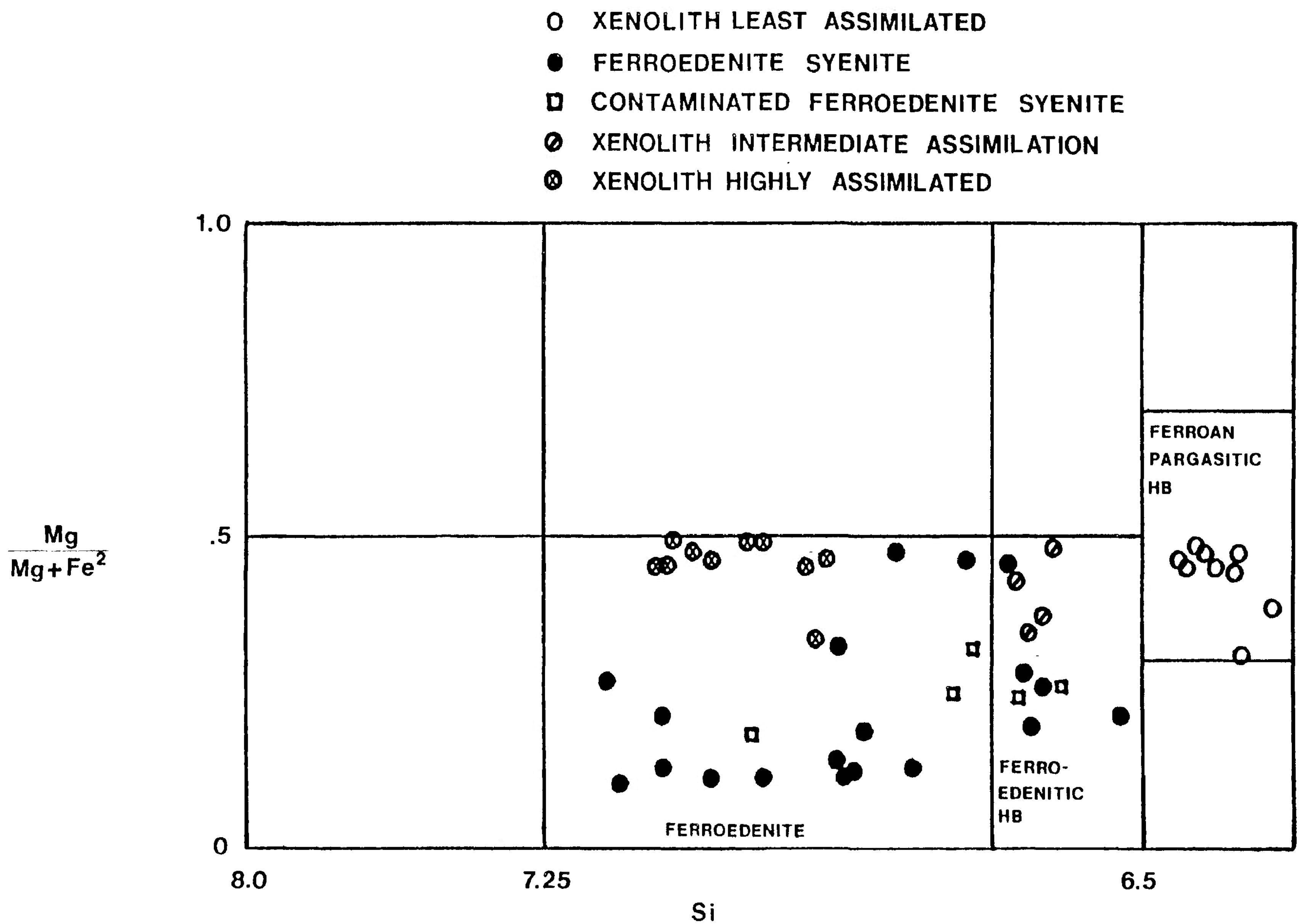

$(Na+K)_A > .5$; $Ti < .5$; $Fe^3 \leq Al^6$

FIGURE 3.2 NEYS LOOKOUT / ASHBURTON
AMPHIBOLE COMPOSITIONS

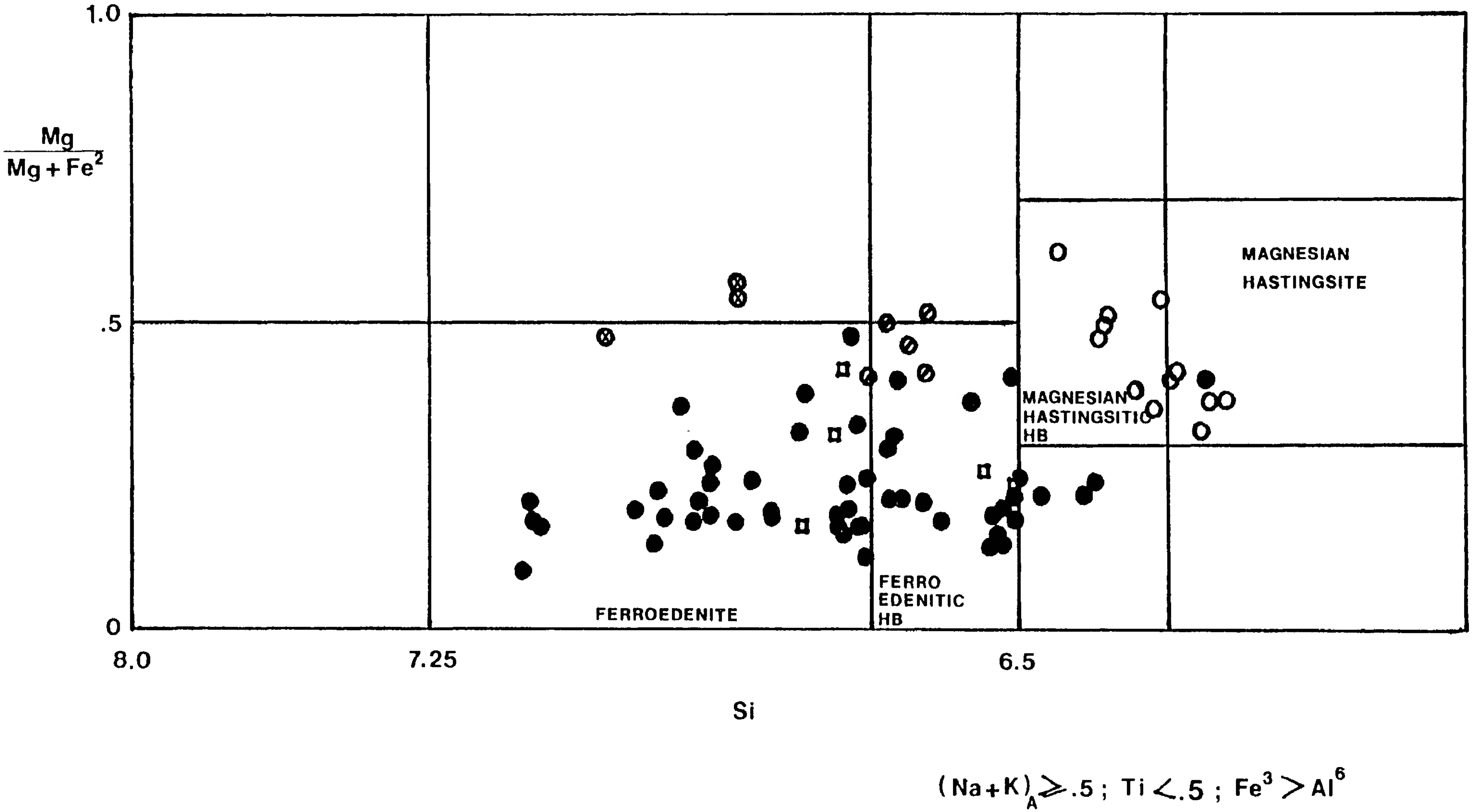

FIGURE 3.3 NEYS LOOKOUT/ASHBURTON
AMPHIBOLE COMPOSITIONS

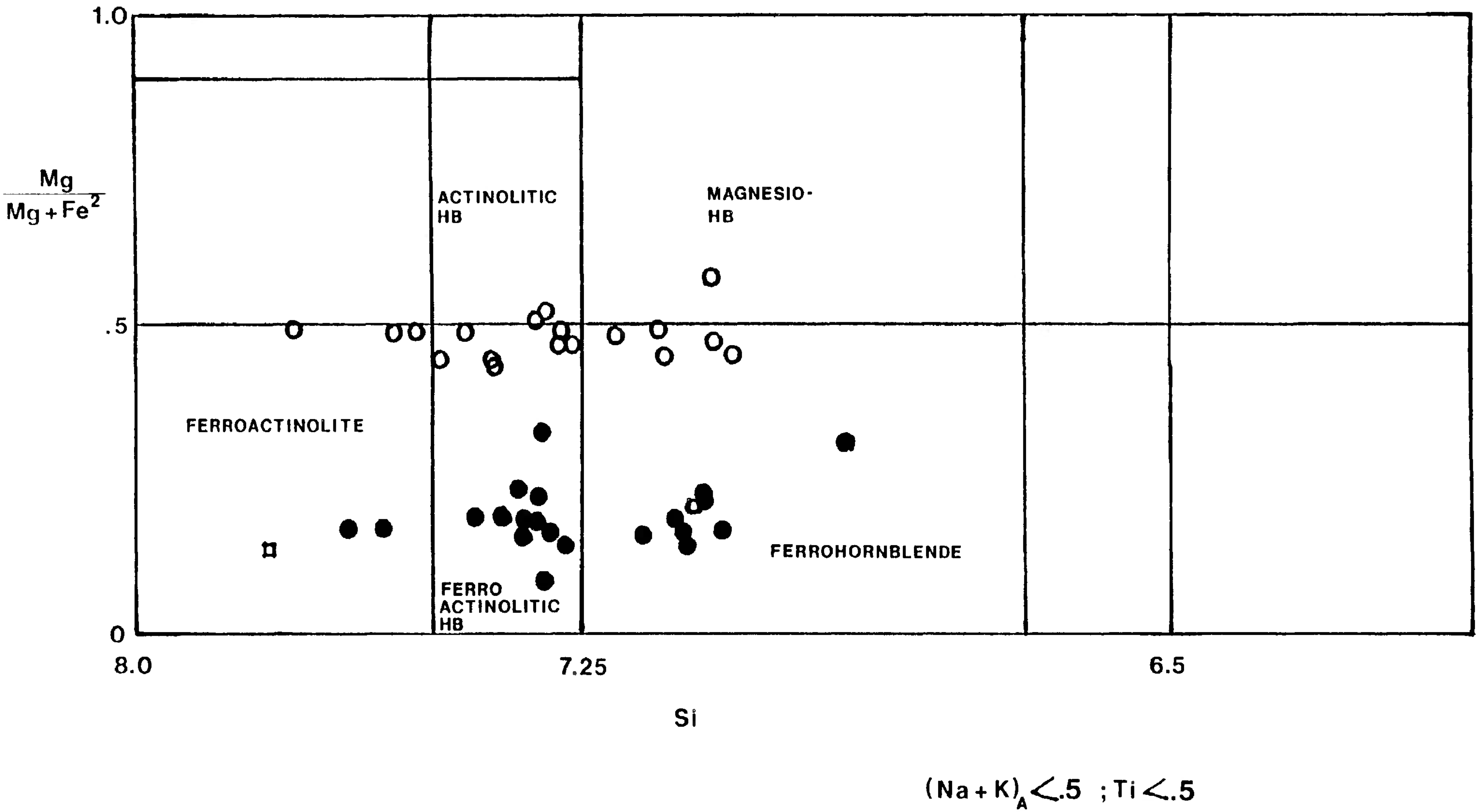

FIGURE 3.4 WOLF CAMP LAKE
AMPHIBOLE COMPOSITIONS

O XENOLITH
● HOST SYENITE

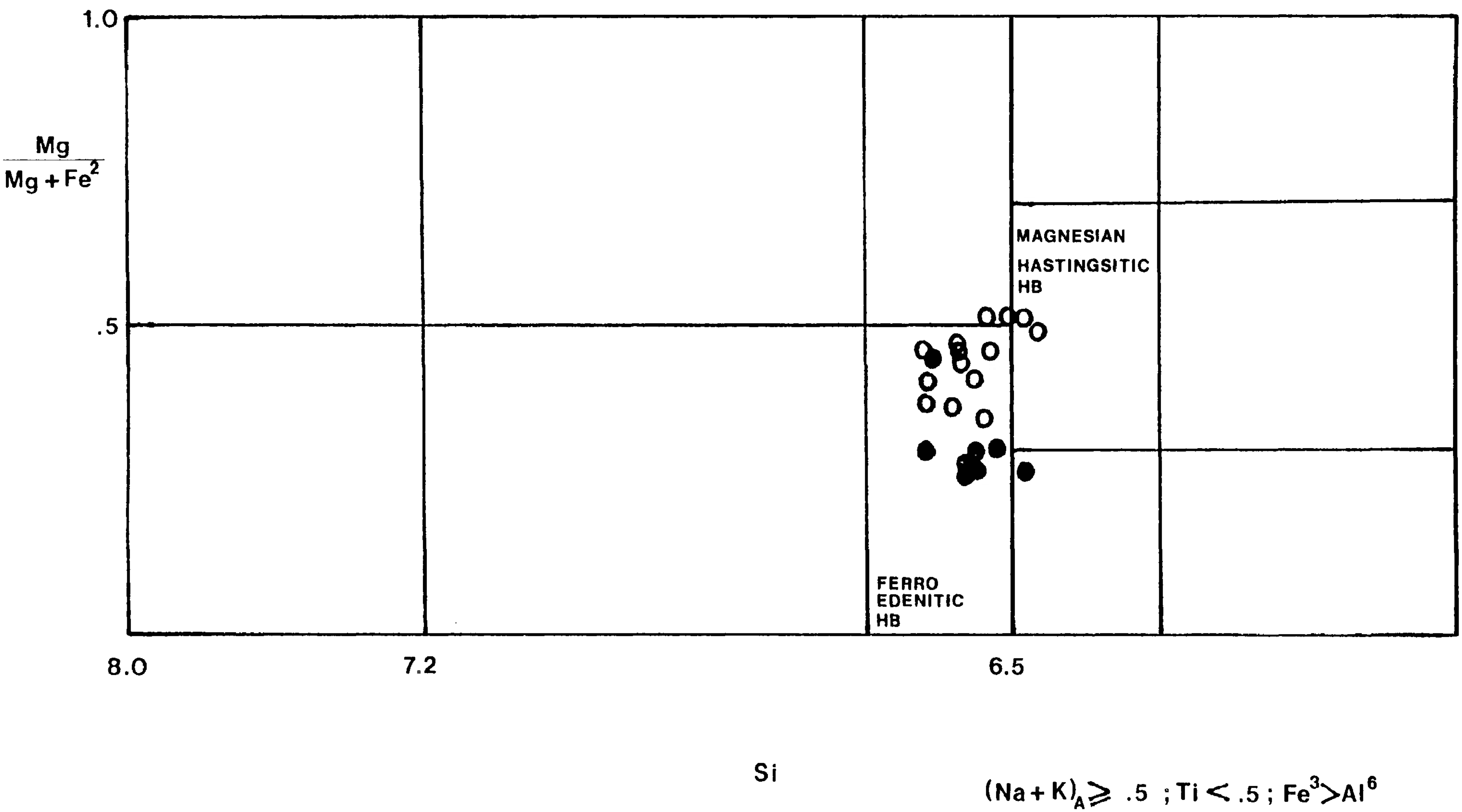

numbers into the ferro-edenite compositional fields. Figure 3.3 shows a considerable scatter of points ranging from ferro-actinolite to ferro-hornblende with near-constant magnesium numbers. Amphibole compositions are similiar to those of the ferro-edenite syenite and contaminated ferro-edenite syenite, except that they have higher amounts of Mg compared to the host syenite amphiboles, with magnesium numbers being 20 to 30 percent higher. This is due to the xenoliths being more magnesium-rich than the syenites. Amphibole formation in the xenoliths involves the replacement of magnesium-rich pyroxenes, and this is in turn is reflected in the composition of the amphibole.

Lukosius-Sanders (1988) reports that groundmass amphiboles replacing pyroxene are ferroan pargasitic hornblende, ferro-actinolitic hornblende and ferro-edenite. Amphibole in biotite ovoids is ferro-edenite or ferro-edenitic hornblende and is more highly evolved than the other amphiboles in the xenoliths as it has higher Si contents.

Amphibole compositions in the xenoliths reflect the degree of assimilation. As the amount of assimilation increases, amphibole compositions become more evolved and exhibit increasing Si contents. This is illustrated in the compositional diagrams (Figure 3.1 to 3.3) which show that Si increases from a low of 6.5 cations per unit cell to a high of around

7.7 cations per unit cell.

3.2.2 Wolf Camp Lake

Amphibole compositions do not show an extensive range of compositional variation (Figure 3.4). They plot in the ferro-edenite hornblende region with minor overlap into edenitic hornblende and hastingsitic hornblende. Amphibole is generally only found in those specimens located near contacts with the host syenites, where assimilation effects are most pronounced. Figure 3.4 shows that the xenolithic amphiboles compositions are slightly more magnesion than amphiboles in host syenite.

3.2.3 Discussion of Amphibole Compositions

In each case, amphibole compositions in the xenoliths are found to extend over the same range of amphibole compositions as found in their syenite hosts, except for those xenoliths least affected by the assimilation process. This is seen for Neys/Ashburton xenoliths (Figures 3.1 and 3.2). On these figures there occurs a cluster of points in the compositional fields of ferroan pargasitic hornblende and magnesian hastingsite respectively with no corresponding amphiboles in the host syenites. These amphibole compositions represent the initial amphibole formed in the xenoliths at the expense of pyroxene. From these clusters, points spread with increasing Si contents and near-constant magnesium numbers to amphiboles corresponding to host syenite amphiboles.

Development of amphibole occurs in the xenoliths because it is the liquidus phase of the host syenite magma. The magma equilibrates with the xenolith and forms within it the mineral phase in which it is saturated. Hence the similarity in composition between xenolith and host amphiboles. Xenolith amphiboles are more magnesian due to the xenolith being more magnesium-rich than the syenite. The range of amphibole compositions is due partly to the various degree of assimilation of the xenoliths studied and evolution of amphiboles in the host syenites. The longer a xenolith is within a syenite magma, the more assimilated it will become and the more evolved the amphiboles become as they equilibrate to those amphiboles in the syenite.

In the case of the Wolf Camp Lake xenoliths, amphibole is only found in proximity to the contacts with host syenites and as such does not show the compositional variation displayed by those amphiboles in Neys/Ashburton xenoliths. This amphibole has only a limited range of composition as the host syenites contain amphibole of limited compositional variation.

3.3 Pyroxene Compositional Variation

Classification and nomenclature used for pyroxene is that proposed by Morimoto (1989). The accuracy of the microprobe analyses was checked by calculating their stiochiometry on the basis of 6 oxygens. End member molecular components were calculated using an APL program "STRUCTURE" (Mitchell, unpublished). A complete list of pyroxene analyses is presented in Appendices 5, 6 and 7.

3.3.1 Neys/Ashburton

Pyroxene is not a common constituent of the xenoliths and few suitable crystals were found for analysis. Figures 3.5 and 3.6 are compositional plots for pyroxene in xenoliths from the Neys/Ashburton study area. All are clinopyroxenes that show little compositional variation. They are classified as augites and diopsides. Sodium was typically not detectable, although some examples do contain up to 1 wt % Na_2O. When compared to host syenites xenolith pyroxenes are deficient in both TiO_2 and Na_2O.

Xenolith pyroxene compositions are notably-different from those reported by Lukosius-Sanders (1988) in that they contain significantly-less TiO_2 and Na_2O. Data reported by Lukosius-Sanders is plotted on the acmite: Ti-pyroxene: CATS diagram (Figure 3.8). They contain TiO_2 up to a few weight % and Na_2O between 2 and 2.2 weight %. Pyroxenes in this study contain a trace-to-nil TiO_2 and a trace-to-nil Na_2O. Al_2O_3 contents of

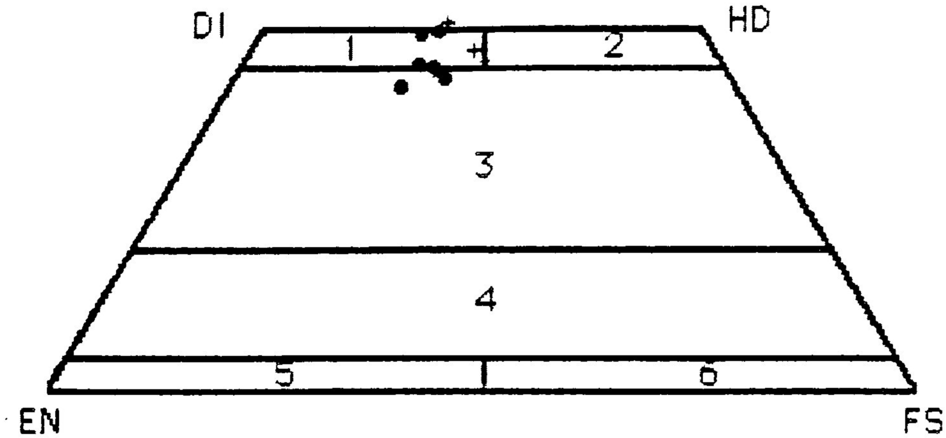

1. DIOPSIDE
2. HEDENBERGITE
3. AUGITE
4. PIGEONITE
5. ENSTATITE
6. FERROSILITE

FIGURE 3.5 PYROXENE COMPOSITIONS FOR C2358(+) AND C2490(•).

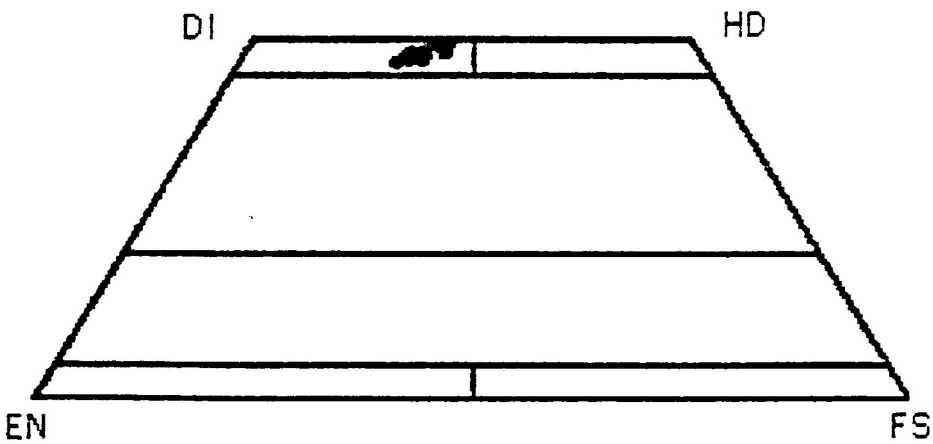

FIGURE 3.6 PYROXENE COMPOSITIONS FOR C2498.

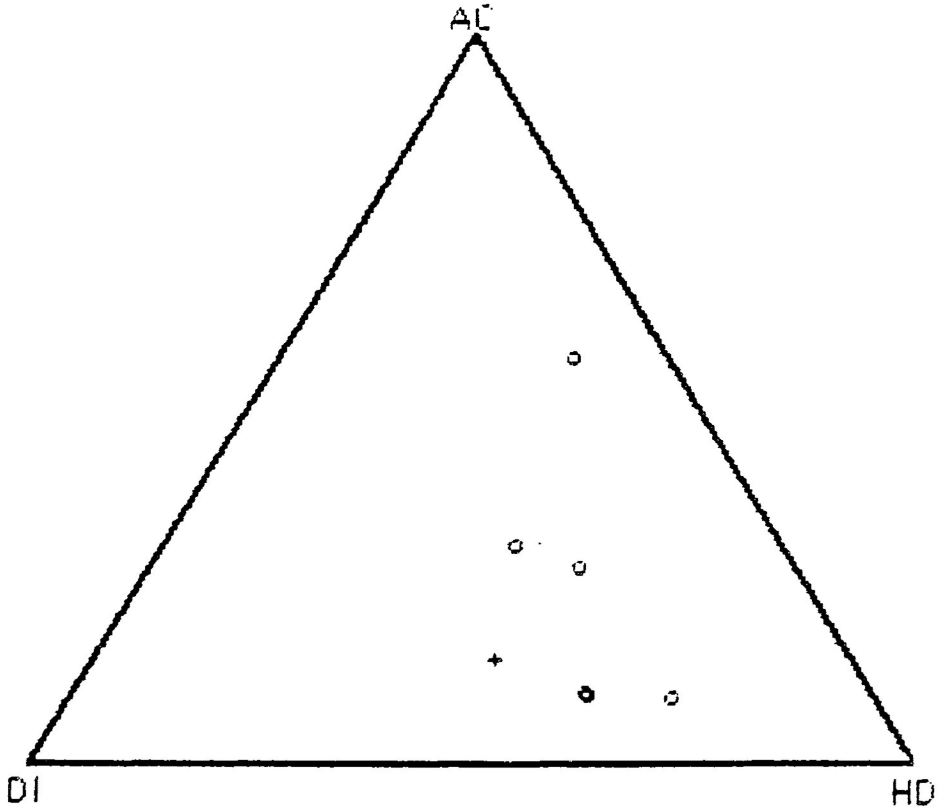

FIGURE 3.7 PYROXENE COMPOSITIONS FOR FERROEDENITE SYENITE(o) AND XENOLITHS(+).

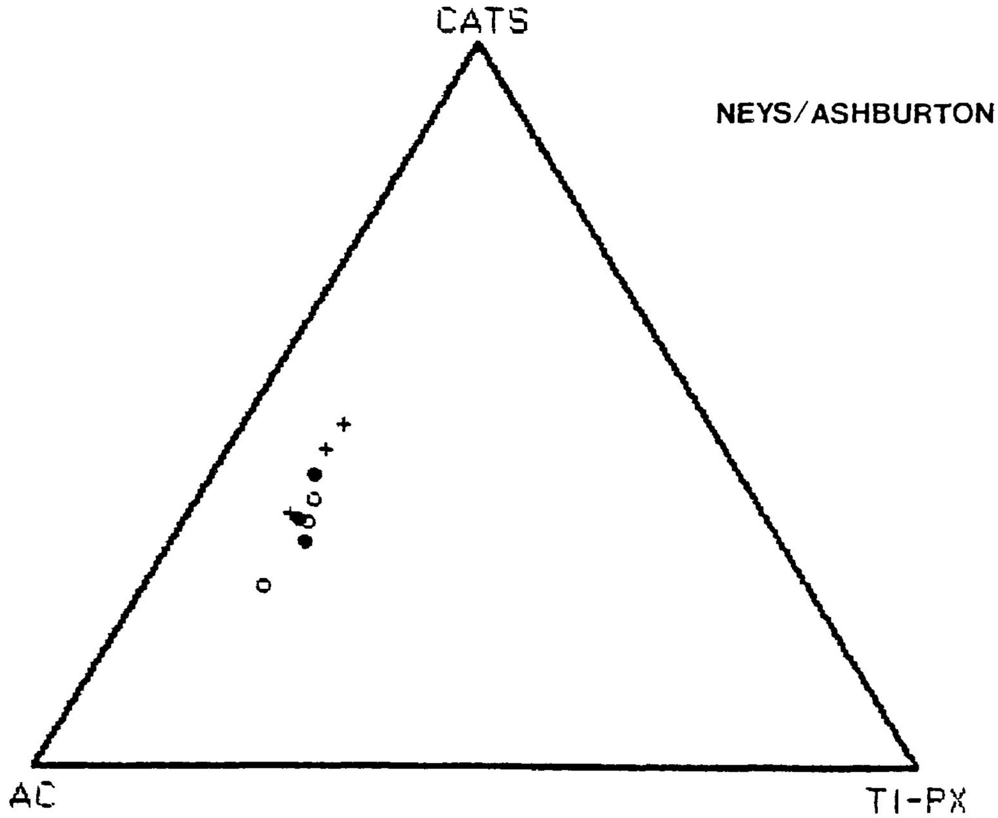

FIGURE 3.8 PYROXENE COMPOSITIONS FOR FERROEDENITE SYENITE(o), CONTAMINATED FERROEDENITE SYENITE(•) AND XENOLITHS(+).

pyroxenes found in this study are also low in comparison to pyroxenes reported by Lukosius-Sanders (1988). Pyroxene compositions reported by Lukosius-Sanders (1988) represent one volcanic xenolith, so little significant comparison is possible.

3.3.2 Wolf Camp Lake

Pyroxene compositions for the Wolf Camp Lake megaxenolith are plotted on Figures 3.9, 3.10 and 3.11. They show the same limited compositional range as Neys/Ashburton pyroxenes. The xenolith C3120 is atypical in that ferrosilite is present in addition to clinopyroxene (Figure 3.12). This indicates that at least some portions of the megaxenolith have possibly undergone effects of contact metamorphism and therefore may be described as a hornfels. It was found that pyroxenes in recrystallized vesicles are clinopyroxene of the same composition as the pyroxene in the groundmass.

Host syenite pyroxene compositions are plotted on Figures 3.13 and 3.14. They are different from those pyroxenes in the megaxenolith in that they contain an appreciable acmite component and thus plot in the acmite: diopside: hedenbergite diagram. Sodium contents range from 1.5 weight % to 5 weight % Na_2O. TiO_2 is present in only trace amounts. Host syenite pyroxenes are also considerably enriched in FeO and moderately enriched in

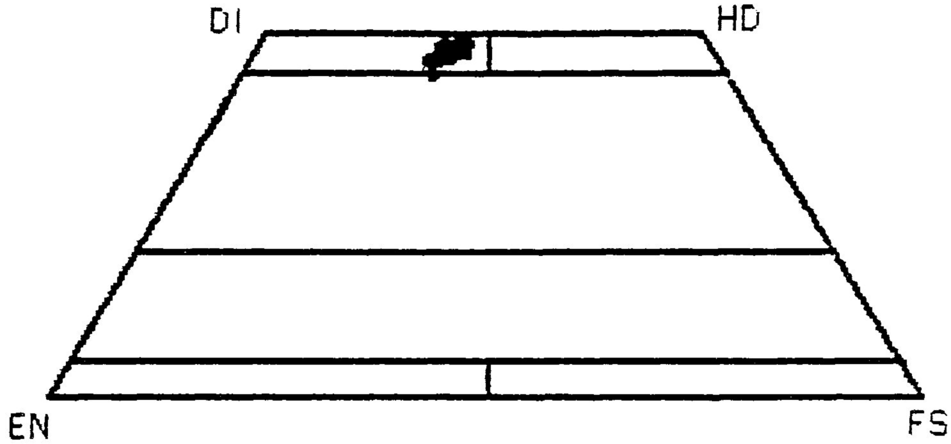

FIGURE 3.9 PYROXENE COMPOSITIONS FOR C2531A.

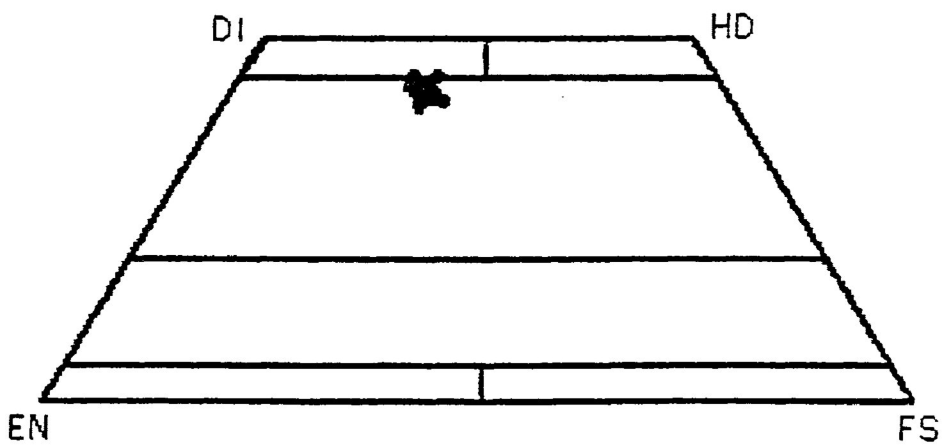

FIGURE 3.10 PYROXENE COMPOSITIONS FOR C3122.

WOLF CAMP LAKE MEGAXENOLITH

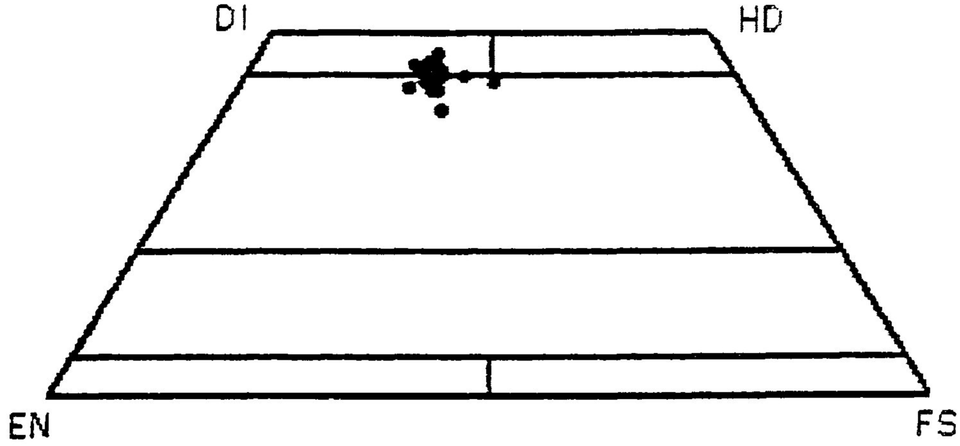

FIGURE 3.11 PYROXENE COMPOSITIONS FOR C3123.

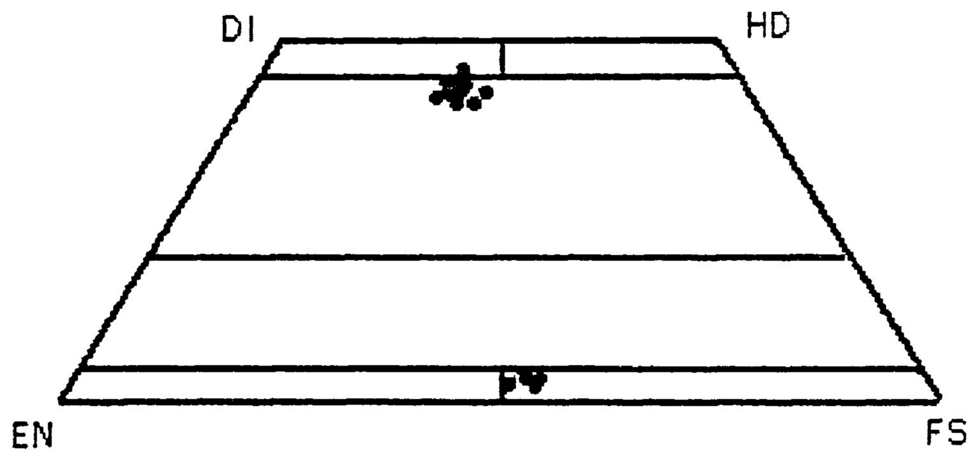

FIGURE 3.12 PYROXENE COMPOSITIONS FOR C3120.

WOLF CAMP LAKE MEGAXENOLITH

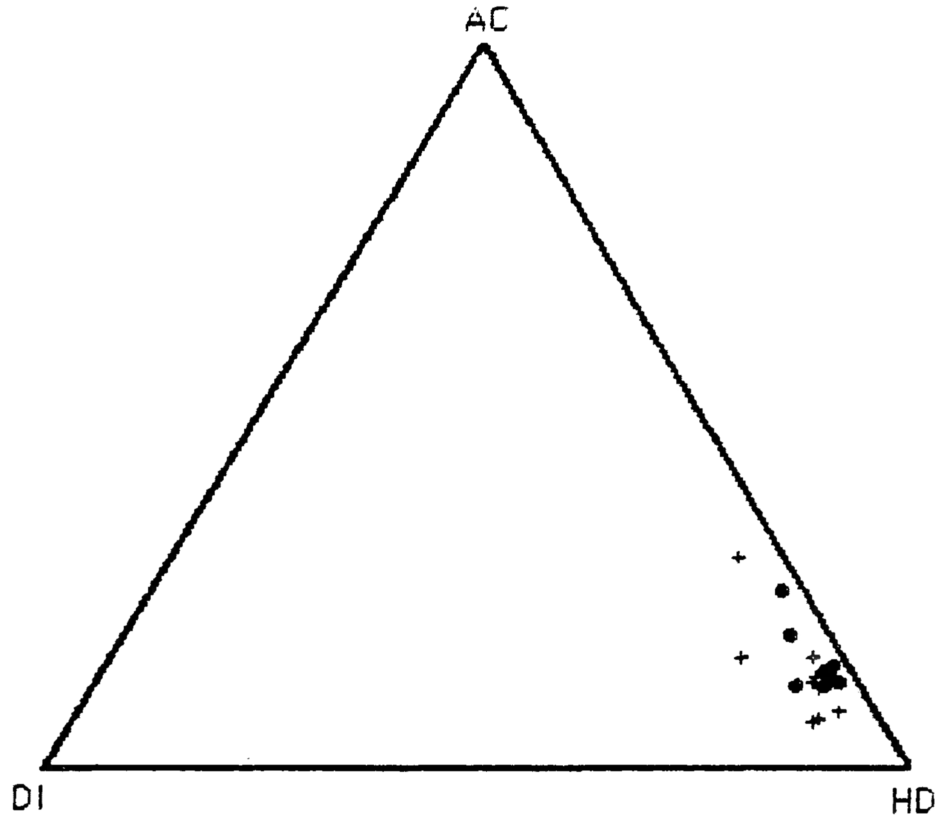

FIGURE 3.13 PYROXENE COMPOSITIONS FOR C2515(+) AND C2516(•).

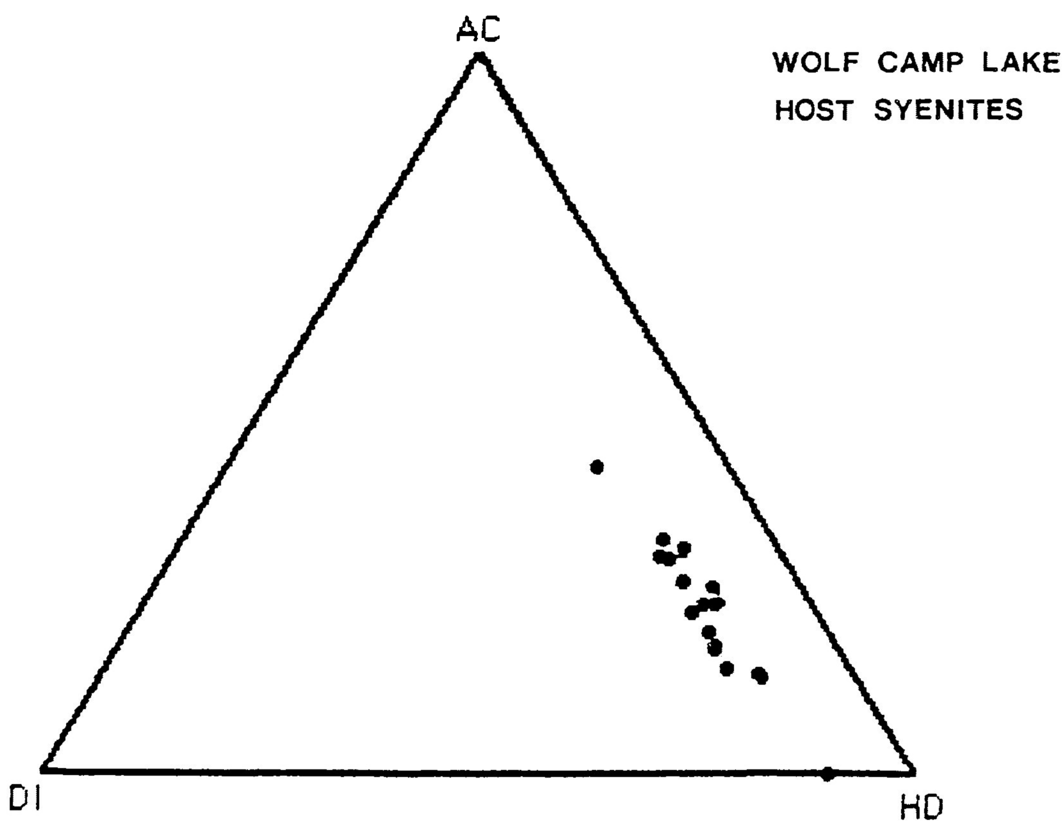

FIGURE 3.14 PYROXENE COMPOSITIONS FOR C2531A.

CaO with respect to xenolith pyroxene compositions. No useful comparison is possible between host and xenolith pyroxene.

3.3.3 Discussion of Pyroxene Compositional Variation

Pyroxenes from both the Neys/Ashburton study area and Wolf Camp Lake have similiar compositions. They also have very different compositions from pyroxenes found in their respective host syenites. This is due to pyroxene in the xenoliths being converted to amphibole early in the assimilation process. As a result no equilibrium is set up between xenolith pyroxenes and liquidus pyroxenes in the host syenites. The amphibole mantle does not allow the host syenite magma to equilibrate with the xenolith pyroxenes.

The pyroxenes however supply information as to the nature of the parental volcanic rocks. This is due to their being relict phases.

Leterrier et al. (1982) devised a method based on statistical study of Ti, Cr, Ca, Al and Na contents of calcic clinopyroxenes which identifies the magmatic affinities of the volcanic rocks within which the clinopyroxenes exist. This method was applied successfully to volcanic rocks which had undergone metamorphism or metasomatism. Magmatic affinities are claimed to be distinguished with better than 80% confidence.

Figure 3.15 is a series of plots based upon the Leterrier et al. (1982)

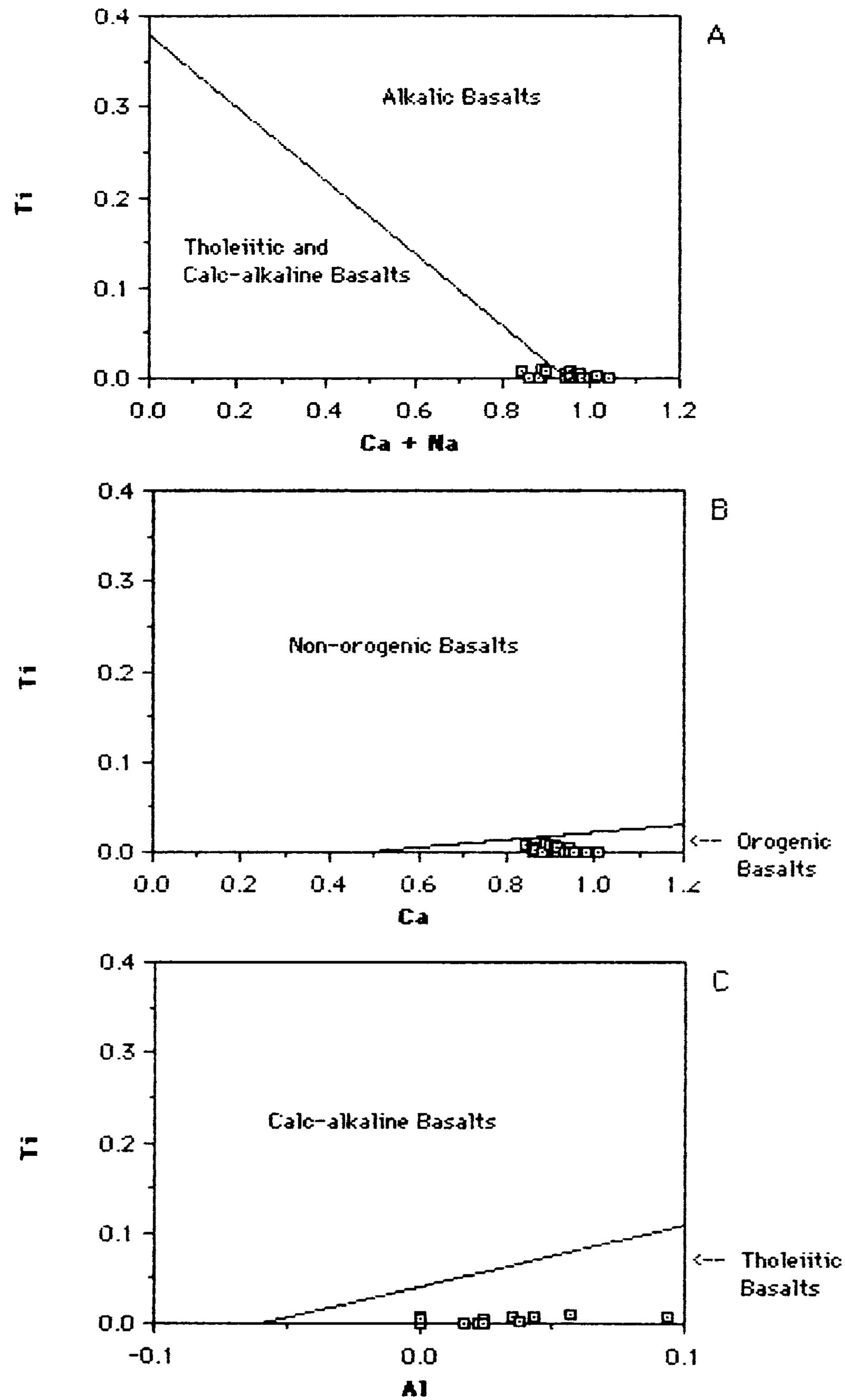

Figure 3.15 Characterization of magmatic parentage for Neys/Ashburton xenoliths from clinopyroxene compositions. After LeTerrier et al, 1982.

method for pyroxene compositions fom Neys/Ashburton xenoliths. Figure 3.15A distinguishes between alkali and tholeiitic plus calc-alkaline basalts. Neys/Ashburton pyroxenes plot stradling the division between the two fields. This could be interpreted as indicating that two xenolith types present at Neys/Ashburton, one a tholeiite and the other an alkali basalt. It may also reflect the addition of sodium to pyroxene in the earliest stages of assimilation.

Figure 3.15B indicates that the source rocks for the xenoliths are orogenic basalts in origin. This is incorrect given the tectonic setting of the Coldwell Complex (Chapter 1). Clinopyroxenes in Neys/Ashburton xenoliths contain less TiO_2 than is needed to plot their compositions into the correct field of non-orogenic basalts. This is due to their evolved nature as clinopyroxenes of tholeiitic basalts decrease TiO_2 contents with fractionation (Deer et al. 1978). Figure 3.15C distinguishes between tholeiites and calc-alkaline basalts from Figure 3.15A. This diagram indicates a definite tholeiitic parentage for Neys/Ashburton xenoliths.

Figure 3.16 applies the method of Leterrier et al (1982) to pyroxene compositions from Wolf Camp Lake. Figure 3.16A indicates the volcanics are not alkali basalts but either tholeiitic or calc-alkaline. Figure 3.16B

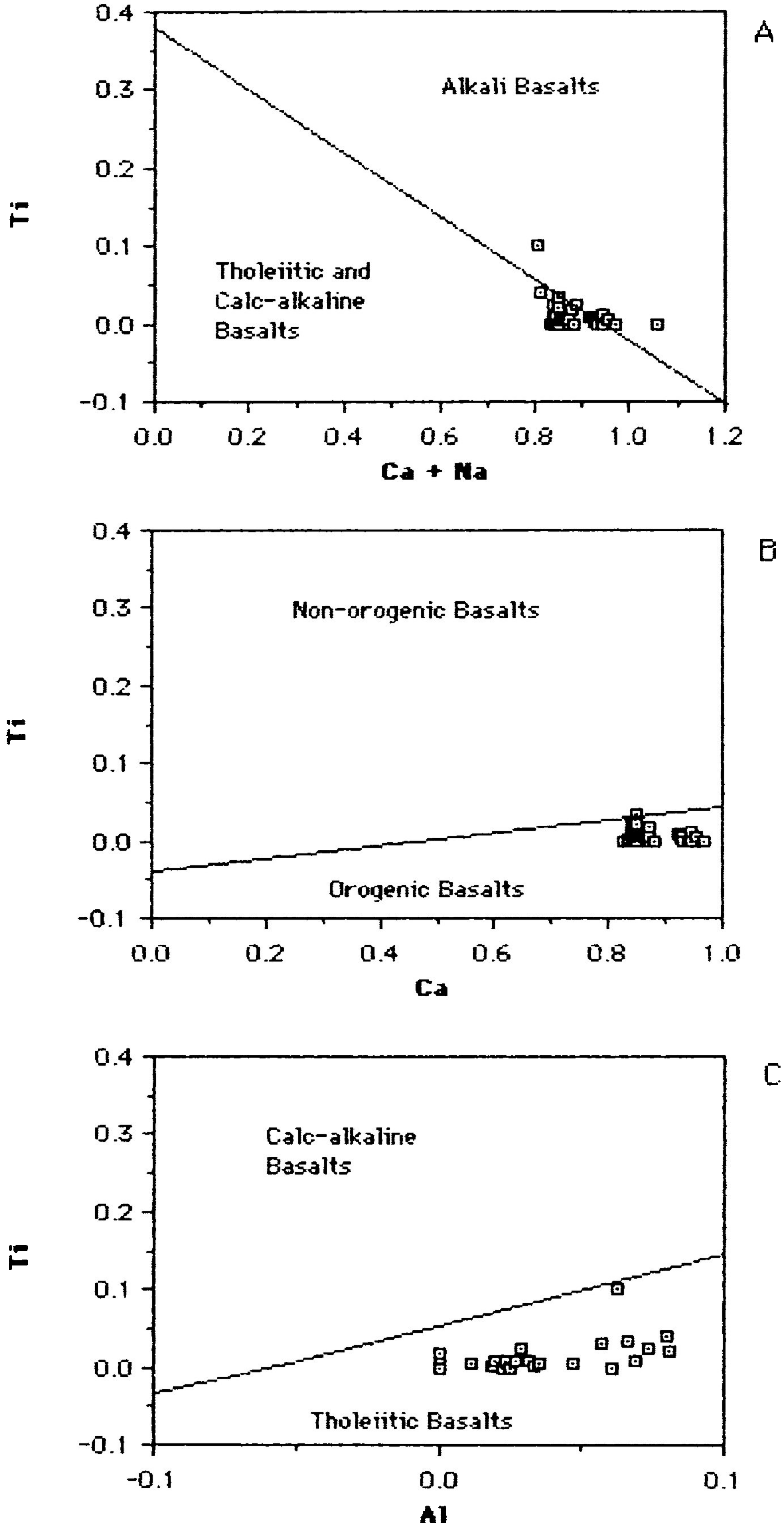

Figure 3.16 Characterization of magmatic parentage for the Wolf Camp Lake megaxenolith from clinopyroxene compositions. After LeTerrier et al, 1982.

indicates incorrectly an orogenic origin for the source volcanics, given the Coldwell Complex tectonic setting. Again low TiO_2 contents of the pyroxenes indicate an evolved nature, such as those in Neys/Ashburton xenoliths. Figury 3.16C indicates a definite tholeiitic affinity for the source volcanics at Wolf Camp Lake.

TiO_2 and Al_2O_3 contents of the pyroxenes for both Neys/Ashburton and Wolf Camp Lake volcanics indicate a tholeiitic basalt parent. It has been documented that clinopyroxenes from undersaturated volcanic rocks, such as alkali olivine basalts, are high in initial TiO_2 and Al_2O_3 and with fractionation of these rock types TiO_2 and Al_2O_3 contents increase (Magonthier and Velde, 1976). Lowdes (1973) concludes also from study of Late Cenozoic basalts in Utah that Al increases in clinopyroxene with increase in fractionation of alkaline basalts. It was also concluded that for tholeiitic basalts, Al shows the opposite trend and decreases with increasing fractionation. Clinopyroxenes for Neys/Ashburton and Wolf Camp Lake contain very little to no TiO_2 and Al_2O_3, indicating fractionation from a tholeiitic basalt, with the small amounts indicating a tholeiitic basalt in an evolved state.

Olivine and/or its alteration products are not seen in either Neys/Ashburton or Wolf Camp Lake xenoliths. This suggests that the basalt was not an alkali olivine basalt, giving credence to the conclusions from pyroxene compositional data.

3.4 Feldspar Compositional Data

Structural formulae and end member molecular components were determined on the basis of 32 oxygens using the feldspar subroutine of the "STRUCTURE" computer program (Mitchell, unpublished). Complete analytical data are presented in Appendices 8 and 9.

3.4.1 Neys/Ashburton

Figures 3.17 through 3.22 illustrate feldspar compositional variation in xenoliths from the Neys/Ashburton area. The compositions of both plagioclase and alkali feldspar reflect the degree of assimilation of the xenoliths.

In sections that appear to be least-affected by assimilation, plagioclase is calcic with compositions up to An_{75}, although on average they lie between An_{40-70} (andesine-labradorite). With increasing assimilation, plagioclase compositions become increasingly-sodic and trend towards more albitic compositions. Highly assimilated xenoliths have plagioclase

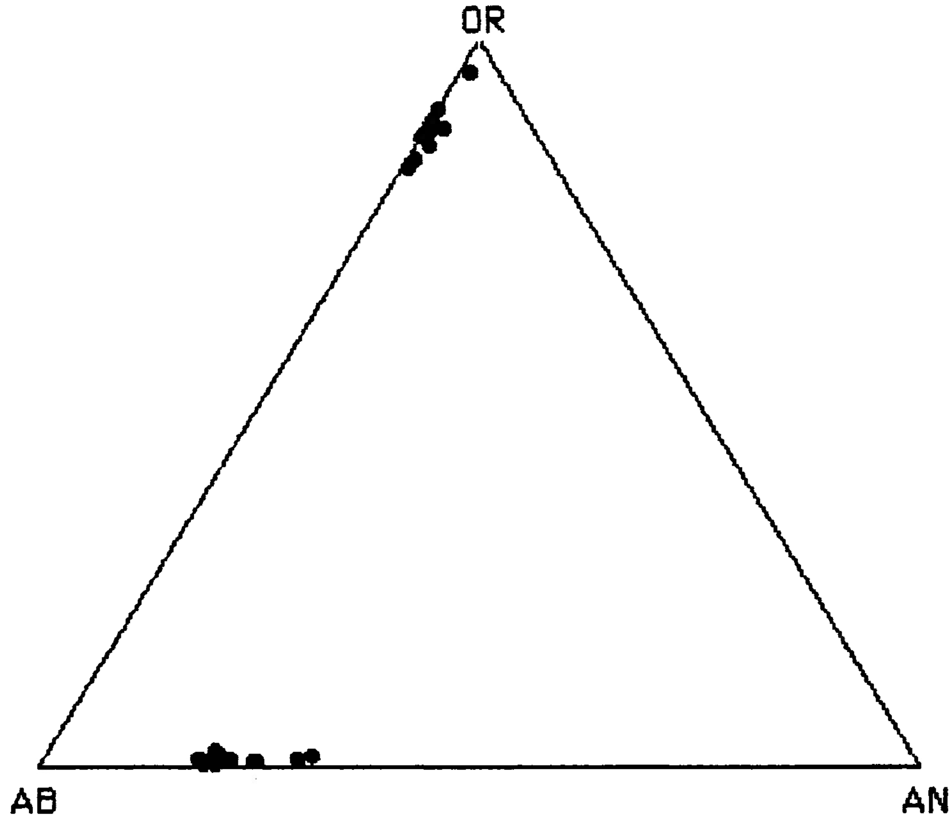

FIGURE 3.17 PLAGIOCLASE COMPOSITIONS FOR C2358.

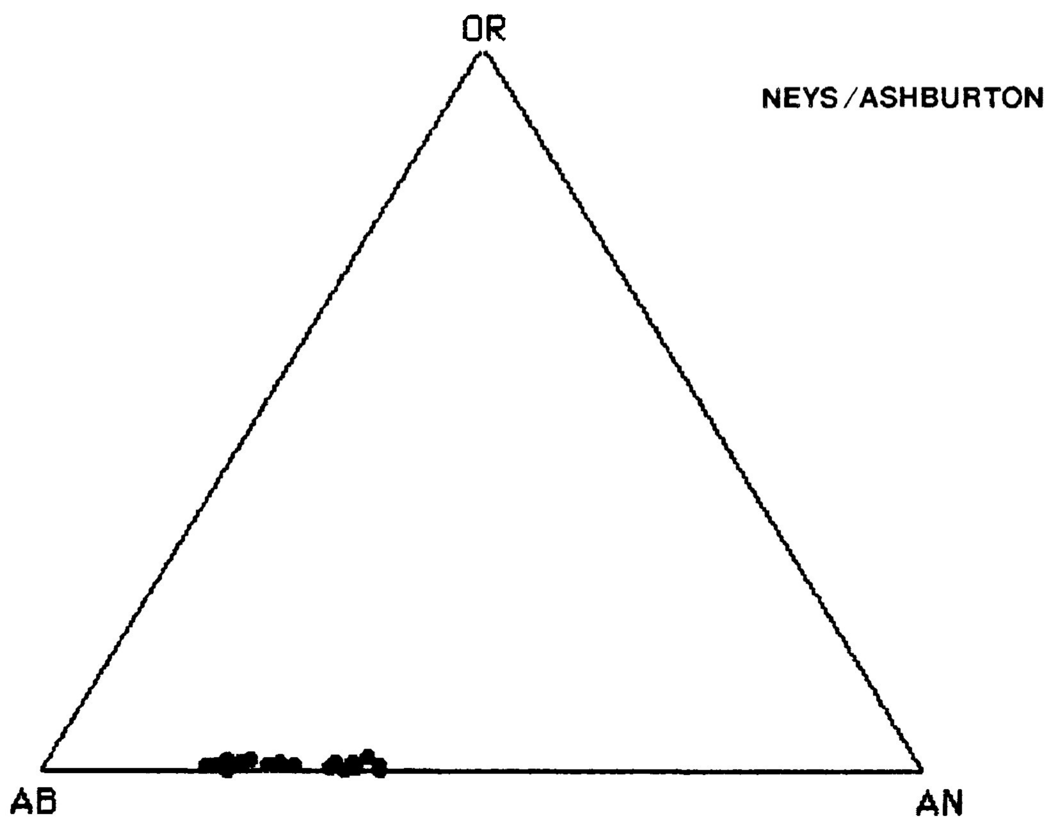

FIGURE 3.18 PLAGIOCLASE COMPOSITIONS FOR C2510.

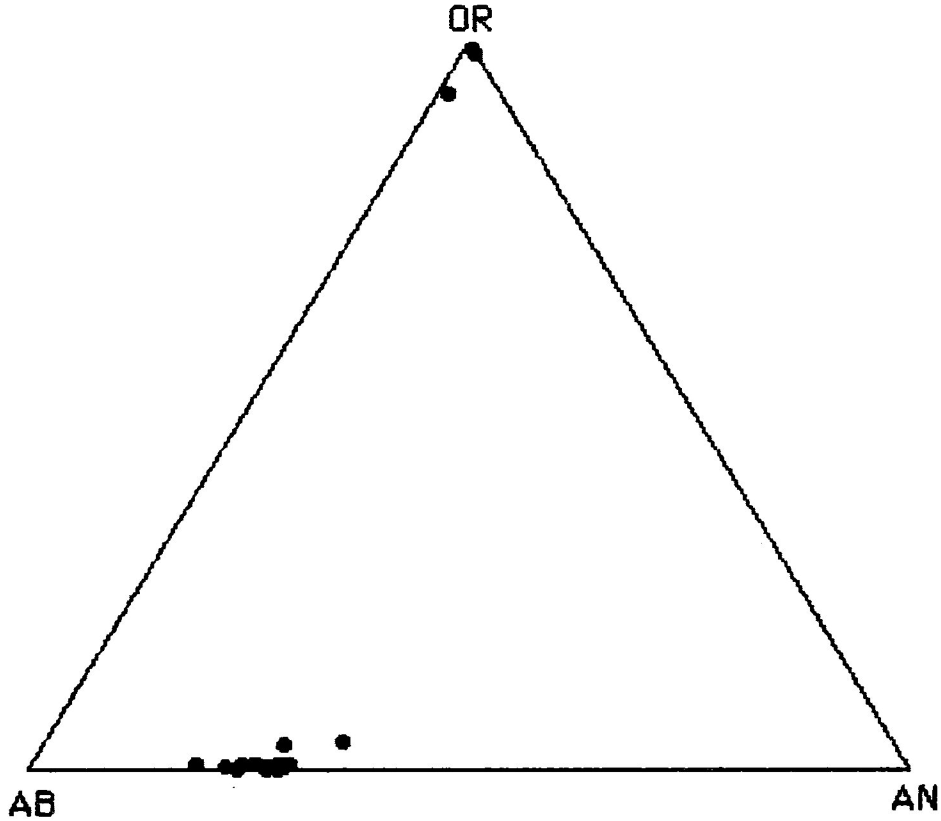

FIGURE 3.19 PLAGIOCLASE COMPOSITIONS FOR C2498.

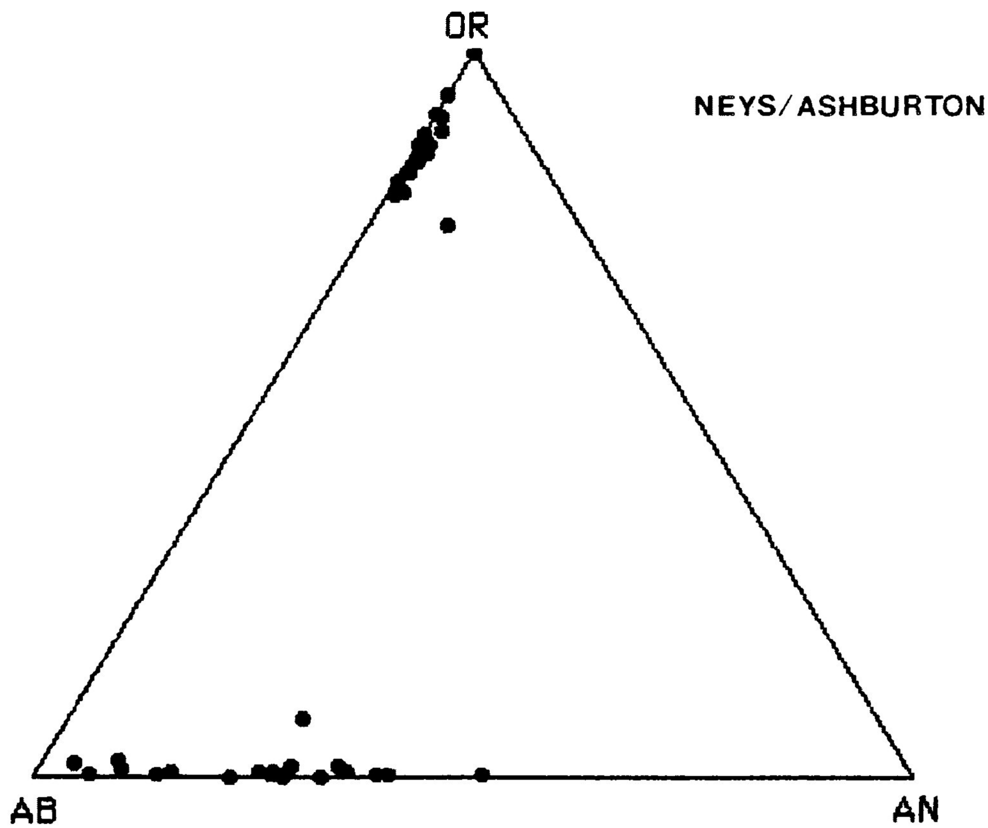

FIGURE 3.20 PLAGIOCLASE COMPOSITIONS FOR C2331.

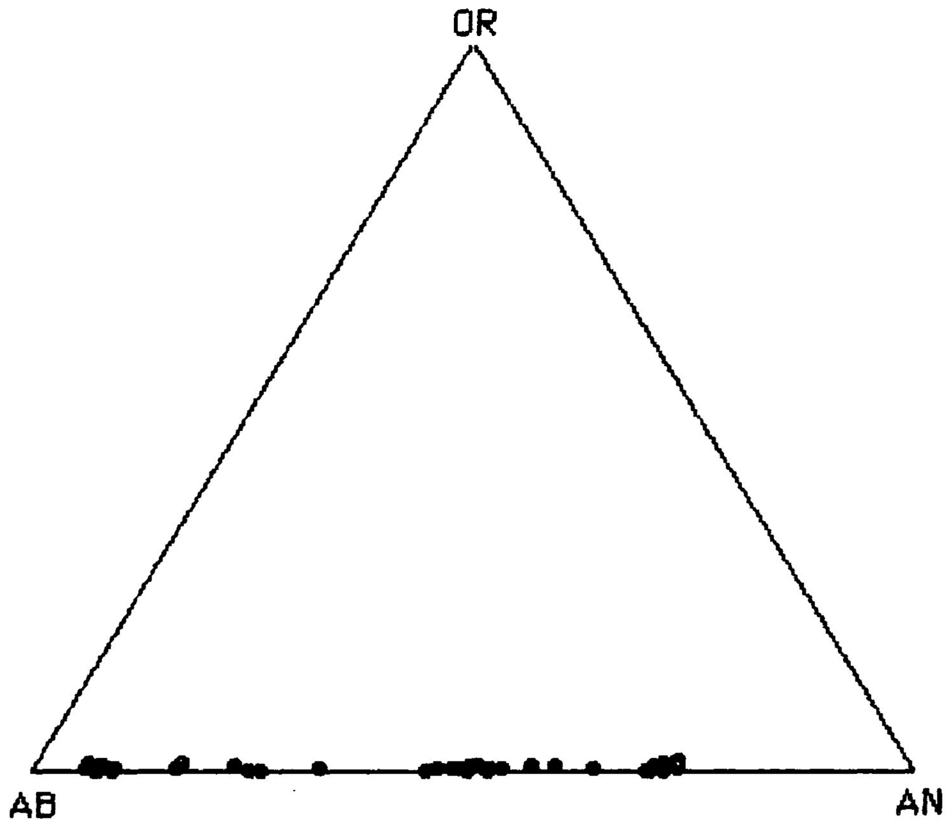

FIGURE 3.21 PLAGIOCLASE COMPOSITIONS FOR C2490.

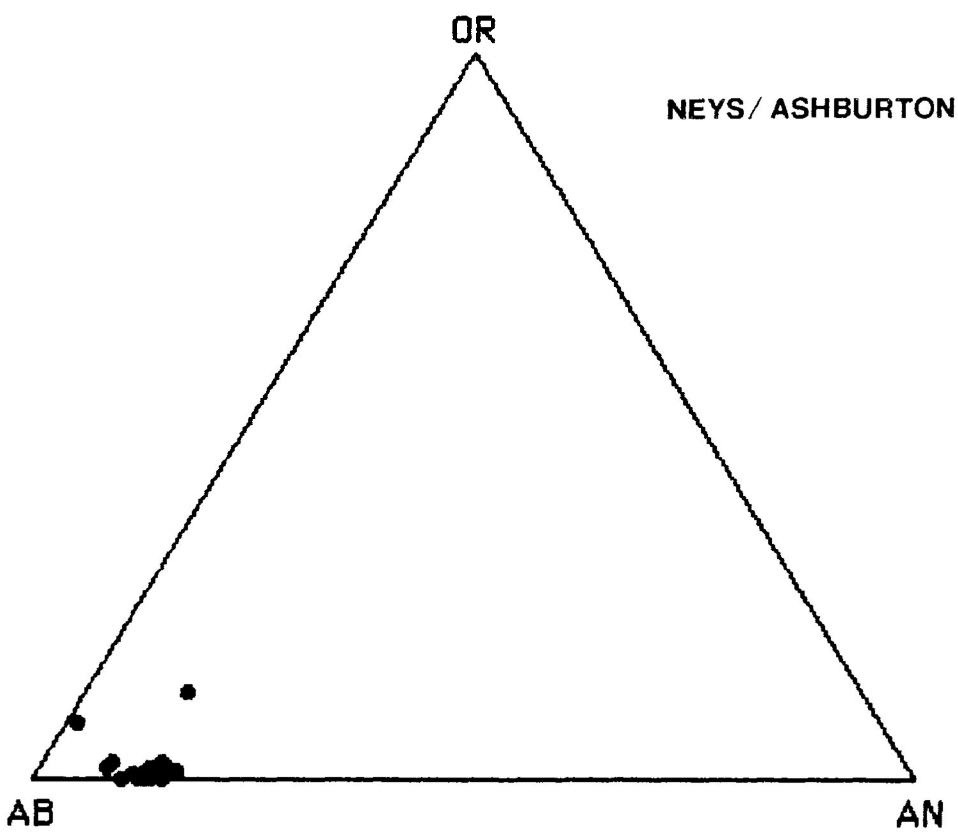

FIGURE 3.22 PLAGIOCLASE COMPOSITIONS FOR C2340.

compositions that are more sodic than Ab_{80} (Figure 3.22).

Recrystallization accompanies this compositional change, and lath-shaped relict plagioclases are converted into a granular texture of rounded crystals exhibiting poor albite twinning. Associated with these changes is the replacement of plagioclase by alkali feldspar. Alkali feldspar compositions are plotted for those specimens where analysis was possible. A common feature of this replacement alkali feldspar, either as distinct crystals in the groundmass or as diffuse patches within relict plagioclase laths, is the presence of appreciable barium contents. These vary from 0.5 to 6.4 wt % BaO. In some cases it is possible to find almost complete replacement of plagioclase by alkali feldspar crystals.

Figure 3.23 shows feldspar compositions for ferro-edenite and contaminated ferro-edenite syenite as reported by Lukosius-Sanders (1988). The feldspars are perthites and antiperthites with secondary feldspars being albite.

3.4.2 Wolf Camp Lake

Compositional data for the Wolf Camp lake megaxenolith are illustrated on figures 3.24 through 3.27. Samples represented by figures 3.24 through 3.26 are from within the block, whereas Figure 3.27 represents a sample

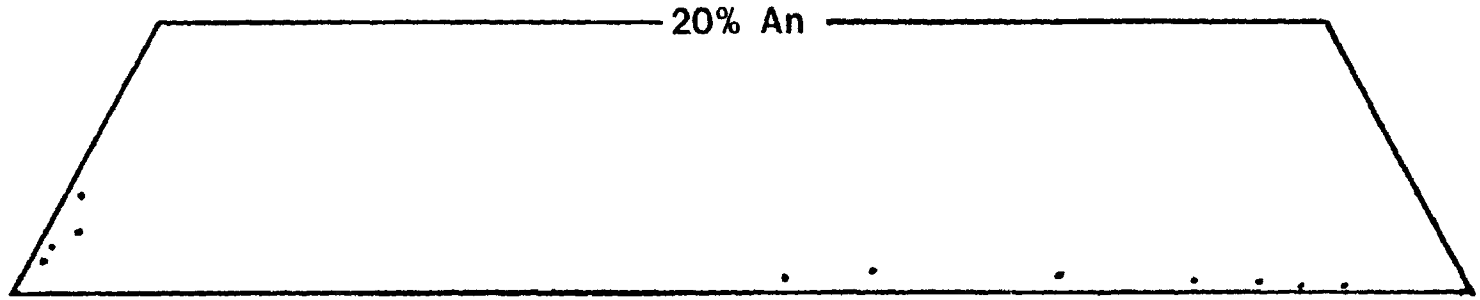

CONTAMINATED FERROEDENITE SYENITE

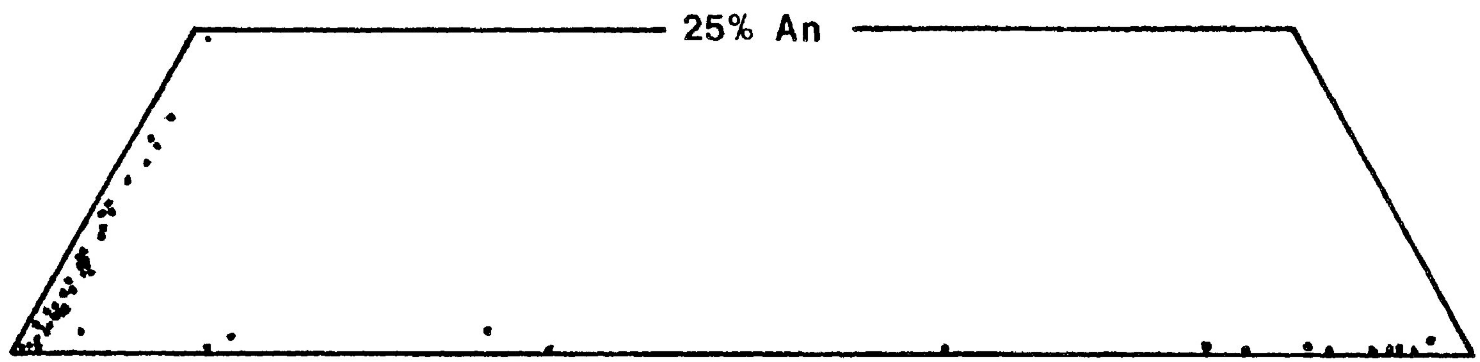

FERROEDENITE SYENITE

FIGURE 3.23 FELDSPARS FROM HOST SYENITES NEYS/ASHBURTON

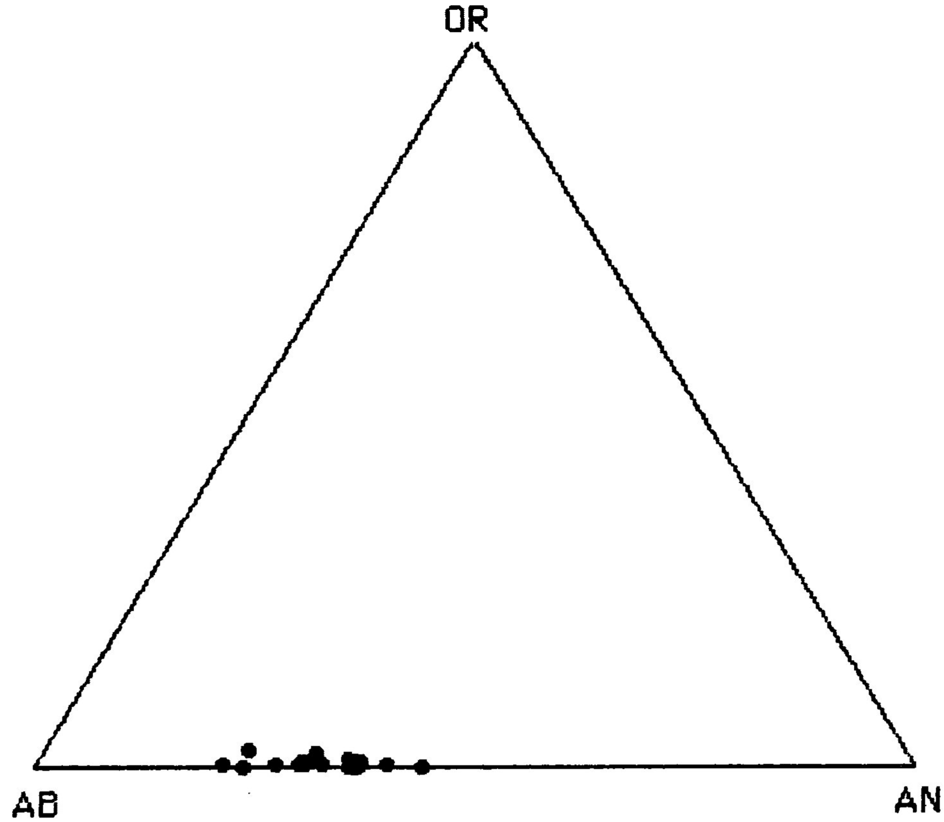

FIGURE 3.24 PLAGIOCLASE COMPOSITIONS FOR C3120.

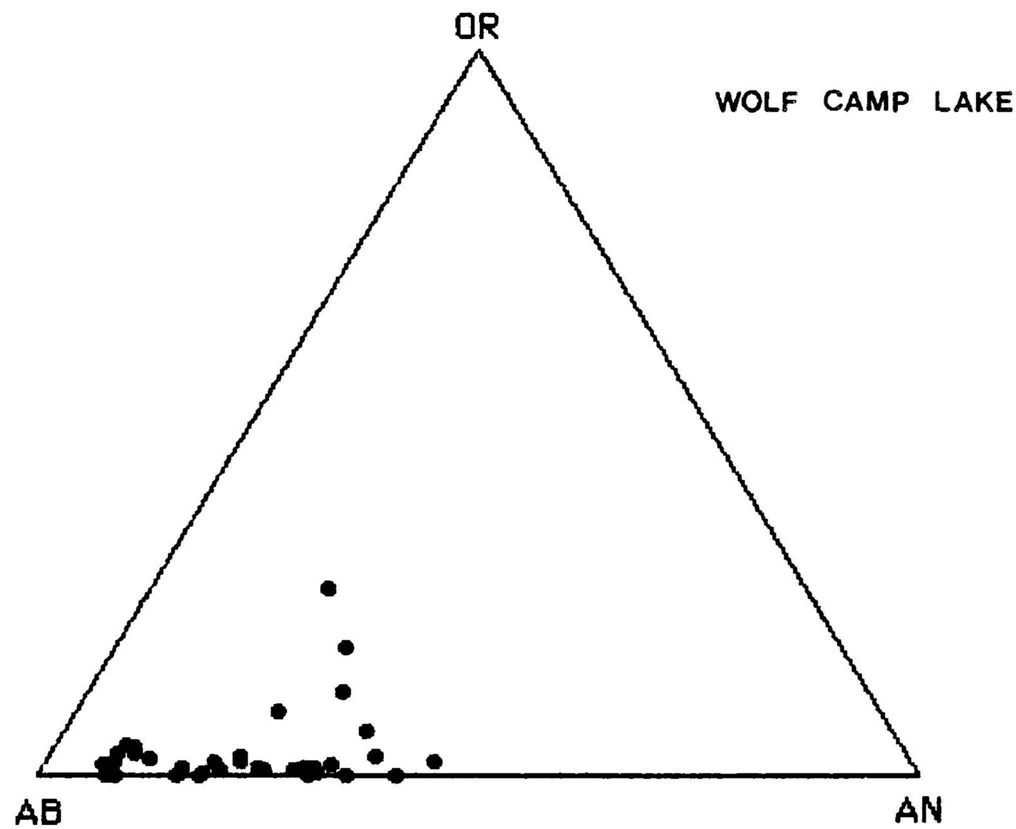

FIGURE 3.25 PLAGIOCLASE COMPOSITIONS FOR C3123.

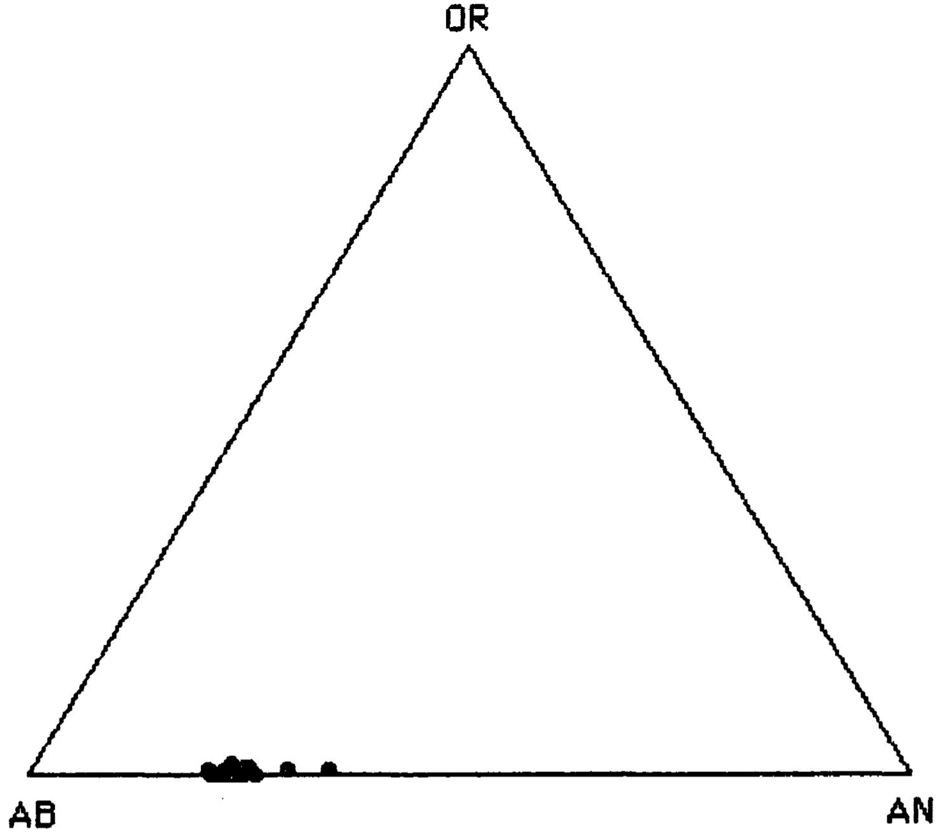

FIGURE 3.26 PLAGIOCLASE COMPOSITIONS FOR C3125.

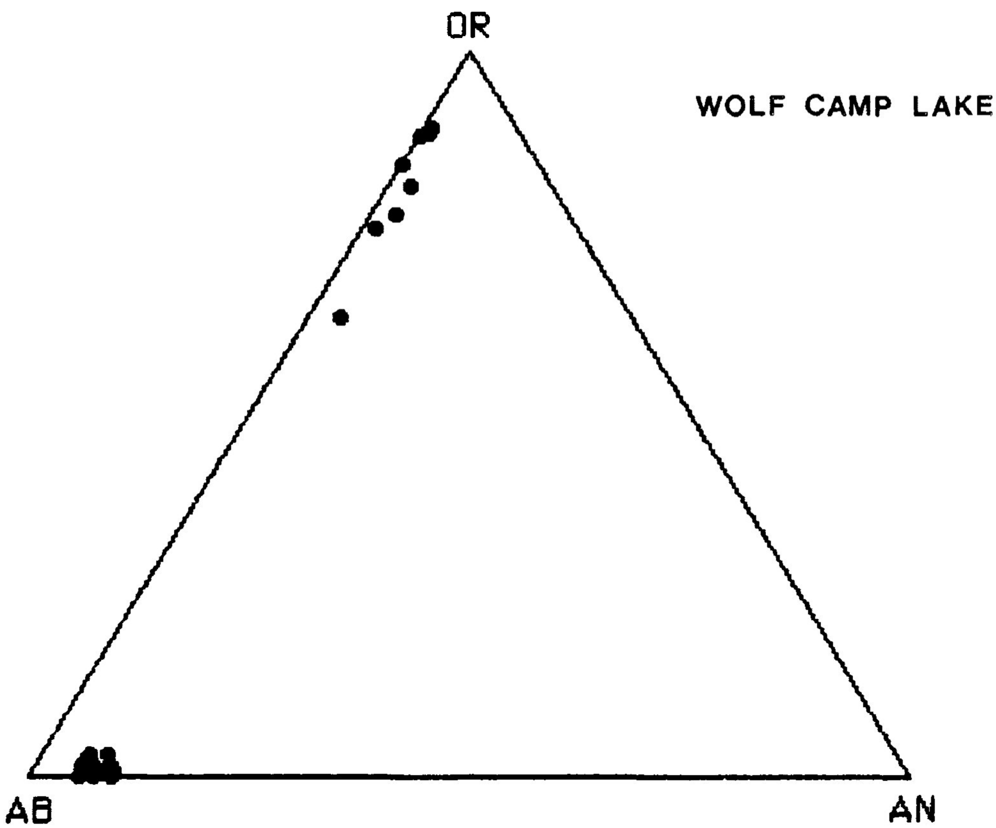

FIGURE 3.27 PLAGIOCLASE COMPOSITIONS FOR C2531A.

collected in contact with the host syenite. Those from within the block have plagioclase compositions in the range of andesine (An_{30-50}). The variation to more sodic compositions is due to effects of assimilation. There is also minor replacement of plagioclase by alkali feldspar, this giving compositions up to 26 mol % orthoclase. The most extreme case of assimilation is represented by xenolith C2531A (Figure 3.27). Recrystallization has occured producing a granular matrix of poorly-twinned albite crystals. Alkali feldspar crystals are also now present in the matrix. The range in orthoclase compositions is due to the presence of minor amounts of sodium.

3.4.3 Summary of Feldspar compositions

Both Neys/Ashburton and Wolf Camp Lake feldspar compositions exhibit the same patterns. With increasing assimilation effects due to incorporation into the host, original plagioclase compositions of oligoclase/andesine are decalcified and converted to albite. Along with this decalcification there occurs 1) recrystallization of plagioclase laths to granular crystals exhibiting poor twinning and 2) replacement of plagioclase and growth of alkali feldspar, this being orthoclase in composition and characterized by high barium content (up to 6.4 wt % BaO).

Phenocrysts are present in the xenoliths of Neys/Ashburton, these being relicts of the original volcanic texture. They are zoned and range from bytownite to labradorite in composition. Groundmass plagioclase is oligoclase-andesine in composition. This plagioclase composition co-existing with a clinopyroxene is similiar to co-existing plagioclase and calcic-clinopyroxene in Nipigon diabase reported by Sutcliffe (1987) and in tholeiitic basalts from southwest Utah reported by Lowder (1973). This indicates the basalt parents to Neys/Ashburton and Wolf Camp Lake xenoliths are common basalts that are not highly evolved.

Chapter Four

Whole Rock Chemistry of Basic Xenoliths

4.1 Introduction

Whole rock analyses for major and minor elements were obtained for ten specimens from Neys/Ashburton and twelve from Wolf Camp Lake. Whole rock analyses for Neys/Ashburton rocks were undertaken by the Centre in Mining and Mineral Exploration Research at Laurentian University. Analyses were performed using XRF methods on glass discs. Accuracy for major elements is ± 2% , for trace elements ± 10% (Lukosius-Sanders, 1988). Trace elements were determined using pressed powder. Whole rock analyses for Wolf Camp Lake rocks were performed by X-Ray Assay Laboratories in Toronto, Ontario using similar methods. Detection limits for major elements were ± 0.01% and ± 10 ppm for trace elements. Major elements determined were SiO_2, TiO_2, Al_2O_3, Fe_2O_3, MnO, CaO, MgO, Na_2O, K_2O and P_2O_5. Trace elements included Cr, Co, Ni, Cu, Zn, Pb, Zr, Y, Sr, Rb, Ba, Ce, La, Nb and Ga.

Normative calculations were processed using a computer program called "ROCALC", written by Stormer (1985) and based on the method in Barker (1983). Also calculated were AFM plotting parameters and F', Q', An parameters used in the Streckeisen-LeMaitre (1979) rock classification plot.

4.2 Neys/Ashburton

4.2.1 Major Elements

Major element compositions for Neys/Ashburton xenoliths and their respective CIPW norms can be found in Table 4.1. Of the ten analyses, four are quartz normative, one is neither quartz nor nepheline normative and the other five are nepheline normative.

Figure 4.1 is a series of variation diagrams for the major oxides vs SiO_2. SiO_2 shows the greatest variation from a low of 45.4% to 54.2%. Points are identified for those samples least assimilated through to those most assimilated. Weak trends are observed in K_2O, Na_2O, CaO and Fe_2O_3 with increasing SiO_2 contents. CaO and Fe_2O_3 are seen to decrease and K_2O, Na_2O are seen to increase from unassimilated to assimilated specimens. Increases in K_2O reflects addition of potassium feldspar into the specimens as assimilation progresses whereas increase in Na_2O and decrease in CaO reflects the decalcification of plagioclase to more sodic compostions. MgO and Al_2O_3 show no identifiable trend as the degree of assimilation

TABLE 4.1 WHOLE ROCK ANALYSES AND CIPW NORMS FOR NEYS/ASHBURTON XENOLITHS

ANALYSES ARE IN ORDER OF INCREASING ASSIMILATION

	C2311	C2503	C2498	C2309	C2490	C2303	C2351	C2386	C2330	C2331
SiO2	49.69	50.21	50.30	51.20	51.45	53.00	53.83	54.16	54.22	45.40
TiO2	0.89	0.74	0.69	0.89	0.64	0.82	0.81	0.79	0.65	1.28
Al2O3	15.21	15.69	15.23	15.93	15.33	15.48	15.24	15.37	15.28	15.36
Fe2O3	11.60	10.28	9.95	11.53	9.72	10.71	10.10	9.56	8.76	14.27
MnO	0.21	0.19	0.19	0.22	0.17	0.19	0.19	0.17	0.16	0.28
CaO	8.04	9.20	7.43	8.16	9.34	7.23	6.80	6.08	7.16	8.72
MgO	4.61	6.00	5.55	4.97	5.90	3.99	4.12	3.90	5.01	4.06
Na2O	6.28	4.26	6.81	3.23	3.91	4.45	4.84	5.81	4.79	4.75
K2O	1.84	1.80	2.25	1.84	2.00	2.31	2.65	2.60	2.22	2.75
P2O5	0.60	0.45	0.38	0.61	0.40	0.55	0.42	0.40	0.37	1.47
TOTAL	98.96	98.82	98.78	98.56	98.87	98.74	99.01	98.84	98.62	98.34

CIPW NORMS

	C2311	C2503	C2498	C2309	C2490	C2303	C2351	C2386	C2330	C2331
Q	-----	-----	-----	5.06	-----	2.01	0.10	-----	0.29	-----
OR	10.96	10.77	13.48	11.04	11.93	13.82	15.79	15.53	13.29	16.50
AB	33.68	33.88	29.30	27.71	33.50	38.17	41.39	46.20	41.12	25.49
AN	7.96	18.60	4.40	23.88	18.57	15.63	12.15	8.31	13.82	12.68
NE	10.85	1.41	15.71	-----	-----	-----	-----	1.90	-----	8.34
DI	20.32	17.75	22.36	8.49	18.72	11.67	13.27	13.56	14.08	14.12
HY	-----	-----	-----	8.63	2.26	4.66	4.22	-----	6.14	-----
OL	1.53	4.83	2.55	-----	2.75	-----	-----	2.48	-----	2.62
IL	0.46	0.42	0.41	0.48	0.36	0.42	0.42	0.37	0.35	0.61
HM	11.72	10.40	10.07	11.69	9.84	10.85	10.20	9.67	8.89	14.51
TN	1.12	0.89	0.82	1.60	1.12	1.49	1.47	1.03	1.16	1.67
AP	1.43	1.08	0.91	1.46	0.96	1.31	1.01	0.97	0.89	3.54

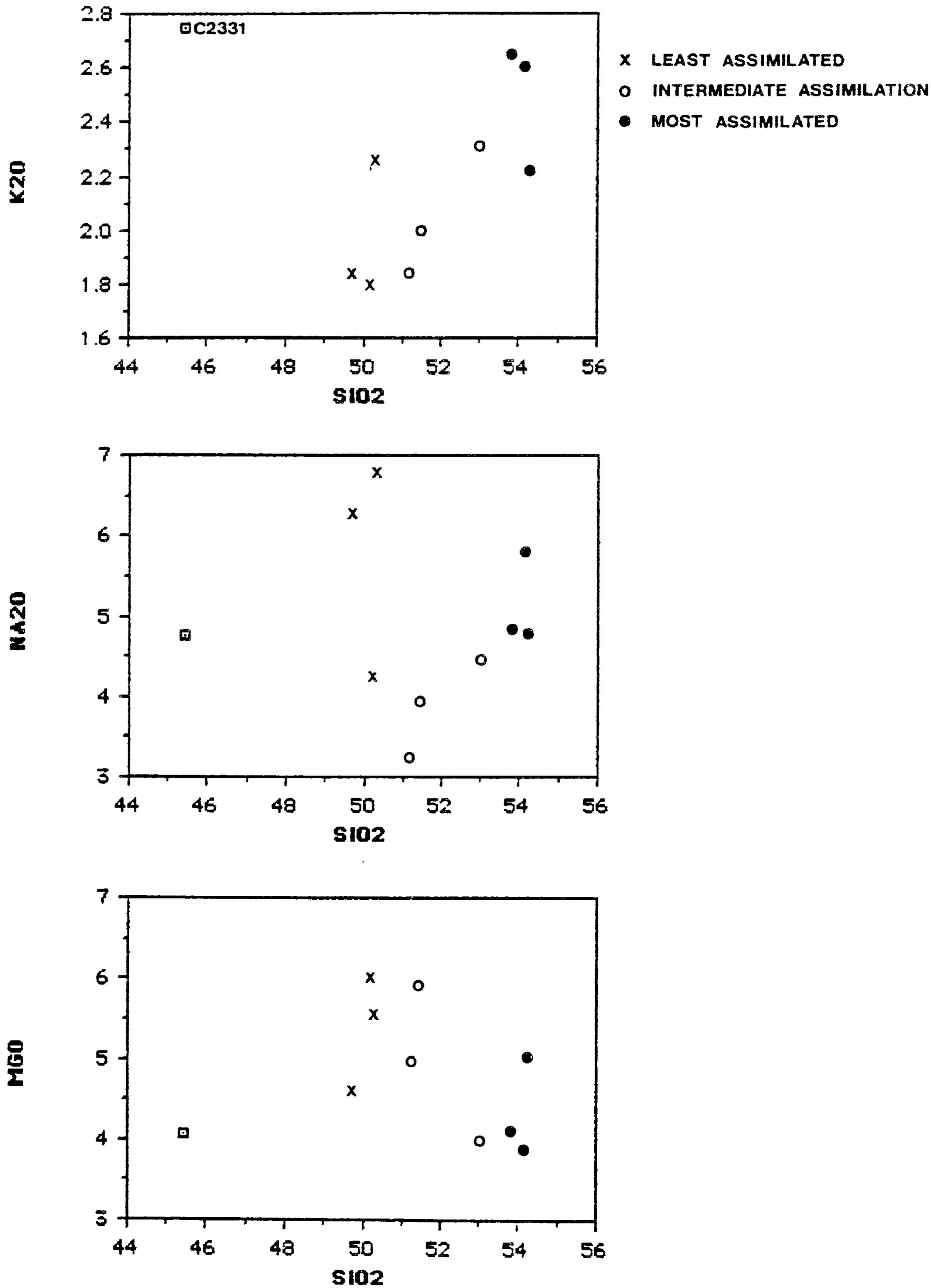

Figure 4.1 Variation diagrams for Neys/Ashburton xenoliths.

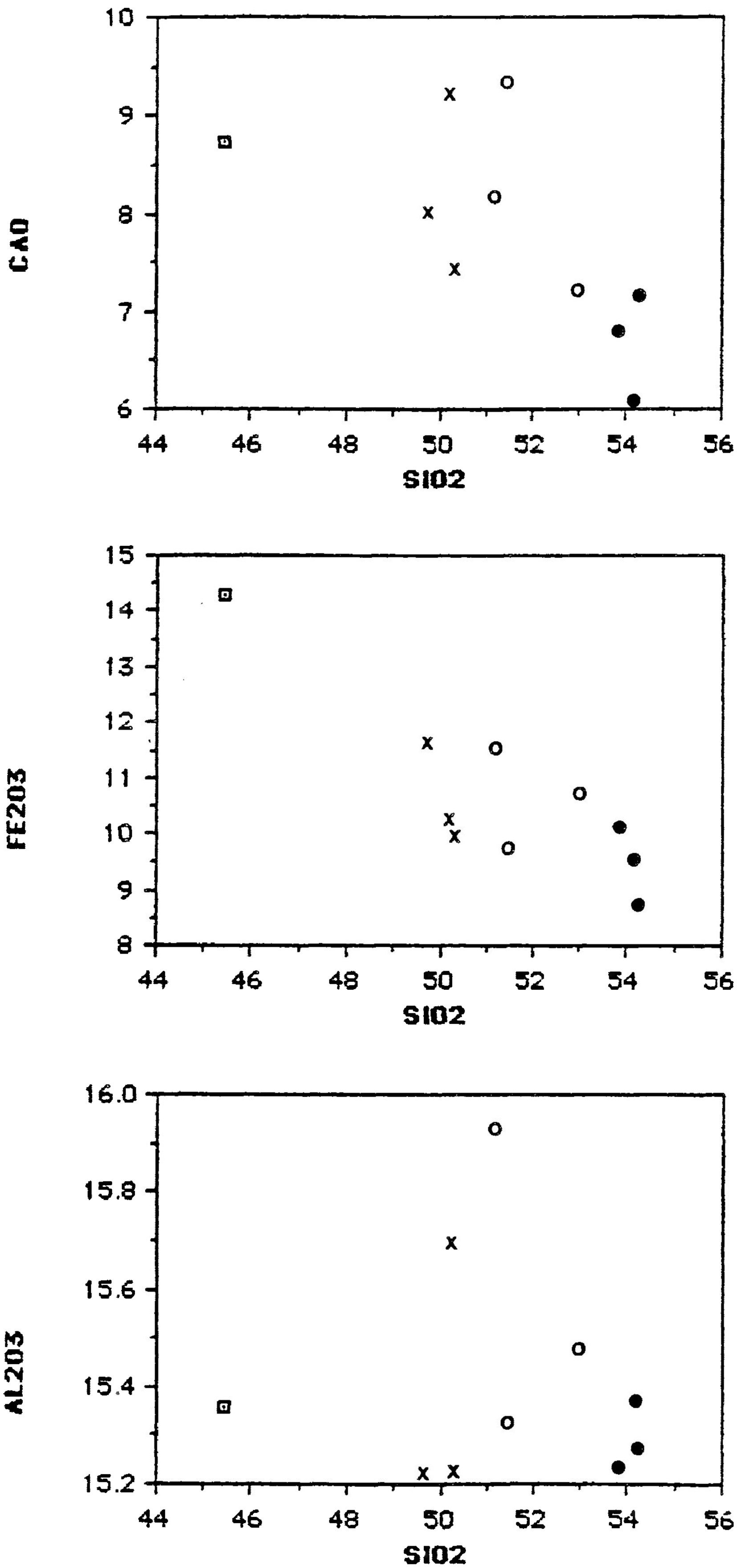

Figure 4.1 continued.

increases.

Sample C2331 is anomalous in that it plots away from the main group of xenoliths. It contains approximately 5% less SiO_2 and has significantly more TiO_2 and Fe_2O_3 than the other xenoliths. Petrologic study shows it to be highly assimilated with a large amount of potassium feldspar growth. It is possible this sample represents another type of xenolith.

C2311, C2331 and C2498 are strongly nepheline normative with C2311 and C2498 exhibiting intermediate assimilation effects and C2331 being highly assimilated. C2386 and C2503 are slightly nepheline normative and exhibit slight effects of assimilation. Those specimens that are quartz normative decrease in their amount of normative quartz as their degree of assimilation increases. These observations seem to indicate two trends in Neys/Ashburton xenoliths. One trend is for quartz normative specimens becoming less saturated with assimilation, the other trend for specimens that are nepheline normative becoming more nepheline normative as assimilation progresses. This indicates there may be two types of volcanics present in the Neys/Ashburton xenoliths syenite. However pyroxene compositional data contradicts this as it indicates that saturated volcanic rocks are parental to the xenoliths. It is possible that the trends reflect the occurence of two different assimilation episodes, each having distinctive chemical characteristics.

Figure 4.2 plots compositions according to the rock classification scheme of Streckeisen and LeMaitre (1979). The data shows a considerable scatter, and range from phonolite and basanite through latite to tholeiitic basalt. As assimilation increases points plot away from the original compositions of a tholeiite towards a latite due to alkali addition. This agrees with plagioclase compositional data as anorthite content decreases. The least assimilated samples plot towards the field of tholeiitic basalt, agreeing with the conclusions derived from pyroxene compositions. Two trends however seem to evident in the data, one from oversaturated to saturated, the other from saturated to highly understaurated. This again could indicate the presence of two types of xenoliths or different assimilation trends. If a second type of xenolith is present the original compositions could lie in the area of alkali basalts.

Compositions of alkali-feldspars are also plotted on figure 4.2. One trend seems to progress towards these compositions whereas the other deviates away from it. The trend that approaches alkali feldspar compositions indicates the xenoliths are becoming more syenitic in nature as their compositions equilibrate with their syenite hosts. The other trend

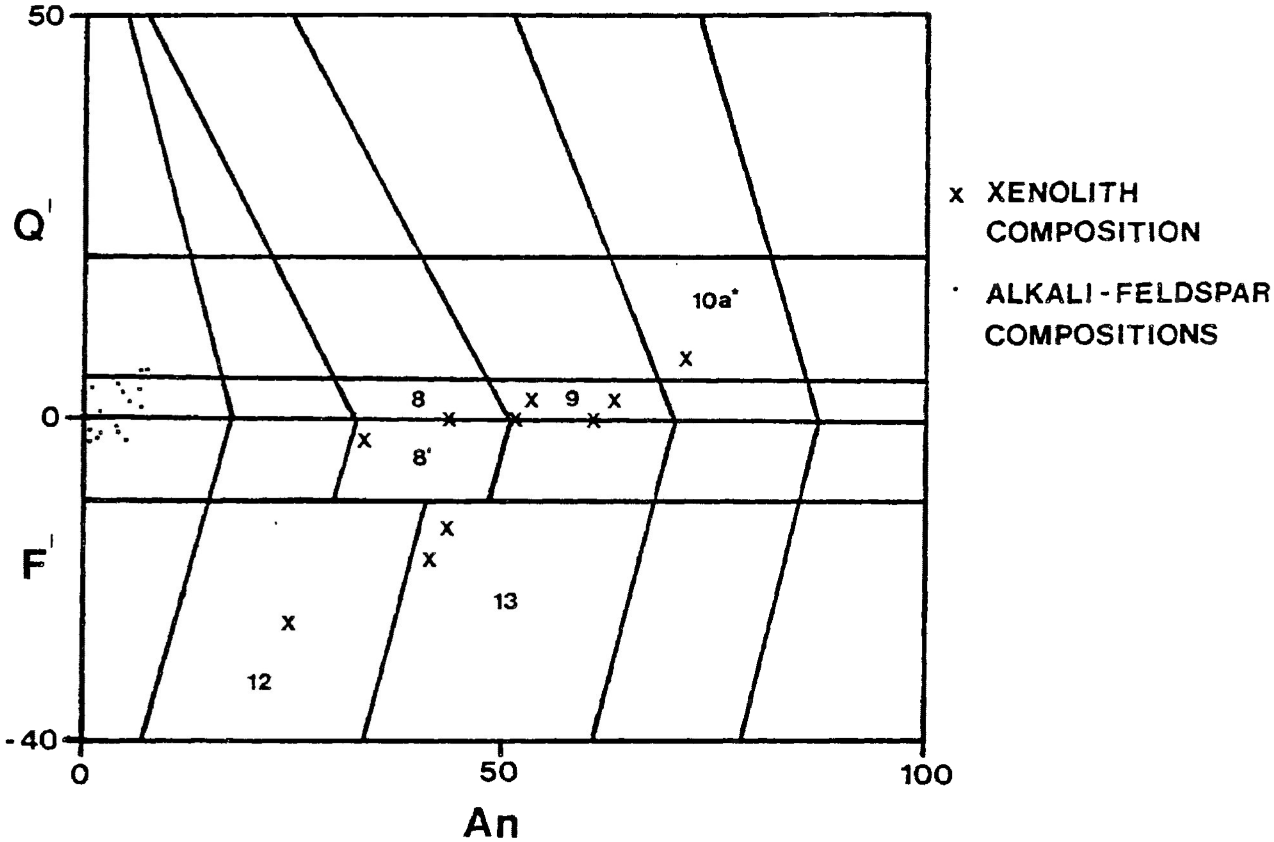

8 LATITE
8' FOID-BEARING LATITE
9 MUGEARITE
10a* THOLEIITIC BASALT
12 TEPHRITIC PHONOLITE
13 BASANITE

FIGURE 4.2 STRECKEISEN-LEMAITRE ROCK CLASSIFICATION PLOT FOR NEYS/ASHBURTON XENOLITHS towards compositions more undersaturated than alkali feldspar may be due to the presence of a different reaction.

4.2.2 Minor Elements

Minor element compositions of the Neys/Ashburton xenoliths are listed in Table 4.2.

Trends in the minor elements of Neys/Ashburton xenoliths are poorly-developed, but it is possible to identify weak trends as SiO_2 increases. Y and Rb are seen to increase and Cr, Co, Ni, Zn, Sr are seen to decrease. Cu, Pb, Zr, La and Ce, do not develop only significant trends. Barium is present in significant amounts, ranging from 471 ppm to 3157 ppm, with the higher amounts in those specimens showing postassium feldspar addition. Sr is also present in significant amounts, ranging from 526 ppm to 916 ppm.

Noticable in all specimens are low contents of Cr and Ni. This indicates that the volcanic parent or parents to the xenoliths is of an evolved nature. This agrees with information obtained from pyroxene compositional variations.

4.2.3 Comparison with other Keweenawan Volcanics

Table 4.3 compares the Neys/Ashburton volcanic xenoliths to other Keweenawan volcanics found in the region. Neys/Ashburton compositions

TABLE 4.2 MINOR ELEMENT COMPOSITIONS FOR NEYS/ASHBURTON XENOLTHS IN PPM

	C2303	C2309	C2311	C2330	C2331	C2351	C2386	C2490	C2498	C2503
Cr	8	15	18	17	26	15	11	20	17	21
Co	46	45	51	45	54	48	36	46	49	49
Ni	27	32	31	55	34	28	28	55	53	55
Cu	105	110	112	48	84	60	42	54	54	70
Zn	115	124	110	106	145	139	99	92	116	95
Pb	0	52	0	0	45	41	35	0	27	46
Zr	234	150	178	332	152	165	194	180	236	156
Y	37	31	31	39	36	29	31	227	29	26
Sr	706	725	741	526	917	621	566	640	592	656
Rb	111	82	86	115	77	140	134	76	115	79
Ba	864	792	804	471	3158	711	791	570	766	715
Ce	162	158	161	208	238	142	132	142	175	129
La	92	86	83	111	128	68	70	74	95	65

TABLE 4.3 COMPARISON OF NEYS/ASHBURTON XENOLITHS TO OTHER KEWEENAWAN VOLCANICS

	NEYS/ASHBURTON	KEW	QUEBEC MINE	SOUTH SHORE
SiO2	49.7-51.2	46.6-48.7	43.4-47.6	50.2-54.0
TiO2	0.69-0.89	0.72-2.33	1.10-1.80	2.10-2.50
Al2O3	15.21-15.93	15.8-19.2	15.2-16.7	13.9-14.2
Fe2O3	9.95-11.6	8.20-14.3	10.9-12.4	11.1-13.9
MnO	0.19-0.22	0.11-0.17	0.17-0.20	0.22-0.27
MgO	4.61-6.0	5.30-8.70	6.30-9.00	4.00-6.40
CaO	7.43-9.20	9.20-12.4	7.10-10.5	6.00-8.10
Na2O	3.22-6.81	2.20-2.60	1.90-2.90	2.90-3.60
K2O	1.80-2.25	0.12-0.54	0.20-1.20	0.60-1.40
P2O5	0.38-0.61	0.03-0.25	0.10-0.18	0.31-0.37

KEW= KEWEENAWAN REFERENCE SUITE (BASALTIC VOLCANISM STUDY PROJECT,1981)
QUEBEC MINE= QUEBEC MINE BASALTS, MICHIPICOTEN ISLAND (ANNELLS,1974)
SOUTH SHORE= SOUTH SHORE BASALTS, MICHIPICOTEN ISLAND (ANNELLS,1974)

are represented by those least-altered by assimilation.

Two groups of tholeiites are found on Michipicoten Island (Annells, 1974), these being the Quebec Mine basalts and the South Shore basalts. When compared to the Quebec Mine Suite, the Neys/Ashburton xenoliths are found to have more SiO_2, Na_2O, K_2O and P_2O_5. Mgo, Al_2O_3, CaO, MnO and Fe_2O_3 are comparable with TiO_2 and MgO less. The South Shore Suite prove to be higher in SiO_2, TiO_2, Fe_2O_3 and MnO with less Al_2O_3, CaO, Na_2O, K_2O, P_2O_5 and comparable MgO.

Neys/Ashburton xenoliths differ significantly from the Keweenawan Reference Suite (Basaltic Volcanism Study Project, 1981) being enriched in SiO_2, Na_2O, K_2O and P_2O_5 and slightly enriched in MnO. They have less Al_2O_3, MgO, CaO, Fe_2O_3 and TiO_2.

In general, Neys/Ashburton least assimilated xenoliths are enriched in the alkalies and P_2O_5 and depleted in TiO_2 relative to other Keweenawan basalts. TiO_2 depletion indicates the parent volcanic(s) of Neys/Ashburton xenoliths to be more evolved than the other volcanics whereas enrichment in alkalies and P_2O_5 shows there is contamination present from the host syenites.

4.3 Wolf Camp Lake

4.3.1 Major Elements

Wolf Camp Lake megaxenolith major element compositions and their respective CIPW norms are presented in Table 4.4. All specimens are quartz normative ranging from less than 1% quartz to over 11% quartz.

Figure 4.3 is a series of variation diagrams for the major oxides vs SiO_2. SiO_2 shows the greatest variation from a low of 48.3% to a high of 53.9%. Points are identified for least-assimilated to most-assimilated specimens.

MgO, Fe_2O_3 and K_2O produce trends when plotted against increasing SiO_2 content. MgO and Fe_2O_3 are seen to decrease while K_2O increases. A weak trend of increasing Na_2O is also evident. CaO and Al_2O_3 show no recognizable trends.

It is observed that the most assimilated samples C2517 and C2518 are distinctly different in composition to the other xenoliths. The specimens plot as the most extreme loss or increase of components with SiO_2 increase. C3121 represents the closest composition to that of the original volcanic rocks.

TABLE 4.4 WHOLE ROCK ANALYSES AND CIPW NORMS FOR WOLF CAMP LAKE MEGAXENOLITH

ANALYSES ARE IN ORDER OF INCREASING ASSIMILATION

	C3121	C2531	C3123	C2530	C2523	C3125	C2526	C2524	C3120	C3124	C2518	C2517
SiO2	48.30	49.50	49.60	49.70	49.80	49.80	50.30	50.50	51.70	52.20	53.80	53.90
TiO2	2.03	1.80	1.90	1.77	1.93	2.00	1.92	1.78	1.97	1.94	1.29	1.40
Al2O3	14.30	14.00	13.90	12.30	13.90	13.90	13.90	13.30	14.20	14.00	15.40	14.50
Fe2O3	15.40	14.30	14.50	13.60	13.90	14.90	15.80	15.20	14.50	14.50	11.00	12.60
MnO	0.27	0.28	0.24	0.30	0.20	0.27	0.27	0.29	0.25	0.22	0.25	0.27
CaO	7.84	7.83	7.85	9.11	7.02	6.56	6.34	5.09	7.15	7.25	4.11	4.37
MgO	4.14	3.42	3.64	4.17	3.56	3.67	4.00	3.08	2.56	2.46	0.76	1.16
Na2O	3.47	4.83	3.85	3.62	4.26	3.95	2.63	4.56	3.81	3.57	5.18	4.74
K2O	1.67	1.68	1.81	2.85	2.52	2.97	2.13	2.85	2.38	2.56	4.36	4.54
P2O5	1.07	0.87	0.99	0.92	1.00	1.02	0.88	0.87	1.05	1.07	0.42	0.48
LOI	1.23	0.47	1.00	1.00	1.16	0.77	1.00	1.70	0.31	0.16	2.77	0.70
TOTAL	99.90	99.20	99.60	99.60	99.50	100.10	99.40	99.50	100.20	100.20	99.80	99.20

CIPW NORMS

	C3121	C2531	C3123	C2530	C2523	C3125	C2526	C2524	C3120	C3124	C2518	C2517
Q	4.73	0.22	4.61	1.15	1.53	1.49	11.25	2.71	7.30	8.57	0.89	2.21
OR	10.02	10.08	10.88	17.13	15.18	17.67	12.82	17.27	14.13	15.16	26.65	27.39
AB	29.81	41.49	33.15	31.15	36.75	33.65	22.67	39.57	32.38	30.28	45.34	40.95
AN	18.80	11.73	15.57	9.05	11.59	11.50	20.20	7.59	14.68	14.65	6.10	4.98
WO	-----	-----	-----	-----	-----	-----	-----	-----	-----	-----	1.29	0.79
DI	5.84	12.99	9.11	20.03	8.73	6.70	0.20	5.67	6.35	6.61	4.22	6.36
HY	7.76	2.63	5.00	1.28	4.99	6.85	10.06	5.24	3.46	3.08	-----	-----
IL	0.59	0.61	0.52	0.65	0.44	0.58	0.59	0.64	0.54	0.47	0.55	0.59
HM	15.64	14.52	14.75	13.83	14.17	15.00	16.09	15.59	14.56	14.53	11.38	12.86
TN	4.30	3.70	4.07	3.57	4.26	4.19	4.04	3.66	4.16	4.16	2.56	2.75
AP	2.57	2.09	2.39	2.22	2.42	2.43	2.12	2.11	2.50	2.54	1.03	1.16

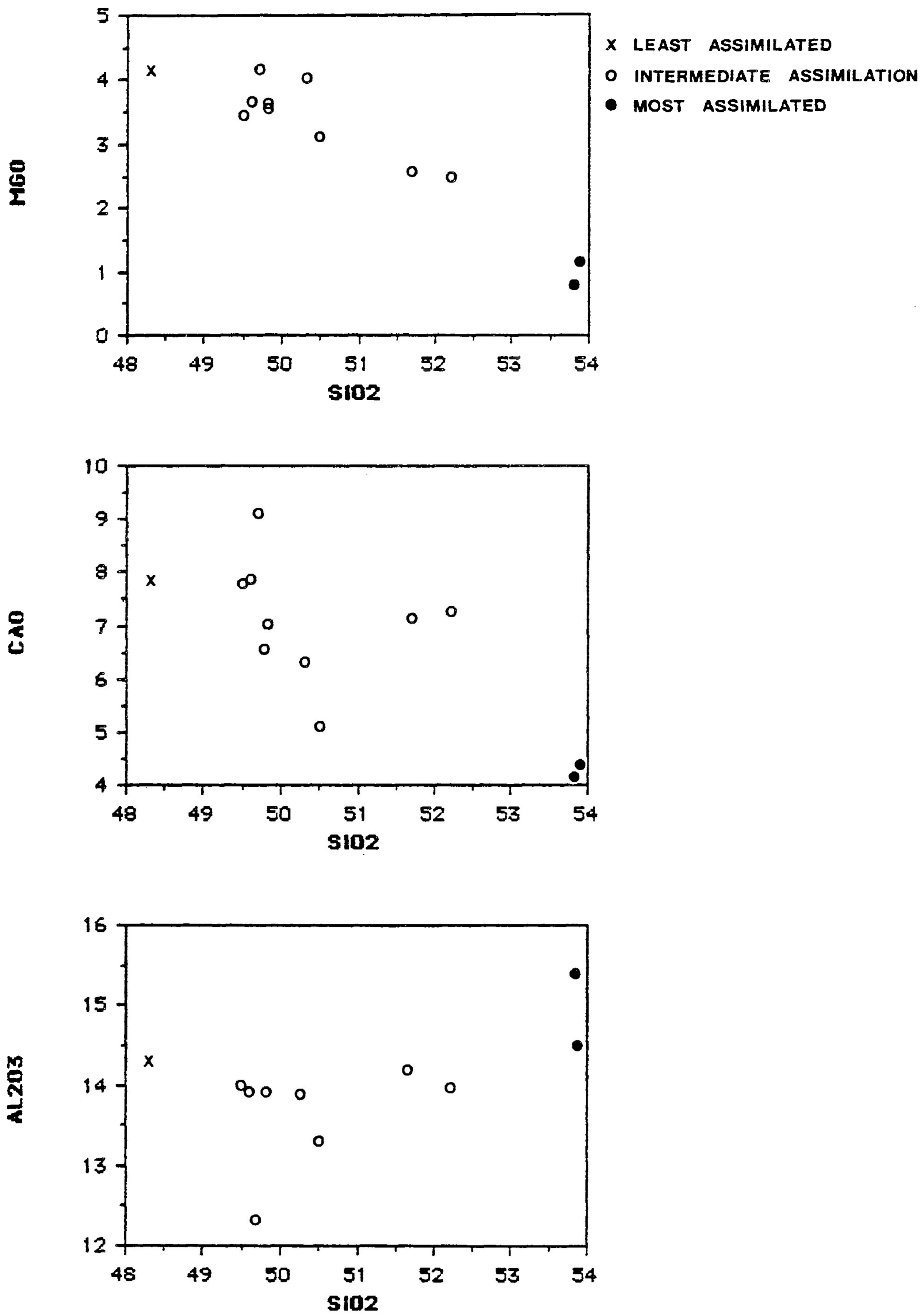

Figure **4.3** Variation diagrams for Wolf Camp Lake megaxenolith samples.

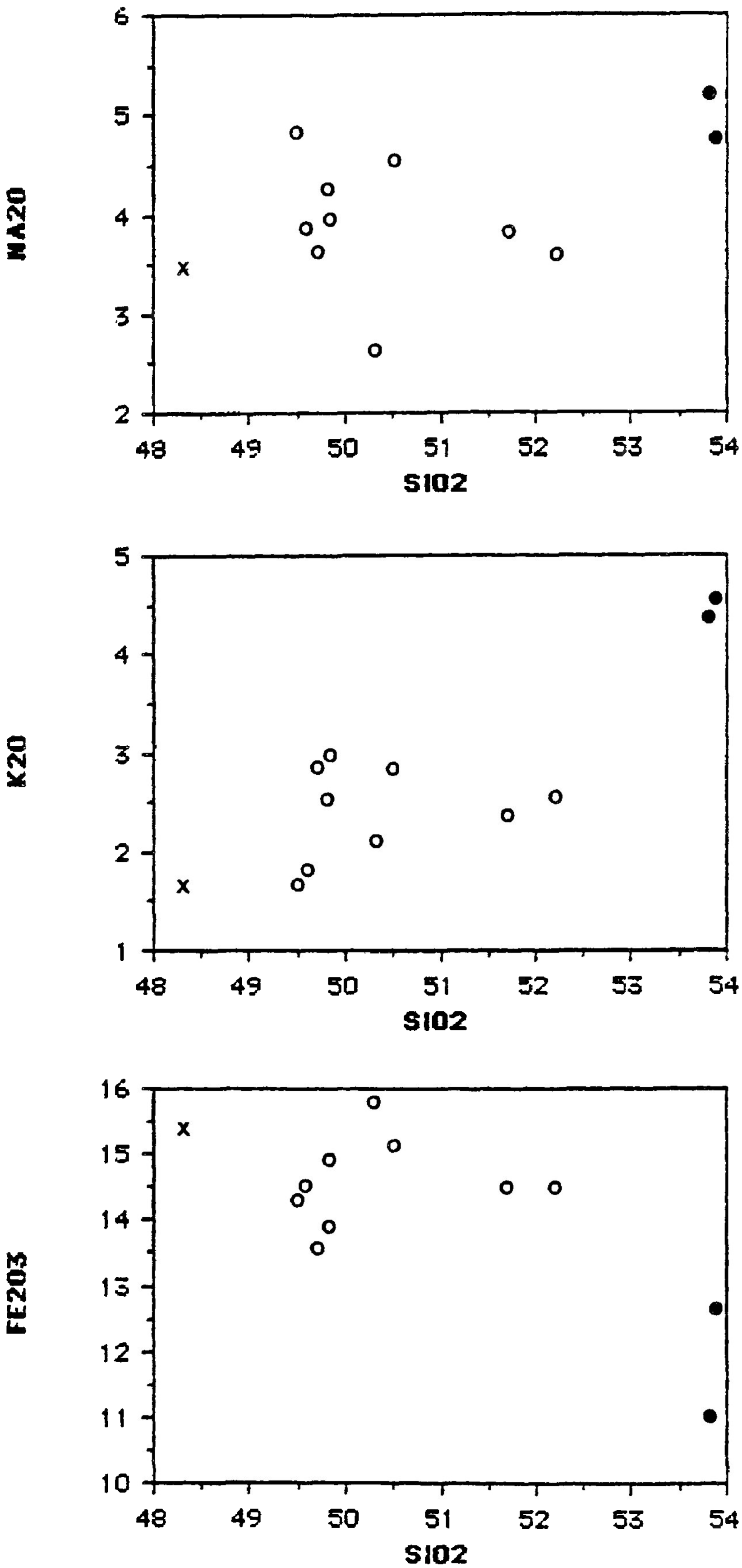

Figure 4.3 continued.

All specimens are quartz normative, with normative hypersthene indicating a parent basalt with tholeiitic affinities.

Figure 4.4 plots compositions according to the rock classification scheme of Streckeisen and LeMaitre (1979). The data shows considerable scatter, with compositions ranging from mugearite and calc-alkaline andesite at the least-assimilated part of the trend to trachyte towards highly-assimilated samples. As assimilation progresses, compositions plot away from the least assimilated samples towards the highly assimilated specimens due to alkali addition. The normative anorthite content is also seen to decrease, this agreeing with observed plagioclase compositional variations. C3121 is the least assimilated of all samples and plots close to the tholeiitic basalt field, showing this rock type to be a likely parent to the megaxenolith basalts. This conclusion agrees with the observed pyroxene compositional variation. All data plots on the same trend indicating only one parental rock type is present. Data also trends towards plotted alkali feldspar compositions, indicating equilibrium to more syenitic compositions of the host.

4.3.2 Minor Elements

Minor element compositions for the Wolf Camp Lake megaxenolith are given in Table 4.5. No significant trends are found in these elements other

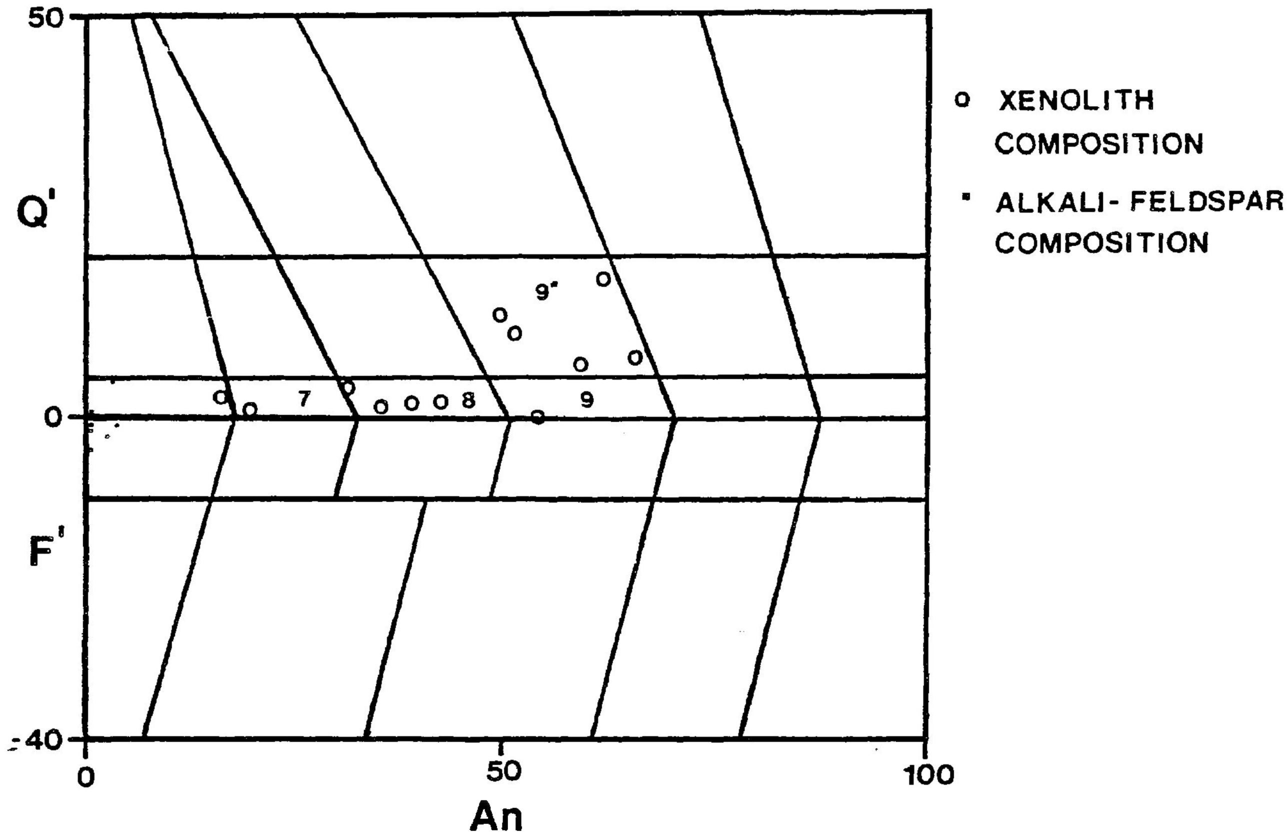

7 TRACHYTE
8 LATITE
9 MUGEARITE
9* CALC-ALKALINE ANDESITE

FIGURE 4.4 STRECKEISEN-LEMAITRE ROCK CLASSIFICATION PLOT FOR WOLF CAMP LAKE

TABLE 4.5 MINOR ELEMENT COMPOSITIONS FOR WOLF CAMP LAKE MEGAXENOLITH IN PPM

	C2517	C2518	C2523	C2524	C2526	C2530	C2531	C3120	C3121	C3123	C3124	C3125
Cr	<10	<10	25	20	19	<10	25	<10	<10	<10	<10	<10
Rb	107	109	115	72	120	127	79	82	86	59	64	118
Sr	314	275	464	259	278	337	430	525	481	499	487	536
Y	60	50	44	40	30	36	24	35	43	42	38	43
Zr	346	356	339	379	332	367	349	329	350	329	332	332
Nb	136	154	104	128	125	126	129	126	135	125	122	114
Ba	3430	2610	1020	1410	1020	1240	768	1370	771	1410	1170	1250
Ni	<2	<2	20	7	32	21	21	22	22	19	24	21
Ga	15	18	18	20	19	14	19	18	19	16	19	17

TABLE 4.6 COMPARISON OF WOLF CAMP LAKE MEGAXENOLTH TO OTHER KEWEENAWAN VOLCANICS

	NEYS/ASHBURTON	KEW	QUEBEC MINE	SOUTH SHORE
SiO2	48.3-52.2	46.6-48.7	43.4-47.6	50.2-54.0
TiO2	1.90-2.03	0.72-2.33	1.10-1.80	2.10-2.50
Al2O3	13.9-14.3	15.8-19.2	15.2-16.7	13.9-14.2
Fe2O3	14.5-15.8	8.20-14.3	10.9-12.4	11.1-13.9
MnO	0.22-0.27	0.11-0.17	0.17-0.20	0.22-0.27
MgO	2.46-4.14	5.30-8.70	6.30-9.00	4.00-6.40
CaO	6.34-7.85	9.20-12.4	7.10-10.5	6.00-8.10
Na2O	2.63-3.95	2.20-2.60	1.90-2.90	2.90-3.60
K2O	1.67-2.97	0.12-0.54	0.20-1.20	0.60-1.40
P2O5	0.88-1.07	0.03-0.25	0.10-0.18	0.31-0.37

KEW= KEWEENAWAN REFERENCE SUITE (BASALTIC VOLCANISM STUDY PROJECT,1981)
QUEBEC MINE= QUEBEC MINE BASALTS, MICHIPICOTEN ISLAND (ANNELLS,1974)
SOUTH SHORE= SOUTH SHORE BASALTS, MICHIPICOTEN ISLAND (ANNELLS,1974)

than slight decreases in Sr and Nb with increasing SiO_2. Ba is seen to increase significantly in the most assimilated samples, reflecting addition of potassium feldspar. Other elements show no trends. Barium and strontium are present in significant amounts ranging from 768 ppm to 3430 ppm and 259 ppm to 536 ppm respectively. Zr is present ranging from 329 ppm to 379 ppm.

Cr and Ni contents are low to nil for Wolf Camp Lake specimens, indicating the parental tholeiitic basalt to be evolved.

4.3.3 Comparison to other Keweenawan Volcanics

Table 4.6 compares Wolf Camp Lake magaxenolith samples to other Keweenawan volcanics. Wolf Camp Lake compositions are represented by least assimilated specimens.

Compared to South Shore tholeiites of Michipicoten Island (Annells, 1974) a close match is observed, except that Wolf Camp Lake is slightly poorer in SiO_2, TiO_2, Fe_2O_3, MnO, Na_2O, K_2O and P_2O_5 and less in Al_2O_3, CaO and MgO. Compared to Quebec Mine basalts, Wolf Camp Lake is found to be higher in SiO_2, TiO_2, Fe_2O_3, MnO, Na_2O, K_2O and P_2O_5 and less in Al_2O_3, CaO and MgO.

Compared to tholeiites of the Keweenawan Reference Suite (Basaltic

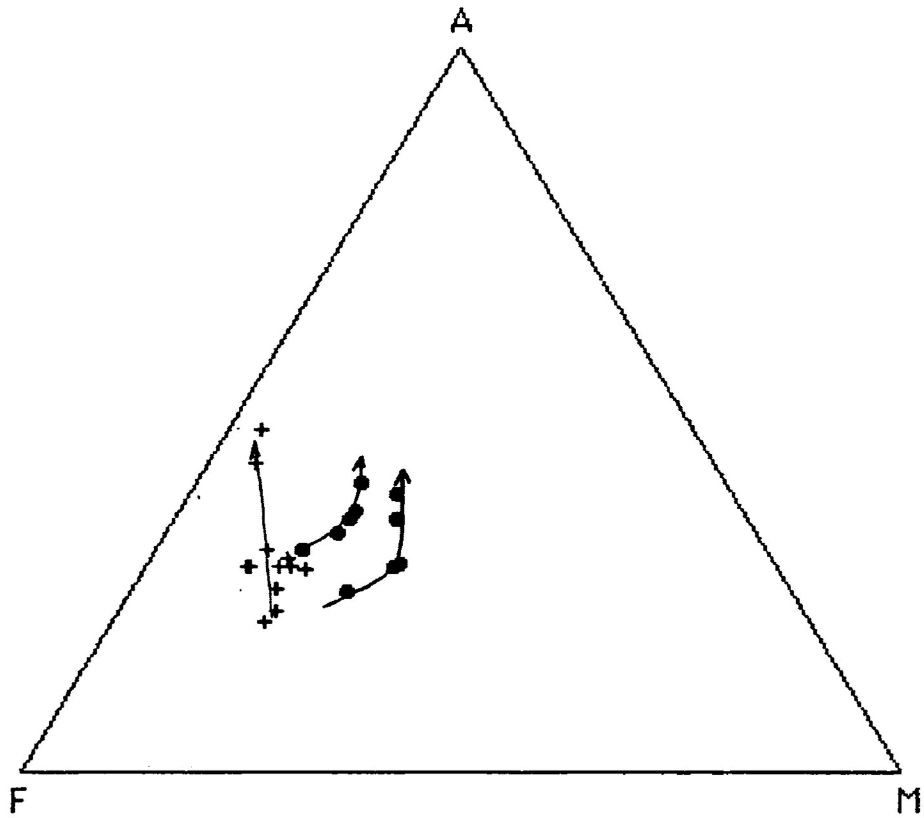

Figure 4.5 AFM diagram for Neys/Ashburton xenoliths (•) and Wolf Camp Lake megaxenolith (+).

$A = Na_2O + K_2O$

$F = (FeO + .8999Fe_2O_3) + (FeO + 2Fe_2O_3)(Fe + Fe)$

$M = MgO$

Volcanism Study Project, 1981), Wolf Camp Lake specimens are significantly different. They are higher in SiO_2, TiO_2, Fe_2O_3, MnO, Na_2O, K_2O and P_2O_5 and lower in Al_2O_3, MgO and CaO.

In general, compared to other Keweenawan volcanics, Wolf Camp Lake xenoliths are higher in alkalies, P_2O_5, MnO and Fe_2O_3 and lower in CaO, MgO and Al_2O_3. Increased alkalies indicate assimilation occuring in the least-altered specimens. South Shore basalts show the closest match indicating a tholeiitic parentage possible. TiO_2 contents show Wolf Camp Lake to be only slightly more evolved than Michipicoten Island tholeiites.

4.4 Comparison of Wolf Camp Lake and Neys/Ashburton

Figure 4.5 is an AFM diagram for Neys/Ashburton xenoliths and the Wolf Camp Lake megaxenolith composition. Neys/Ashburton xenoliths have slightly more total Fe, MgO and higher alkalies than Wolf Camp Lake samples. Both however show the same response to assimilation as alkalies increases. The most assimilated samples in each case plot with higher alkali content. Neys/Ashburton data suggests development of two trends, each increasing with alkali content. This may indicate the presence of two xenolith types.

Both Neys/Ashburton and Wolf Camp Lake show the same trends on the Streckeisen-LeMaitre rock classification plot of decreasing normative anorthite with increasing assimilation, agreeing with observed plagioclase compositional variation.

Bulk rock compositions from both areas and CIPW norms indicate the xenoliths are derived from a tholeiitic basalt parent. Neys/Ashburton displays trends suggesting the presence of a second undersaturated xenolith type. Pyroxene compositional variation indicates an evolved tholeiitic parentage. Trace element data from the xenoliths agree with this conclusion as Ni and Cr contents are low. Wolf Camp Lake xenoliths are slightly more evolved than Neys/Ashburton xenoliths as they contain less Ni and Cr. In the case of the Neys/Ashburton xenoliths, identification of two rock types is difficult due to the absence of completely-fresh rocks and few analyses available.

Chapter Five

Relationship between the Xenoliths and Host Syenites

5.1 Introduction

It was suggested by Jago (1980) and Lukosius-Sanders (1988) that assimilation of the basic xenoliths in the Western Contact Zone and Neys/Ashburton has resulted in the production of contaminated ferro-edenite syenites from uncontaminated ferro-edenite syenite. This hypothesis is tested in this study by modelling the contamination of a ferro-edenite syenite by the addition of basic xenoliths. This is accomplished by mass balance mixing calculations and principal component analysis. The compositional changes found in the xenoliths are also modelled using these techniques.

5.2 Xenolith Compositional Changes

Mass balance mixing calculations are used to study the compositional changes in the xenoliths due to assimilation. The calculations are based on the procedure orginally devised by Bryan et al (1969), and incorporated into the Geochemical Program Package of Geist et al (1985). Proportions of a specified set of components are added to or subtracted from a parent to produce a least squares best fit to a given daughter composition. This procedure permits the modelling of assimilation or mixing processes. The sum of the squared values of residuals (R-squared) is used as a test of whether or not a solution is acceptable. R-squared values less than 1 are considered acceptable with values less than 0.3 a good fit and values less than 0.1 an excellent fit.

To assess compositional changes during xenolith assimilation, the parents used are Keweenawan volcanics from the area of the North Shore, Lake Superior, these being from Michipicoten Island (Annells, 1974) and the Keweenawan Reference Suite (Basaltic Volcanism Study Project, 1981). The daughters are the xenoliths observed at Neys/Ashburton. Components added to the xenoliths are minerals found within the host ferro-edenite syenites, as they are the source of the components added.

Figures 5.1 and 5.2 are mass balance mixing calculations modelling a Michipicoten Island tholeiite (AK 108) as the parent for volcanic xenoliths at Neys/Ashburton. By adding various combinations of minerals to this volcanic it was found the best solution was obtained by the addition of albite, potassium feldspar, magnetite and apatite. This combination of minerals produce R-squared values of 0.199 and 0.091 for the daughter compositions C2490 and C2330 respectively. C2490 is a xenolith displaying

UNWEIGHTED INPUT DATA:

	PARENT	albite	mag	kspar	apat	DAUGHTER
SIO2	47.60	67.41	0.27	63.66	0.00	51.45
TIO2	1.44	0.00	0.00	0.00	0.00	0.64
AL2O3	15.20	20.50	0.21	19.54	0.00	15.33
FE2O3	0.00	0.00	0.00	0.00	0.00	0.00
FEO	10.52	0.06	92.73	0.09	0.00	8.75
MNO	0.18	0.00	0.00	0.00	0.10	0.17
MGO	7.90	0.10	0.00	0.00	0.10	5.90
CAO	8.80	0.81	0.00	0.50	55.84	9.34
NA2O	2.90	10.97	0.00	0.80	0.00	3.91
K2O	0.60	0.36	0.00	15.60	0.00	2.00
H2O+	0.00	0.15	0.00	0.00	1.86	0.00
H2O-	0.00	0.00	0.00	0.00	0.00	0.00
P2O5	0.14	0.00	0.00	0.00	42.05	0.40

(PARENT-MINERALS=DAUGHTER)

PARENT: ak 108
DAUGHTER: c2490

	SOL'N	% CUMULATE
ak 108	1.000	
albite	0.252	58.484
mag	0.006	1.342
kspar	0.154	35.608
apat	0.020	4.565
c2490	1.431	

R SQUARED = 0.199

	PARENT ANALYSIS	DAUGHTER ANALYSIS	DAUGHTER CALC	WEIGHTED RESID	BULK D
SIO2	22.50	22.94	22.85	0.33	
TIO2	0.68	0.29	0.48	-0.19	
AL2O3	7.19	6.83	7.20	-0.07	
FEO	4.97	3.90	3.89	0.02	
MNO	0.09	0.07	0.06	0.01	
MGO	3.73	2.63	2.62	0.01	
CAO	4.16	4.16	4.10	0.06	
NA2O	1.37	1.75	1.72	0.03	
K2O	0.28	0.89	0.87	0.02	
P2O5	0.07	0.18	0.89	-0.21	
cr	210.000	20.220	146.974	-126.754	0.000
co	52.000	45.600	36.393	9.207	0.000
ni	150.000	54.880	104.981	-50.101	0.000
cu	59.000	54.130	41.293	12.837	0.000
zr	160.000	179.706	111.980	67.726	0.000
y	47.000	28.597	32.894	-4.297	0.000
sr	250.000	639.918	174.969	464.949	0.000
ba	200.000	569.750	139.975	429.775	0.000

FIGURE 5.1

UNWEIGHTED INPUT DATA:

	PARENT	albite	mag	kspar	apat	DAUGHTER
SIO2	47.60	67.41	0.27	63.66	0.00	54.22
TIO2	1.44	0.00	0.00	0.00	0.00	0.65
AL2O3	15.20	20.50	0.21	19.54	0.00	15.28
FE2O3	0.00	0.00	0.00	0.00	0.00	0.00
FEO	10.52	0.06	92.73	0.09	0.00	7.89
MNO	0.18	0.00	0.00	0.00	0.10	0.16
MGO	7.90	0.10	0.00	0.00	0.10	5.01
CAO	8.80	0.31	0.00	0.50	55.84	7.16
NA2O	2.90	10.97	0.00	0.80	0.00	4.79
K2O	0.60	0.36	0.00	15.60	0.00	2.22
H2O+	0.00	0.15	0.00	0.00	1.86	0.00
H2O-	0.00	0.00	0.00	0.00	0.00	0.00
P2O5	0.14	0.00	0.00	0.00	42.05	0.37

(PARENT-MINERALS=DAUGHTER)

PARENT: ak 108
DAUGHTER: c2330

	SOL'N	% CUMULATE
ak 108	1.000	
albite	0.520	68.826
mag	0.010	1.286
kspar	0.213	28.249
apat	0.012	1.640
c2330	1.755	

R SQUARED = 0.091

	PARENT ANALYSIS	DAUGHTER ANALYSIS	DAUGHTER CALC	WEIGHTED RESID
SIO2	22.50	23.41	23.35	0.22
TIO2	0.68	0.28	0.39	-0.11
AL2O3	7.19	6.59	7.30	-0.14
FEO	4.97	3.40	3.40	0.01
MNO	0.09	0.07	0.05	0.02
MGO	3.73	2.16	2.14	0.02
CAO	4.16	3.09	3.06	0.03
NA2O	1.37	2.07	2.04	0.03
K2O	0.28	0.96	0.94	0.02
P2O5	0.07	0.16	0.47	-0.09

					BULK D
cr	210.000	16.630	119.892	-103.262	0.000
co	52.000	45.400	29.688	15.712	0.000
ni	150.000	55.220	85.637	-30.417	0.000
cu	59.000	48.090	33.684	14.406	0.000
zr	160.000	331.950	91.346	240.604	0.000
y	47.000	39.321	26.833	12.488	0.000
sr	250.000	526.099	142.729	383.370	0.000
ba	200.000	471.180	114.183	356.997	0.000

FIGURE 5.2

few effects of assimilation whereas C2330 is a highly assimilated xenolith. Amounts of components added depend on the degree of assimilation of the xenolith. Only 25.2% albite was added to the least assimilated C2490 whereas 52% albite was added to the more highly assimilated xenolith C2330. Potassium feldspar and magnetite also show this relationship of increased addition to the more assimilated xenolith. Apatite results are variable as P_2O_5 contents of the xenoliths show no relationship to degree of assimilation only that concentrations are higher in assimilated xenoliths.

Figures 5.3 and 5.4 are mass balance mixing calculations using a Keweenawan tholeiite, KEW5, as the parent. Addition of the same four minerals used in calculations for AK 108 produces R-squared values of 0.172 and 0.170, with the components showing the relationship of more addition to produce more-assimilated xenoliths. This indicates that the modelling procedure is valid for the general case. Both examples demonstrate that addition of albite, potassium feldspar, magnetite and apatite produce assimilated xenoliths, the amounts added governing the degree of assimilation.

To test further the modelling process, these four minerals were added to a xenolith displaying no effects of assimilation to investigate whether or

UNWEIGHTED INPUT DATA:

	PARENT	albite	mag	kspar	apat	DAUGHTER
SIO2	48.73	67.41	0.27	63.66	0.00	51.45
TIO2	0.82	0.00	0.00	0.00	0.00	0.64
AL2O3	18.02	20.50	0.21	19.54	0.00	15.33
FE2O3	0.00	0.00	0.00	0.00	0.00	0.00
FEO	8.67	0.06	92.73	0.09	0.00	8.75
MNO	0.11	0.00	0.00	0.00	0.10	0.17
MGO	7.77	0.10	0.00	0.00	0.10	5.90
CAO	10.13	0.81	0.00	0.50	55.84	9.34
NA2O	2.39	10.97	0.00	0.80	0.00	3.91
K2O	0.21	0.36	0.00	15.60	0.00	2.00
H2O+	3.29	0.15	0.00	0.00	1.86	0.00
H2O-	0.00	0.00	0.00	0.00	0.00	0.00
P2O5	0.06	0.00	0.00	0.00	42.05	0.40

(PARENT-MINERALS=DAUGHTER)

PARENT: kew 5
DAUGHTER: c2490

	SOL'N	% CUMULATE
kew 5	1.000	
albite	0.260	57.768
mag	0.016	3.605
kspar	0.160	35.448
apat	0.014	3.179
c2490	1.450	

R SQUARED = 0.172

	PARENT ANALYSIS	DAUGHTER ANALYSIS	DAUGHTER CALC	WEIGHTED RESID
SIO2	22.77	22.94	22.98	-0.15
TIO2	0.38	0.29	0.26	0.02
AL2O3	8.42	6.83	8.03	-0.24
FEO	4.05	3.90	3.91	-0.01
MNO	0.05	0.07	0.04	0.04
MGO	3.63	2.63	2.51	0.12
CAO	4.73	4.16	4.14	0.02
NA2O	1.12	1.75	1.55	0.20
K2O	0.10	0.89	0.76	0.13
P2O5	0.03	0.18	0.62	-0.13

					BULK D
cr	140.000	20.220	96.466	-76.246	0.000
co	48.200	45.600	33.212	12.388	0.000
ni	270.000	54.880	186.041	-131.161	0.000
sr	210.000	639.918	144.699	495.220	0.000
rb	2.000	75.469	1.378	74.091	0.000
ba	51.000	569.750	35.141	534.609	0.000
ce	10.500	141.670	7.235	134.435	0.000
la	4.290	73.750	2.956	70.794	0.000

FIGURE 5.3

UNWEIGHTED INPUT DATA:

	PARENT	albite	mag	kspar	apat	DAUGHTER
SIO2	48.73	67.41	0.27	63.66	0.00	54.22
TIO2	0.82	0.00	0.00	0.00	0.00	0.65
AL2O3	18.02	20.50	0.21	19.54	0.00	15.28
FE2O3	0.00	0.00	0.00	0.00	0.00	0.00
FEO	8.67	0.06	92.73	0.09	0.00	7.89
MNO	0.11	0.00	0.00	0.00	0.10	0.16
MGO	7.77	0.10	0.00	0.00	0.10	5.01
CAO	10.13	0.81	0.00	0.50	55.84	7.16
NA2O	2.39	10.97	0.00	0.80	0.00	4.79
K2O	0.21	0.36	0.00	15.60	0.00	2.22
H2O+	3.29	0.15	0.00	0.00	1.86	0.00
H2O-	0.00	0.00	0.00	0.00	0.00	0.00
P2O5	0.06	0.00	0.00	0.00	42.05	0.37

(PARENT-MINERALS=DAUGHTER)

PARENT: kew 5
DAUGHTER: c2330

	SOL'N	% CUMULATE
kew 5	1.000	
albite	0.537	68.257
mag	0.020	2.603
kspar	0.222	28.226
apat	0.007	0.914
c2330	1.786	

R SQUARED = 0.170

	PARENT ANALYSIS	DAUGHTER ANALYSIS	DAUGHTER CALC	WEIGHTED RESID	BULK D
SIO2	22.77	23.41	23.45	-0.18	
TIO2	0.38	0.28	0.21	0.07	
AL2O3	8.42	6.59	7.98	-0.28	
FEO	4.05	3.40	3.41	-0.01	
MNO	0.05	0.07	0.03	0.04	
MGO	3.63	2.16	2.04	0.12	
CAO	4.73	3.09	3.09	0.00	
NA2O	1.12	2.07	1.91	0.16	
K2O	0.10	0.96	0.85	0.10	
P2O5	0.03	0.16	0.26	-0.03	
cr	140.000	16.630	78.241	-61.611	0.000
co	48.200	45.400	26.937	18.463	0.000
ni	270.000	55.220	150.893	-95.673	0.000
sr	210.000	526.099	117.361	408.738	0.000
rb	2.000	114.757	1.118	113.639	0.000
ba	51.000	471.180	28.502	442.678	0.000
ce	10.500	208.320	5.868	202.452	0.000
la	4.290	110.470	2.398	108.072	0.000

FIGURE 5.4

not a contaminated xenolith could be produced. The results are presented in figure 5.5. Using C2490 as the parent and C2330 as the daughter composition, an R-squared value of 0.019 is obtained, indicating that this model is valid also for the Neys/Ashburton xenoliths. Apatite in this case is subtracted as P_2O_5 is present in varying amounts within the xenoliths with no relationship to degree of assimilation, other than being present in increased amounts in affected xenoliths.

The program also allows for the inclusion of trace elements in the calculations, without affecting the result of mass balance mixing. The program predicts the distribution of trace elements in the daughter based on the proportions of minerals added to produce the daughter. For all calculations, trace element distributions do not match those observed in the daughter compositions. This suggests that the trace elements in the assimilation process are controlled by some other process not modelled by these calculations.

5.3 Origin of Contaminated Ferro-edenite Syenite

Modelling of the origin of contaminated ferro-edenite syenites involves the addition of volcanic compositions to a parent ferro-edenite syenite to determine if a contaminated ferro-edenite syenite can be produced.

UNWEIGHTED INPUT DATA:

	PARENT	albite	mag	kspar	apat	DAUGHTER
SIO2	51.45	67.41	0.27	63.66	0.00	54.22
TIO2	0.64	0.00	0.00	0.00	0.00	0.65
AL2O3	15.33	20.50	0.21	19.54	0.00	15.28
FE2O3	0.00	0.00	0.00	0.00	0.00	0.00
FEO	8.75	0.06	92.73	0.09	0.00	7.89
MNO	0.17	0.00	0.00	0.00	0.10	0.16
MGO	5.90	0.10	0.00	0.00	0.10	5.01
CAO	9.34	0.81	0.00	0.50	55.84	7.16
NA2O	3.91	10.97	0.00	0.80	0.00	4.79
K2O	2.00	0.36	0.00	15.60	0.00	2.22
H2O+	0.00	0.15	0.00	0.00	1.86	0.00
H2O-	0.00	0.00	0.00	0.00	0.00	0.00
P2O5	0.40	0.00	0.00	0.00	42.05	0.37

(PARENT-MINERALS=DAUGHTER)

PARENT: c2490
DAUGHTER: c2330

	SOL'N	% CUMULATE
c2490	1.000	
albite	0.139	82.386
mag	0.003	1.243
kspar	0.043	18.538
apat	-0.005	-2.167
c2330	1.230	

R SQUARED = 0.019

	PARENT ANALYSIS	DAUGHTER ANALYSIS	DAUGHTER CALC	WEIGHTED RESID	BULK D
SIO2	22.94	23.41	23.42	-0.05	
TIO2	0.29	0.28	0.23	0.05	
AL2O3	6.83	6.59	7.01	-0.08	
FEO	3.90	3.40	3.41	-0.00	
MNO	0.07	0.07	0.06	0.01	
MGO	2.63	2.16	2.14	0.02	
CAO	4.16	3.09	3.11	-0.02	
NA2O	1.75	2.07	2.07	0.00	
K2O	0.89	0.96	0.96	0.00	
P2O5	0.18	0.16	-0.10	0.08	
cr	20.220	16.630	16.438	0.192	0.000
co	45.600	45.400	37.070	8.330	0.000
ni	54.880	55.220	44.614	10.606	0.000
cu	54.130	48.090	44.004	4.086	0.000
zn	91.810	106.650	74.635	32.015	0.000
pb	0.030	0.060	0.065	-0.005	0.000
zr	179.706	331.950	146.089	185.861	0.000
y	28.597	39.321	23.247	16.074	0.000
sr	639.918	526.099	520.211	5.888	0.000
rb	75.469	114.757	61.351	53.406	0.000
ba	569.750	471.180	463.169	8.011	0.000
ce	141.670	208.320	115.168	93.152	0.000
la	73.750	110.470	59.954	50.516	0.000

Volcanic rocks added are from Michipicoten Island (Annells, 1974) and the Keweenawan Reference Suite (Basaltic Volcanism Study Project, 1981). Contamination of quartz syenite to form contaminated ferro-edenite syenite was also investigated.

Figures 5.6 through 5.8 are the results of mass balance mixing calculations using a variety of contaminated ferro-edenite syenites from least-contaminated to highly-contaminated. The volcanic xenolith composition added is from Michipicoten Island. Results indicate the addition of a volcanic xenolith into a ferro-edenite syenite may produce a contaminated ferro-edenite syenite. For the least contaminated ferro-edenite syenite composition xenolith addition of 12.5% produces the closest match. This increases to 24% and 75.7% for the more contaminated syenites. The amount of xenolith added varies with the degree of contamination. Little addition results in slight contamination whereas large additions produce highly contaminated compositions.

This trend of differing xenolith amounts added producing varying degrees of assimilation is also seen in figures 5.9 through 5.11 which models origin of contaminated ferro-edenite syenite with the added volcanic rocks being from the Keweenawan Reference Suite. The results obtained are comparable

UNWEIGHTED INPUT DATA:

	PARENT	ak144	DAUGHTER
SIO2	64.75	46.70	62.97
TIO2	0.37	1.80	0.45
AL2O3	15.65	16.30	15.44
FE2O3	0.00	0.00	0.00
FEO	4.50	11.85	5.55
MNO	0.11	0.20	0.12
MGO	0.57	6.90	1.57
CAO	1.66	9.80	2.34
NA2O	5.70	2.40	5.27
K2O	5.30	0.40	4.70
H2O+	0.00	3.80	0.00
H2O-	0.00	0.00	0.00
P2O5	0.01	0.18	0.08

(PARENT-MINERALS=DAUGHTER)

PARENT: c2334
DAUGHTER: c2329

	SOL'N	% CUMULATE
c2334	1.000	
ak144	0.125	%100.000
c2329	1.125	

R SQUARED = 0.337

	PARENT ANALYSIS	DAUGHTER ANALYSIS	DAUGHTER CALC	WEIGHTED RESID
SIO2	65.66	63.94	63.75	0.19
TIO2	0.37	0.46	0.54	-0.08
AL2O3	15.87	15.67	15.99	-0.31
FEO	4.57	5.64	5.42	0.22
MNO	0.11	0.12	0.12	-0.01
MGO	0.58	1.59	1.30	0.29
CAO	1.68	2.38	2.62	-0.24
NA2O	5.78	5.35	5.41	-0.06
K2O	5.37	4.77	4.82	-0.05
P2O5	0.01	0.08	0.03	0.05

FIGURE 5.6

UNWEIGHTED INPUT DATA:

	PARENT	ak144	DAUGHTER
SIO2	64.75	46.70	61.00
TIO2	0.37	1.80	0.48
AL2O3	15.65	16.30	16.00
FE2O3	0.00	0.00	0.00
FEO	4.50	11.85	5.84
MNO	0.11	0.20	0.15
MGO	0.57	6.90	1.75
CAO	1.66	9.80	3.45
NA2O	5.70	2.40	5.16
K2O	5.30	0.40	4.63
H2O-	0.00	3.80	0.00
H2O-	0.00	0.00	0.00
P2O5	0.01	0.13	0.14

(PARENT-MINERALS=DAUGHTER)

PARENT: c2334
DAUGHTER: c2335

	SOL'N	% CUMULATE
c2334	1.000	
ak144	0.240	%100.000
c2335	1.240	

R SQUARED = 0.404

	PARENT ANALYSIS	DAUGHTER ANALYSIS	DAUGHTER CALC	WEIGHTED RESID
SIO2	65.66	61.87	62.30	-0.44
TIO2	0.37	0.49	0.66	-0.18
AL2O3	15.87	16.22	16.07	0.15
FEO	4.57	5.92	6.06	-0.14
MNO	0.11	0.15	0.13	0.02
MGO	0.58	1.77	1.85	-0.08
CAO	1.68	3.50	3.33	0.18
NA2O	5.78	5.24	5.14	0.10
K2O	5.37	4.70	4.41	0.29
P2O5	0.01	0.14	0.04	0.09

FIGURE 5.7

UNWEIGHTED INPUT DATA:

	PARENT	ak144	DAUGHTER
SIO2	64.75	46.70	54.70
TIO2	0.37	1.00	0.61
AL2O3	15.65	16.30	15.50
FE2O3	0.00	0.00	0.00
FEO	4.50	11.83	7.68
MNO	0.11	0.20	0.16
MGO	0.57	6.90	4.17
CAO	1.66	9.80	7.02
NA2O	5.70	2.40	4.35
K2O	5.30	0.40	2.79
H2O-	0.00	3.80	1.79
H2O-	0.00	0.00	0.00
P2O5	0.01	0.18	0.37

(PARENT-MINERALS=DAUGHTER)

PARENT: c2034
DAUGHTER: c2059

	SOL'N	% CUMULATE
c2034	1.000	
ak144	1.130	%100.000
c2059	2.130	

R SQUARED = 2.576

	PARENT ANALYSIS	DAUGHTER ANALYSIS	DAUGHTER CALC	WEIGHTED RESID
SIO2	65.66	56.19	56.44	-0.25
TIO2	0.37	0.62	1.17	-0.54
AL2O3	15.87	15.92	16.41	-0.49
FEO	4.57	7.89	8.68	-0.79
MNO	0.11	0.16	0.16	-0.00
MGO	0.58	4.28	4.08	0.20
CAO	1.68	7.21	6.20	1.01
NA2O	5.78	4.47	4.02	0.45
K2O	5.37	2.87	2.73	0.14
P2O5	0.01	0.38	0.10	0.27

FIGURE 5.8

UNWEIGHTED INPUT DATA:

	PARENT	kew11	DAUGHTER
SIO2	64.75	50.54	62.97
TIO2	0.37	1.49	0.45
AL2O3	15.65	16.59	15.44
FE2O3	0.00	0.00	0.00
FEO	4.50	10.55	5.55
MNO	0.11	0.16	0.12
MGO	0.57	4.51	1.57
CAO	1.66	10.06	2.34
NA2O	5.70	3.23	5.27
K2O	5.30	0.76	4.70
H2O+	0.00	1.38	0.00
H2O-	0.00	0.74	0.00
P2O5	0.01	0.23	0.08

(PARENT-MINERALS=DAUGHTER)

PARENT: c2334
DAUGHTER: c2329

	SOL'N	% CUMULATE
c2334	1.000	
kew11	0.140	%100.000
c2329	1.140	

R SQUARED = 0.620

	PARENT ANALYSIS	DAUGHTER ANALYSIS	DAUGHTER CALC	WEIGHTED RESID
SIO2	65.66	63.94	63.92	0.02
TIO2	0.37	0.46	0.51	-0.06
AL2O3	15.87	15.67	16.00	-0.33
FEO	4.57	5.64	5.33	0.31
MNO	0.11	0.12	0.12	-0.00
MGO	0.58	1.59	1.07	0.52
CAO	1.68	2.38	2.74	-0.36
NA2O	5.78	5.35	5.47	-0.12
K2O	5.37	4.77	4.81	-0.03
P2O5	0.01	0.08	0.04	0.04

FIGURE 5.9

UNWEIGHTED INPUT DATA:

	PARENT	kew 3	DAUGHTER
SIO2	64.75	47.19	61.00
TIO2	0.37	0.95	0.48
AL2O3	15.65	17.04	16.00
FE2O3	0.00	0.00	0.00
FEO	4.50	10.06	5.34
MNO	0.11	0.14	0.15
MGO	0.57	8.11	1.75
CAO	1.66	10.76	3.45
NA2O	5.70	2.23	5.16
K2O	5.30	0.35	4.63
H2O+	0.00	2.55	0.00
H2O-	0.00	0.00	0.00
P2O5	0.01	0.13	0.14

(PARENT-MINERALS=DAUGHTER)

PARENT: c2334
DAUGHTER: c2335

	SOL'N	% CUMULATE
c2334	1.000	
kew 3	0.232	%100.000
c2335	1.232	

R SQUARED = 0.569

	PARENT ANALYSIS	DAUGHTER ANALYSIS	DAUGHTER CALC	WEIGHTED RESID
SIO2	65.66	61.87	62.43	-0.57
TIO2	0.37	0.49	0.49	-0.00
AL2O3	15.87	16.22	16.20	0.03
FEO	4.57	5.92	5.67	0.25
MNO	0.11	0.15	0.12	0.03
MGO	0.58	1.77	2.06	-0.28
CAO	1.68	3.50	3.47	0.03
NA2O	5.78	5.24	5.12	0.12
K2O	5.37	4.70	4.42	0.28
P2O5	0.01	0.14	0.03	0.10

FIGURE 5.10

UNWEIGHTED INPUT DATA:

	PARENT	kew 3	DAUGHTER
SIO2	64.75	47.19	54.70
TIO2	0.37	0.95	0.61
AL2O3	15.65	17.04	15.50
FE2O3	0.00	0.00	0.00
FEO	4.50	10.06	7.68
MNO	0.11	0.14	0.16
MGO	0.57	8.11	4.17
CAO	1.66	10.76	7.02
NA2O	5.70	2.23	4.35
K2O	5.30	0.35	2.79
H2O+	0.00	2.55	1.79
H2O-	0.00	0.00	0.00
P2O5	0.01	0.13	0.37

(PARENT-MINERALS=DAUGHTER)

PARENT: c2334
DAUGHTER: c2059

	SOL'N	% CUMULATE
c2334	1.000	
kew 3	1.095	%100.000
c2059	2.095	

R SQUARED = 1.906

	PARENT ANALYSIS	DAUGHTER ANALYSIS	DAUGHTER CALC	WEIGHTED RESID
SIO2	65.66	56.19	56.69	-0.50
TIO2	0.37	0.62	0.69	-0.07
AL2O3	15.87	15.92	16.77	-0.85
FEO	4.57	7.89	7.63	0.26
MNO	0.11	0.16	0.13	0.03
MGO	0.58	4.28	4.69	-0.40
CAO	1.68	7.21	6.65	0.56
NA2O	5.78	4.47	3.94	0.53
K2O	5.37	2.87	2.73	0.14
P2O5	0.01	0.38	0.08	0.30

FIGURE 5.11

to the above calculations. Addition of basic volcanics to ferro-edenite syenite results in the production of contaminated ferro-edenite syenite with the degree of contamination varying with the amounts of volcanic material added.

Figures 5.12 through 5.14 show that addition of least-assimilated Neys/Ashburton xenolith compositions also results in the production of contaminated ferro-edenite syenite from ferro-edenite syenite. When the composition of xenolith C2311 is added, it produces the same trends as seen by addition of Michipcoten Island and Keweenawan Reference Suite volcanic rocks.

In the above cases it is observed the R-squared value is high (2.576, 1.906 and 6.333 respectively) for the most contaminated samples. This is the result of two possibilities. Either the xenolith composition chosen is not compositionally similiar to that of the Neys/Ashburton xenoliths or it is possible that addition of more contaminated xenoliths is needed to produce highly contaminated ferro-edenite syenite. To test the latter possibility, conditions were remodelled using addition of a more assimilated xenolith, C2490, to an uncontamined ferro-edenite syenite. The results are presented in figure 5.15. The R-squared value is 0.159 for 253.3% volcanic xenolith

UNWEIGHTED INPUT DATA:

	PARENT	c2311	DAUGHTER
SIO2	64.75	49.69	62.97
TIO2	0.37	0.89	0.45
AL2O3	15.65	15.21	15.44
FE2O3	0.00	0.00	0.00
FEO	4.50	10.43	5.55
MNO	0.11	0.21	0.12
MGO	0.57	4.61	1.57
CAO	1.66	8.04	2.34
NA2O	5.70	6.28	5.27
K2O	5.30	1.84	4.70
H2O+	0.00	0.00	0.00
H2O-	0.00	0.00	0.00
P2O5	0.01	0.60	0.08

(PARENT-MINERALS=DAUGHTER)

PARENT: c2334
DAUGHTER: c2329

	SOL'N	% CUMULATE
c2334	1.000	
c2311	0.165	%100.000
c2329	1.165	

R SQUARED = 0.720

	PARENT ANALYSIS	DAUGHTER ANALYSIS	DAUGHTER CALC	WEIGHTED RESID
SIO2	65.66	63.94	63.56	0.38
TIO2	0.37	0.46	0.45	0.01
AL2O3	15.87	15.67	15.83	-0.16
FEO	4.57	5.64	5.43	0.21
MNO	0.11	0.12	0.13	-0.01
MGO	0.58	1.59	1.16	0.43
CAO	1.68	2.38	2.60	-0.23
NA2O	5.78	5.35	5.87	-0.51
K2O	5.37	4.77	4.88	-0.11
P2O5	0.01	0.08	0.09	-0.01

FIGURE 5.12

UNWEIGHTED INPUT DATA:

	PARENT	c2311	DAUGHTER
SIO2	64.75	49.69	61.00
TIO2	0.37	0.89	0.48
AL2O3	15.65	15.21	16.00
FE2O3	0.00	0.00	0.00
FEO	4.50	10.43	5.84
MNO	0.11	0.21	0.15
MGO	0.57	4.61	1.75
CAO	1.66	8.04	3.45
NA2O	5.70	6.28	5.16
K2O	5.30	1.84	4.63
H2O+	0.00	0.00	0.00
H2O-	0.00	0.00	0.00
P2O5	0.01	0.60	0.14

(PARENT-MINERALS=DAUGHTER)

PARENT: c2334
DAUGHTER: c2335

	SOL'N	% CUMULATE
c2334	1.000	
c2311	0.339	%100.000
c2335	1.339	

R SQUARED = 0.812

	PARENT ANALYSIS	DAUGHTER ANALYSIS	DAUGHTER CALC	WEIGHTED RESID
SIO2	65.66	61.87	61.90	-0.04
TIO2	0.37	0.49	0.51	-0.02
AL2O3	15.87	16.22	15.79	0.43
FEO	4.57	5.92	6.11	-0.19
MNO	0.11	0.15	0.14	0.01
MGO	0.58	1.77	1.62	0.15
CAO	1.68	3.50	3.33	0.17
NA2O	5.78	5.24	5.94	-0.70
K2O	5.37	4.70	4.49	0.21
P2O5	0.01	0.14	0.16	-0.02

FIGURE 5.13

UNWEIGHTED INPUT DATA:

	PARENT	c2311	DAUGHTER
SIO2	64.73	49.69	54.70
TIO2	0.37	0.89	0.61
AL2O3	15.65	15.21	15.50
FE2O3	0.00	0.00	0.00
FEO	4.50	10.43	7.63
MNO	0.11	0.21	0.16
MGO	0.57	4.61	4.17
CAO	1.66	0.04	7.02
NA2O	5.70	6.23	4.35
K2O	5.30	1.34	2.79
H2O-	0.00	0.00	1.79
H2O-	0.00	0.00	0.00
P2O5	0.01	0.60	0.37

(PARENT-MINERALS=DAUGHTER)

PARENT: c2334
DAUGHTER: c2059

	SOL'N	% CUMULATE
c2334	1.000	
c2311	2.309	%100.000
c2059	3.309	

R SQUARED = 6.333

	PARENT ANALYSIS	DAUGHTER ANALYSIS	DAUGHTER CALC	WEIGHTED RESID
SIO2	63.66	56.19	55.41	0.78
TIO2	0.37	0.62	0.74	-0.12
AL2O3	15.37	15.92	15.65	0.27
FEO	4.57	7.89	8.78	-0.89
MNO	0.11	0.16	0.18	-0.02
MGO	0.58	4.28	3.43	0.85
CAO	1.63	7.21	6.19	1.02
NA2O	5.78	4.47	6.22	-1.75
K2O	5.37	2.87	2.96	-0.09
P2O5	0.01	0.38	0.42	-0.05

FIGURE 5.14

UNWEIGHTED INPUT DATA:

	PARENT	c2490	DAUGHTER
SIO2	64.75	51.45	54.70
TIO2	0.37	0.64	0.61
AL2O3	13.65	13.33	15.50
FE2O3	0.00	0.00	0.00
FEO	4.50	8.75	7.68
MNO	0.11	0.17	0.16
MGO	0.57	5.90	4.17
CAO	1.66	9.34	7.02
NA2O	5.70	3.91	4.35
K2O	5.30	2.00	2.79
H2O-	0.00	0.00	1.79
H2O-	0.00	0.00	0.00
P2O5	0.01	0.40	0.37

(PARENT-MINERALS=DAUGHTER)

PARENT: c2334
DAUGHTER: c2059

	SOL'N	% CUMULATE
c2334	1.000	
c2490	2.533	%100.000
c2059	3.533	

R SQUARED = 0.159

	PARENT ANALYSIS	DAUGHTER ANALYSIS	DAUGHTER CALC	WEIGHTED RESID
SIO2	65.66	56.19	56.26	-0.07
TIO2	0.37	0.62	0.58	0.05
AL2O3	13.87	15.92	15.72	0.20
FEO	4.57	7.89	7.70	0.19
MNO	0.11	0.16	0.15	0.01
MGO	0.58	4.28	4.49	-0.20
CAO	1.68	7.21	7.32	-0.11
NA2O	5.78	4.47	4.50	-0.03
K2O	5.37	2.87	2.98	-0.12
P2O5	0.01	0.38	0.30	0.08

FIGURE 5.15

added. The large amount of xenolith addition required is implausible and suggests that the simple mixing procedure is not valid for this case..

Figures 5.16 and 5.17 are the results of mass balance mixing calculations modelling quartz syenites as parents to the contaminated ferro-edenite syenites. On average R-squared values are greater than one, this indicating they are not possible parents. Ferro-edenite syenites produce a much better fit to the model as potential parents.

5.4 Principal Component Analysis

Variation diagrams for SiO_2 vs major oxide components for whole rock compositions of xenoliths and host syenites are plotted on figure 5.18. Compositions from this study are combined with those reported by Lukosius-Sanders (1988). The plots show linear relationships between the end-members ferro-edenite syenite and xenoliths with contaminated ferro-edenite syenite lying intermediate between the two. This suggests that the three rock types are related. To study further the relationship between Neys/Ashburton xenoliths, ferro-edenite syenite and contaminated ferro-edenite syenite, principal component analysis is used.

Principal component analysis was carried out using the subroutine principal components of Multivariant Methods contained within the

UNWEIGHTED INPUT DATA:

	PARENT	kew 3	DAUGHTER
SIO2	64.10	47.19	62.97
TIO2	0.39	0.95	0.45
AL2O3	16.00	17.04	15.44
FE2O3	0.00	0.00	0.00
FEO	4.92	10.06	5.55
MNO	0.14	0.14	0.12
MGO	0.36	8.11	1.57
CAO	1.30	10.76	2.34
NA2O	5.99	2.23	5.27
K2O	5.66	0.35	4.70
H2O+	0.00	2.55	0.00
H2O-	0.00	0.00	0.00
P2O5	0.06	0.13	0.08

(PARENT-MINERALS=DAUGHTER)

PARENT: c2473
DAUGHTER: c2329

	SOL'N	% CUMULATE
c2473	1.000	
kew 3	0.127	%100.000
c2329	1.127	

R SQUARED = 1.628

	PARENT ANALYSIS	DAUGHTER ANALYSIS	DAUGHTER CALC	WEIGHTED RESID
SIO2	64.80	63.94	63.00	0.93
TIO2	0.39	0.46	0.46	-0.00
AL2O3	16.17	15.67	16.33	-0.66
FEO	4.97	5.64	5.57	0.06
MNO	0.14	0.12	0.14	-0.03
MGO	0.36	1.59	1.25	0.34
CAO	1.31	2.38	2.40	-0.02
NA2O	6.06	5.35	5.64	-0.28
K2O	5.72	4.77	5.13	-0.35
P2O5	0.06	0.08	0.07	0.01

FIGURE 5.16

UNWEIGHTED INPUT DATA:

	PARENT	kew 5	DAUGHTER
SIO2	64.10	48.73	62.97
TIO2	0.39	0.82	0.45
AL2O3	16.00	18.02	15.44
FE2O3	0.00	0.00	0.00
FEO	4.92	8.67	5.55
MNO	0.14	0.11	0.12
MGO	0.36	7.77	1.57
CAO	1.30	10.13	2.34
NA2O	5.99	2.39	5.27
K2O	5.66	0.21	4.70
H2O+	0.00	3.29	0.00
H2O-	0.00	0.00	0.00
P2O5	0.06	0.06	0.08

(PARENT-MINERALS=DAUGHTER)

PARENT: c2473
DAUGHTER: c2329

	SOL'N	% CUMULATE
c2473	1.000	
kew 5	0.132	%100.000
c2329	1.132	

R SQUARED = 1.614

	PARENT ANALYSIS	DAUGHTER ANALYSIS	DAUGHTER CALC	WEIGHTED RESID
SIO2	64.80	63.94	63.13	0.81
TIO2	0.39	0.46	0.45	0.01
AL2O3	16.17	15.67	16.45	-0.78
FEO	4.97	5.64	5.43	0.20
MNO	0.14	0.12	0.14	-0.02
MGO	0.36	1.59	1.25	0.34
CAO	1.31	2.38	2.37	0.01
NA2O	6.06	5.35	5.64	-0.29
K2O	5.72	4.77	5.09	-0.31
P2O5	0.06	0.08	0.06	0.02

FIGURE 5.17

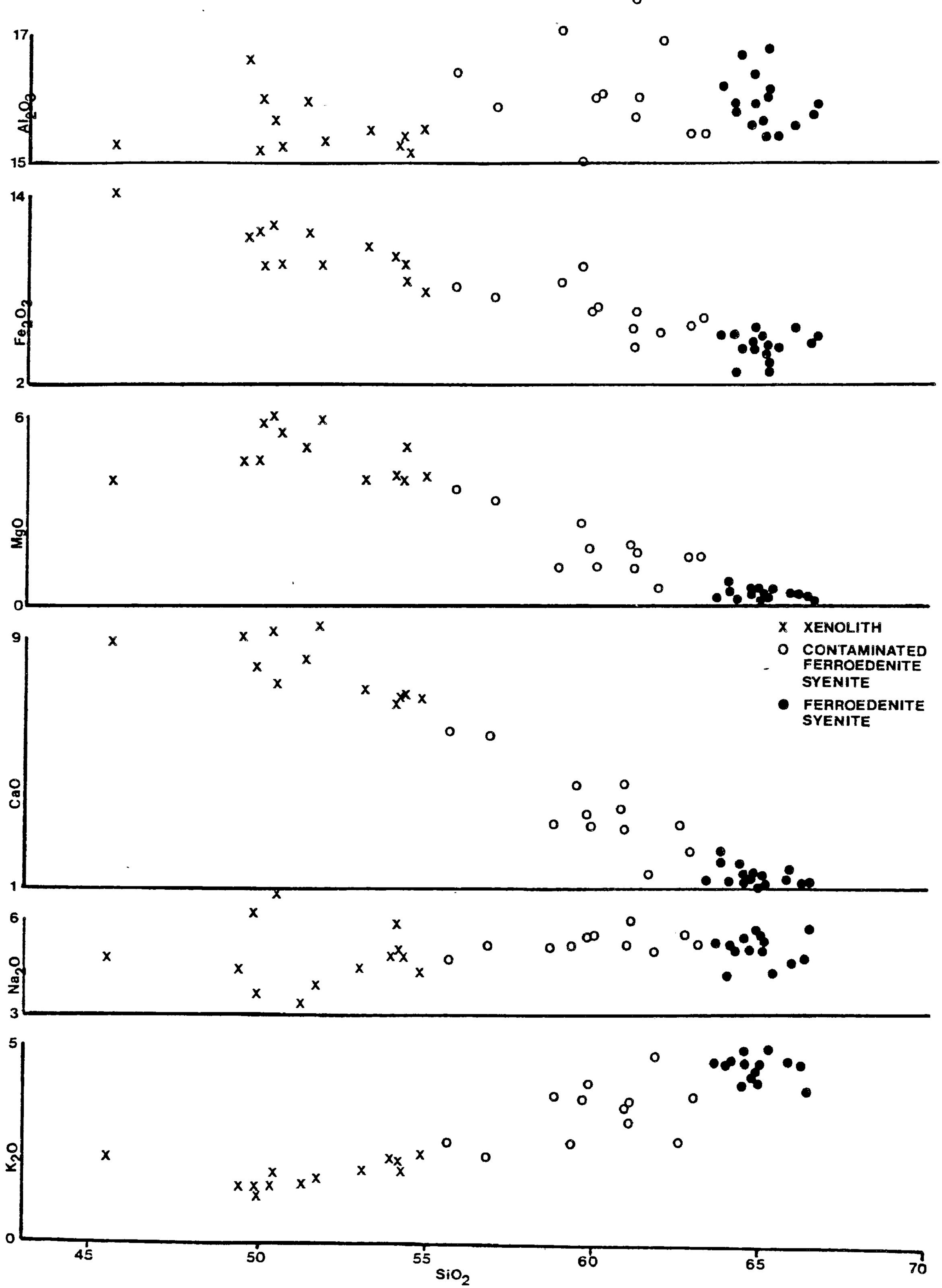

FIGURE 5.18 HARKER DIAGRAM FOR NEYS/ASHBURTON WHOLE ROCK ANALYSES

Statgraphics Statistical Graphics System, designed by the Statistical Graphics Corporation. Ordinary variation diagrams do not account for all the variation inherent in the data set. In principal component analysis all data is used such that all variance in the raw data is accounted for. Principal components that explain most of the variance can be identified in a data set such that the others may be discarded reducing the number of variables to consider. Plots of principal components are equivalent to n-dimensional orthogonal variation diagrams.

In this study the data set is the whole rock composition of xenoliths and host syenites. MnO and P_2O_5 are deleted from the principal component analysis as they contribute very little to the variance in the data set. Principal component analysis of the eight major oxides SiO_2, TiO_2, Al_2O_3, Fe_2O_3, CaO, MgO, Na_2O, and K_2O generates Table 5.1 which shows the proportion of the total variance accounted for by each component. In this case the first three components account for over 90% of the total variance encountered.

Figures 5.19 and 5.20 are scatter plots of component 1 vs components 2

TABLE 5.1 PRINCIPAL COMPONENTS ANALYSIS FOR FERRO-EDENITE SYENITE, CONTAMINATED FERRO-EDENITE SYENITE AND XENOLITHS FROM NEYS/ASHBURTON

COMPONENT NUMBER	PERCENT OF VARIANCE	CUMULATIVE PERCENTAGE
1	63.75933	63.75933
2	19.35054	83.10987
3	7.41613	90.52599
4	5.31908	95.84507
5	2.41470	98.25978
6	1.20900	99.46877
7	0.47446	99.94323
8	0.05677	100.00000

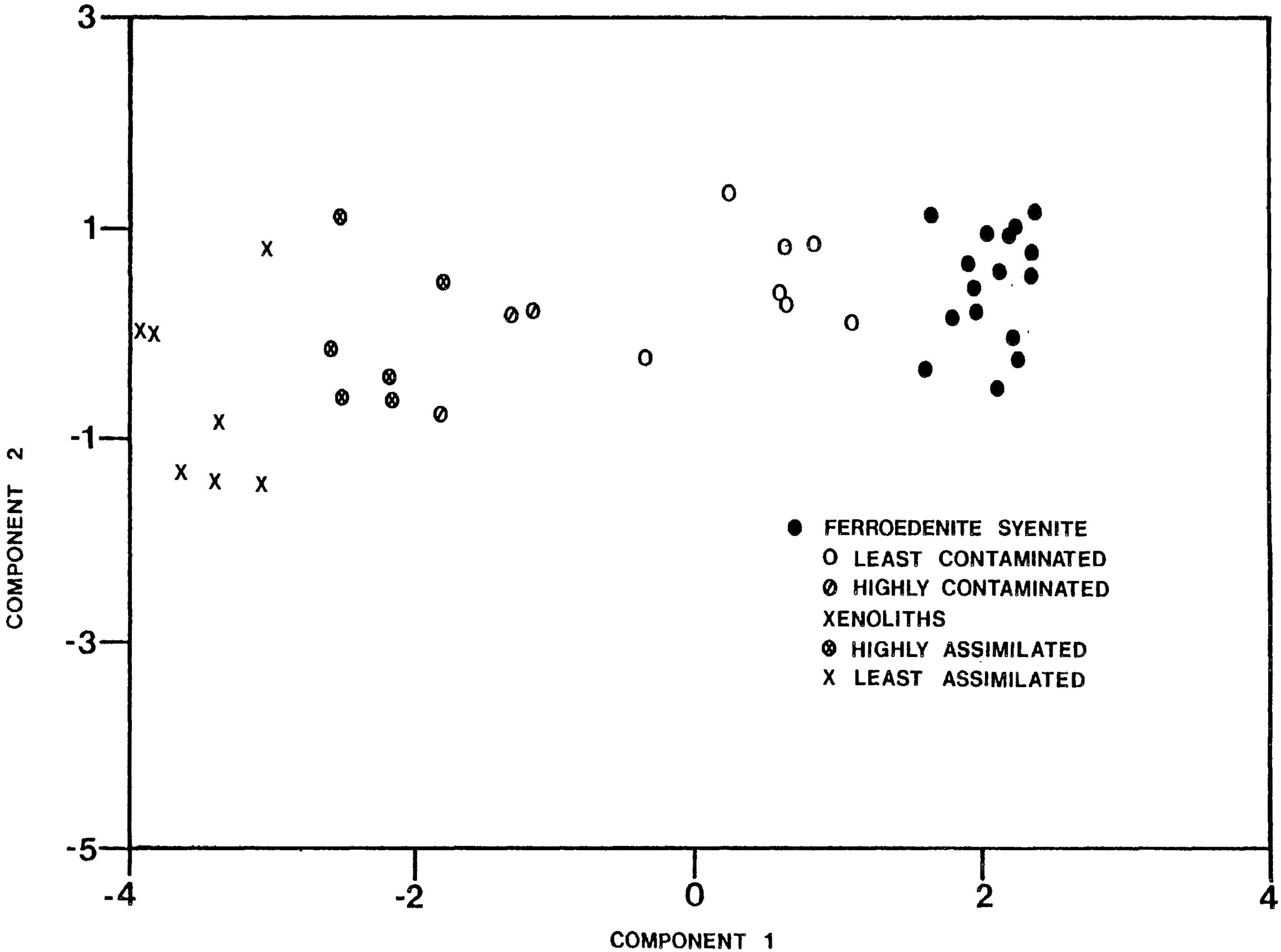

FIGURE 5.19 SCATTERPLOT OF PRINCIPAL COMPONENTS ANALYSIS

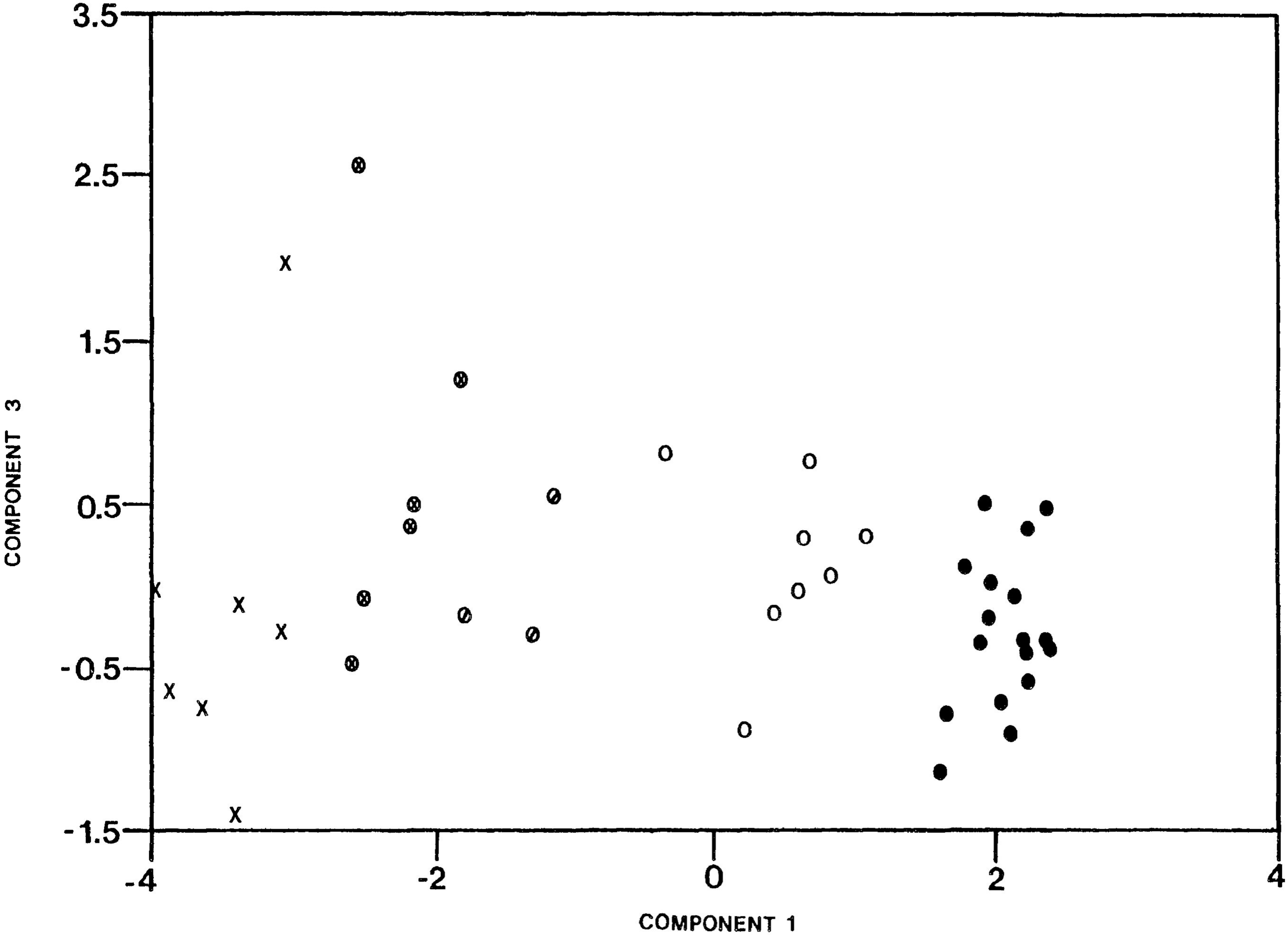

FIGURE 5.20 SCATTERPLOT OF PRINCIPAL COMPONENTS

and 3 respectively. Xenoliths plot to the left-hand side of each figure within a small field. Within this field it is found that least assimilated xenoliths range to more assimilated xenoliths.

Ferro-edenite syenites all plot together in a tight group on the right-hand side of each diagram.

Between ferro-edenite syenite and the xenoliths is a wide spread of data points representing contaminated ferro-edenite syenite. Identification of data points (figures 5.19 and 5.20) leads to the observation that highly-contaminated ferro-edenite syenites plot towards the xenolith end of the distribution pattern and slightly-contaminated ferro-edenite syenite plots toward the ferro-edenite syenite end of the distribution pattern. This is significant in that it suggests that contaminated ferro-edenite syenites are the result of the direct assimilation of Neys/Ashburton volcanic xenoliths by ferro-edenite syenite. This supports the conclusions reached from the mass balance mixing calculations outlined in section 5.3.

Summary

Volcanics that produced the xenoliths found in the Neys/Ashburton study area and the megaxenolith are postulated to be coeval with the production of the Coldwell Alkaline Complex and to have formed cap rock lavas. Bulk rock composition and pyroxene compositional variation indicate they were of an evolved tholeiitic basalt character. Cauldron subsidence may have caused their brecciation and subsequent inclusion into the Coldwell syenites.

Modelling by mass balance mixing calculations indicate volcanic xenoliths are assimilated by the equilibration of their mineral assemblages with that of the host syenites. Ferro-edenite syenite is seen to be the parent of contaminated ferro-edenite syenite.

Further study of the xenoliths in the Neys/Ashburton area is needed to determine if there are two types of xenoliths present. Trace element behavior in the assimilation process also requires further investigation as mass balance mixing modelled in this study is inadequate.

REFERENCES

Annells,R.,1974. Keweenawan volcanic rocks of Michipicoten Island Lake Superior, Ontario, an eruptive centre of Proterozoic age. Geol.Surv.Can.Bull.218, 141p.

Basaltic Volcanism Study Project, 1981. Basaltic volcanism on the terrestrial planets. Pergamon Press,Inc., New York, 1286p.

Deer,W., Howie,R. & Zussman,J.,1978. Rock Forming Minerals. Volume 2A. Single Chain Silicates(2nd ed.). John Wiley & Sons. 668p.

Geist,D.,Baker,B., & McBirney,A.,1985. GPP: A program package for creating and using Geochemical Data Files.

Hawthorne,F.,1981. Crystal chemistry of the amphiboles in Veblen.D.(ed). Amphiboles and other hydrous Pyriboles-Mineralogy. Reviews in Mineralogy,Vol.9A, Min.Soc.Am., pp1-120.

Jago,B.,1980. Geology of a Portion Of the Weatern Contact Margin, the Coldwell Complex. Unpublished BSc. thesis, Lakehead University, Thunder Bay, Ontario. 98p.

LeTerrier,J., Maury,R., Thonon,P., Girard,D. & Marchal,M.,1982. Clinopyroxene composition as a method of identification of the magmatic affinities of paleo-volcanic series. Earth Plan.Sci.Lett., Vol.59, 139-154.

Lowder,G.,1973. Late Cenozoic Transitional Alkali-Olivine-Tholeiitic Basalt and Andesite from the Margin of the Great Basin, Southwest Utah. Geol.Soc.Am.Bull., Vol.84, pp2993-3012.

Lukosius-Sanders,J.,1988. Petrology of Syenites from Centre 3 of the Coldwell Alkaline Complex, Northwest Ontario. Unpublished MSc. thesis, Lakehead University, Thunder Bay, Ontario.110p.

Magonthier,M. & Velde,D.1976. Mineralogy and Petrology of some Tertiary Leucite-Rhonite basanites from central France. Mineral Mag., 40, pp817-826.

Mitchell,R. & Platt,R.G.,1978. Mafic mineralogy of Ferro-augite Syenite from the Coldwell Alkaline Complex, Ontario, Canada. Jour.Pet.,Vol.19, Part 4, pp627-651.

Mitchell,R. & Platt,R.G.,1982. Mineralogy and Petrology of Nepheline Syenites from the Coldwell Alkaline Complex, Ontario, Canada. Jour.Pet., Vol.23, Part 2, pp186-214.

Mitchell,R., Platt,R.G. & Cheadle,S.,1983. A gravity Study of the Coldwell Complex, Northwestern Ontario and its Petrological Significance. Can.Jour,Earth Sci., Vol.20, No.11, pp1631-1638.

Morimoto,N.,1989. Nomenclature of Pyroxenes. Can.Min., Vol.27, pp143-156.

Platt,R.G. & Mitchell,R., 1982. Rb-Sr Geochronolgy of the Coldwell Complex, Northwestern Ontario, Canada. Can.Jour.Earth Sci., Vol.19, pp1796-1801.

Statistical Graphics Corporation 1986. STATGRAPHICS,Statistical Graphics System, Rockville.MD.

Stormer,J.,1985. ROCALC. A program for calculating normative calculations.

Streckeisen,A. & LeMaitre,R.,1979. A chemical approximation to the Modal QAPF Classification of the Igneous Rocks. N.Jb.Miner.Abh., Vol.136. pp169-206.

Sutcliffe,R.,1987. Petrology of Middle Proterozoic diabases and Picrites from Lake Nipigon, Canada. Contrib.Min.Petrl., Vol.96, pp201-211.

Walker,J.,1967 Geology of the Jackfish-Middleton Area. Ont.Dept. of Mines, Geol.Rpt. 50, 41p

APPENDIX 1

MICROPROBE ANALYSIS

Circular, one-inch diameter polished discs were studied using a Hitachi S-570 Scanning Electron Microscope at Lakehead University, Thunder Bay, Ontario. Quantitative analysis was accomplished using energy dispersive x-ray spectrometry and the Tracor Northern MICROQ program(full ZAF correction procedure). Counting time ranged from 80 to 100 seconds with an accelerating voltage of 20 KeV, a beam current of 0.38 nA and spot size of approximately 1 um. Standards used were minerals similiar in composition to those analysed.

APPENDIX 2 AMPHIBOLE COMPOSITIONS FOR NEYS/ASHBURTON XENOLITHS

	C2328A	C2328A	C2328A	C2328A	C2328A	C2328A	C2328A	C2328A	C2328A	C2331
SiO2	43.14	44.33	43.88	43.15	43.57	43.48	41.60	42.29	42.92	40.50
Al2O3	7.40	7.36	8.04	7.19	8.10	7.77	7.84	7.43	8.54	10.68
FeO	21.10	21.07	22.12	22.05	21.51	21.86	21.58	22.14	20.91	23.04
MnO	0.04	0.03	0.05	0.04	0.02	0.03	0.05	0.04	0.04	0.07
TiO2	1.04	0.98	1.16	1.26	1.18	1.05	0.91	1.38	1.21	1.92
MgO	8.65	9.59	8.41	8.38	9.17	8.00	8.29	8.06	10.29	5.92
CaO	11.33	11.23	11.28	11.67	11.52	11.78	11.35	11.65	9.68	11.23
Na2O	3.49	2.26	1.52	1.34	2.45	1.21	2.96	2.28	1.92	1.94
K2O	1.28	1.20	1.25	1.26	1.29	1.34	1.55	1.21	2.61	1.65
TOTAL	97.48	98.06	97.72	96.33	98.81	96.52	96.46	96.49	98.12	96.95

	C2331	C2331	C2331	C2331	C2331	C2331	C2331	C2331	C2331	C2331
SiO2	39.71	39.66	40.53	40.22	40.28	40.10	40.15	40.43	39.30	40.15
Al2O3	10.29	11.23	10.90	10.78	10.78	10.92	10.16	11.26	10.78	10.75
FeO	22.94	22.59	22.08	20.92	20.25	21.59	22.47	21.73	21.28	21.61
MnO	0.07	0.04	0.05	0.04	0.02	0.04	0.05	0.06	0.04	0.06
TiO2	1.82	2.49	2.39	2.61	2.66	2.25	2.24	2.16	2.30	2.34
MgO	6.57	6.79	6.64	7.67	7.02	6.83	6.80	6.61	6.84	7.33
CaO	11.53	11.36	11.55	11.76	11.54	11.31	11.29	11.08	11.41	11.58
Na2O	2.03	2.15	1.63	1.65	2.91	3.16	1.36	2.07	1.60	2.31
K2O	1.84	1.87	1.75	1.79	1.83	1.70	1.66	1.44	1.68	1.75
TOTAL	96.81	98.17	97.51	97.44	97.30	97.89	96.17	96.84	95.24	97.87

	C2331	C2331	C2331	C2331	C2331	C2331	C2331	C2331	C2331	C2331
SiO2	39.89	40.46	40.50	40.50	39.15	40.06	40.23	40.36	39.91	38.13
Al2O3	10.41	10.75	10.92	10.45	10.91	10.62	10.77	10.91	10.50	10.50
FeO	22.84	22.82	21.35	23.09	24.76	20.85	22.26	23.47	23.27	22.65
MnO	0.05	0.05	0.03	0.05	0.03	0.04	0.05	0.04	0.04	0.05
TiO2	2.18	1.81	2.60	2.32	0.73	2.93	2.21	2.17	2.33	2.05
MgO	6.43	5.94	7.44	5.63	6.48	6.40	5.90	6.35	6.99	6.30
CaO	11.53	11.17	11.69	11.54	10.87	11.14	11.48	11.38	11.32	10.95
Na2O	1.85	1.88	2.07	2.84	3.25	2.14	2.43	2.81	3.01	3.18
K2O	1.70	1.84	1.56	1.67	1.86	1.77	1.61	1.64	1.73	1.85
TOTAL	96.89	97.04	98.16	98.07	98.05	95.96	96.93	99.12	99.11	95.66

APPENDIX 2 CONTINUED...

	C2331	C2331	C2331	C2358	C2358	C2358	C2358	C2358	C2358	C2358
SiO2	39.66	41.08	40.47	46.80	47.38	48.95	47.93	51.40	48.91	48.86
Al2O3	10.63	11.08	10.92	6.02	4.76	4.70	4.77	4.27	4.07	3.93
FeO	21.67	20.95	20.77	19.85	19.34	19.90	19.95	19.66	20.01	19.60
MnO	0.03	0.04	0.03	0.32	0.28	0.52	0.38	0.41	0.37	0.33
TiO2	2.18	2.32	2.65	1.78	1.29	0.75	0.96	0.66	1.01	0.91
MgO	7.13	7.59	6.96	8.88	9.30	9.97	9.25	9.49	10.20	9.68
CaO	11.40	11.37	11.55	11.45	11.48	10.41	11.19	10.64	11.09	11.34
Na2O	2.83	2.19	2.45	1.71	1.53	1.72	1.85	1.73	1.66	0.88
K2O	1.67	1.73	1.72	0.64	0.52	0.59	0.64	0.47	0.35	0.44
TOTAL	97.21	98.35	97.52	98.29	96.76	98.35	97.53	98.74	98.56	97.20

	C2358	C2358	C2358	C2358	C2358	C2358	C2358	C2358	C2358	C2358
SiO2	48.62	48.69	48.46	48.03	51.08	50.35	48.97	47.48	46.23	46.72
Al2O3	4.19	3.25	4.46	4.81	2.49	3.33	4.66	5.12	6.25	4.22
FeO	20.56	20.80	20.67	21.10	18.80	19.08	20.43	20.36	20.59	20.31
MnO	0.17	0.34	0.40	0.42	0.46	0.36	0.27	0.30	0.56	0.42
TiO2	0.74	0.84	1.06	1.40	0.32	0.46	0.96	1.33	1.57	1.45
MgO	9.01	9.04	9.39	8.76	10.16	10.13	9.41	9.38	8.71	9.50
CaO	11.82	11.63	11.21	10.72	11.68	11.57	11.08	10.94	10.78	10.91
Na2O	1.33	1.05	2.27	1.02	0.71	1.82	3.16	1.23	1.42	2.15
K2O	0.41	0.55	0.44	0.46	0.34	0.29	0.58	0.57	0.64	0.47
TOTAL	97.32	97.31	99.59	98.00	97.12	97.38	99.89	96.72	96.75	96.98

	C2358	C2490	C2490	C2490	C2490	C2498	C2498	C2498	C2498	C2498
SiO2	45.29	47.07	46.60	46.39	47.21	41.51	40.69	40.94	42.98	41.11
Al2O3	6.02	5.93	5.83	6.58	5.98	10.18	10.11	9.79	7.80	9.83
FeO	20.69	18.22	17.85	18.27	18.77	19.47	19.66	19.88	19.55	20.50
MnO	0.41	0.36	0.18	0.28	0.25	0.49	0.38	0.47	0.36	0.44
TiO2	1.59	1.09	1.07	1.09	0.81	1.56	1.46	1.28	0.45	0.99
MgO	8.62	10.15	11.64	10.64	11.07	9.14	9.43	8.84	9.93	8.66
CaO	11.02	11.44	11.54	11.26	11.08	11.35	11.21	11.12	11.71	11.66
Na2O	1.78	2.20	2.53	2.21	1.82	2.35	2.63	2.88	2.51	2.49
K2O	0.64	0.57	0.60	0.79	0.66	1.26	1.15	1.11	1.10	1.01
TOTAL	97.30	97.98	98.88	98.17	97.65	98.19	97.87	97.52	97.41	96.69

APPENDIX 3 AMPHIBOLE COMPOSITIONS FOR WOLF CAMP LAKE MEGAXENOLITH

	C2519	C2519	C2519	C2519	C2519	C2519	C2519	C2519	C2519	C2519
SiO2	44.46	44.60	42.07	42.54	43.35	42.93	43.06	41.85	43.21	42.94
Al2O3	7.97	8.23	7.71	8.32	8.23	7.81	8.16	8.79	8.19	8.22
MgO	9.34	9.09	9.10	8.50	8.95	8.58	8.63	8.73	8.28	7.94
CaO	11.47	11.00	11.23	10.93	11.48	11.22	11.11	11.37	10.91	10.85
Na2O	2.23	1.31	3.31	2.37	2.27	1.75	2.48	1.55	1.49	1.58
K2O	1.18	1.33	1.24	1.22	1.26	1.43	1.41	1.44	1.60	1.39
FeO	20.48	21.89	21.21	21.28	21.18	21.31	21.24	21.42	21.39	21.93
MnO	0.04	0.07	0.04	0.05	0.06	0.04	0.05	0.04	0.05	0.04
TiO2	0.77	0.75	1.53	1.38	1.71	1.43	1.25	1.34	1.76	1.67
TOTAL	97.95	98.28	97.44	96.59	98.49	96.83	97.81	96.53	96.90	96.57

	C2519	C2519	C2519	C2519	C2519	C2519	C2519	C2519	C2519	C2519
SiO2	42.76	41.76	44.72	42.53	42.22	43.47	42.22	42.32	43.15	43.71
Al2O3	8.44	8.28	6.80	7.75	8.37	8.35	7.97	8.58	8.30	8.17
MgO	8.22	7.78	7.89	7.84	6.87	7.14	9.37	6.75	7.19	7.81
CaO	11.21	11.05	10.59	10.77	11.15	11.37	11.30	11.07	11.26	11.22
Na2O	2.98	2.52	0.62	1.64	2.16	1.91	2.02	2.96	1.89	1.81
K2O	1.25	1.30	1.44	1.43	1.41	1.40	1.29	1.25	1.36	1.42
FeO	21.33	21.95	23.73	23.04	23.39	23.40	21.57	24.11	22.29	22.05
MnO	0.04	0.02	0.05	0.06	0.07	0.06	0.03	0.06	0.07	0.06
TiO2	1.48	1.49	1.08	1.54	1.49	1.80	1.47	1.64	1.76	1.49
TOTAL	97.94	96.15	96.92	96.60	97.12	98.89	97.24	98.75	97.27	97.74

	C2531A	C2531A	C2531A	C2531A	C2531A	C2531A
SiO2	40.68	42.62	43.19	39.57	41.14	39.57
Al2O3	9.92	9.21	8.80	10.52	8.89	11.13
MgO	7.10	10.23	10.07	8.42	5.86	8.24
CaO	11.28	11.13	11.58	13.22	10.73	11.67
Na2O	3.59	3.52	2.89	2.84	3.57	3.14
K2O	1.38	1.35	1.38	1.35	1.48	1.25
FeO	21.54	18.62	19.30	16.71	23.60	19.08
MnO	0.39	0.27	0.51	0.56	0.47	0.61
TiO2	2.58	0.94	0.80	4.84	2.03	3.26
TOTAL	98.47	97.88	98.51	98.04	97.77	97.95

APPENDIX 4 AMPHIBOLE COMPOSITIONS FOR WOLF CAMP LAKE HOST SYENITE

	C2515	C2515	C2515	C2515	C2515	C2515	C2515	C2515	C2515	C2515
SiO2	47.08	49.05	47.85	47.91	47.39	47.31	47.10	46.51	48.07	47.20
Al2O3	2.08	1.01	1.09	1.62	1.46	1.56	1.74	1.77	1.43	1.68
MgO	1.45	0.00	0.00	0.00	0.00	0.70	0.73	0.00	0.45	0.81
CaO	6.20	9.11	4.83	4.81	5.18	4.93	5.43	5.30	5.10	5.23
Na2O	5.02	1.38	5.51	5.21	4.18	5.04	4.56	3.71	4.36	4.25
K2O	1.24	0.40	1.05	1.19	1.08	1.21	1.02	1.00	0.96	1.20
FeO	33.16	35.39	36.06	35.14	35.70	35.62	34.92	35.72	34.85	35.21
MnO	0.58	2.06	1.23	1.19	0.94	0.86	1.37	0.87	0.77	0.90
TiO2	1.57	0.00	0.38	0.77	0.63	0.43	0.51	1.28	0.51	0.35
TOTAL	98.38	98.40	98.00	98.74	97.65	97.67	98.73	97.53	96.50	97.79

	C2515	C2515	C2516	C2516	C2516	C2516	C2516	C2516	C2516	C2516
SiO2	47.95	45.80	46.40	47.07	45.99	47.18	45.80	46.80	47.63	46.97
Al2O3	1.76	2.10	2.04	2.22	2.23	2.22	2.13	2.87	1.95	1.65
MgO	1.07	0.00	0.00	0.43	0.00	0.00	0.48	0.84	0.00	0.00
CaO	5.02	5.72	6.30	6.38	6.43	6.23	6.69	6.07	5.80	5.93
Na2O	4.50	4.97	3.82	3.99	3.32	3.74	3.69	4.84	3.47	4.11
K2O	1.14	1.20	1.08	1.17	1.21	1.15	1.15	1.00	1.11	0.89
FeO	34.98	34.22	34.44	34.21	34.44	34.34	34.44	32.65	35.78	35.57
MnO	0.99	0.85	0.88	0.77	0.83	0.71	0.60	0.72	0.71	0.70
TiO2	0.26	1.61	2.10	2.18	2.36	2.52	2.28	2.02	0.81	0.86
TOTAL	98.89	97.21	98.09	98.42	98.01	98.08	98.67	98.81	98.55	98.14

	C2516	C2516	C2516	C2531A	C2531A	C2531A	C2531A	C2531A	C2531A	C2531A
SiO2	47.80	47.36	46.05	42.16	41.77	42.88	41.55	41.09	41.90	41.25
Al2O3	1.79	1.83	2.17	7.60	7.80	6.94	7.84	7.79	8.17	8.24
MgO	0.00	0.62	0.00	5.94	5.53	4.97	5.01	4.03	5.53	4.91
CaO	5.96	6.10	6.33	10.58	10.19	10.71	10.18	10.22	10.19	10.25
Na2O	3.06	3.45	4.11	3.44	3.13	3.01	3.05	3.24	3.26	2.94
K2O	0.94	0.87	1.05	1.27	1.33	1.13	1.27	1.28	1.49	1.48
FeO	35.82	34.57	34.15	23.33	24.77	26.08	26.40	26.94	26.06	25.79
MnO	0.80	0.89	1.05	0.59	0.55	0.65	0.56	0.46	0.73	0.45
TiO2	0.43	0.82	1.37	1.95	1.65	1.30	1.68	2.02	1.62	1.86
TOTAL	98.05	97.94	97.16	96.90	96.71	97.67	98.75	97.08	99.27	97.16

APPENDIX 4 CONTINUED...

	C2531A	C2531A	C2531A
SiO2	41.63	40.86	40.80
Al2O3	8.32	7.90	8.75
MgO	4.99	4.59	4.79
CaO	10.06	10.23	10.27
Na2O	2.12	2.80	3.48
K2O	1.49	1.24	1.30
FeO	25.99	26.21	26.27
MnO	0.61	0.64	0.52
TiO2	1.70	1.61	1.49
TOTAL	97.16	96.74	98.86

APPENDIX 5 PYROXENE COMPOSITIONS FOR NEYS/ASHBURTON XENOLITHS

	C2358	C2358	C2358	C2490	C2490	C2490	C2490	C2490	C2490	C2490
SiO2	52.67	51.99	52.34	51.82	51.90	53.35	50.75	51.45	51.06	50.27
AL2O3	0.33	0.84	0.77	0.97	0.50	0.55	1.25	2.10	0.36	0.00
MnO	0.59	0.48	0.64	0.55	0.65	0.56	0.68	0.39	0.51	0.52
FeO	15.27	15.12	15.99	12.25	14.81	13.68	13.33	11.59	13.54	13.51
MgO	9.10	8.32	8.74	11.82	11.26	11.54	11.03	12.63	9.83	10.51
CaO	21.94	21.01	20.43	22.07	20.99	22.05	21.41	20.70	22.55	22.53
Na2O	0.00	2.00	0.00	0.00	0.00	0.00	0.00	0.00	0.89	1.31
K2O	0.00	0.30	0.00	0.13	0.00	0.00	0.00	0.00	0.00	0.00
TiO2	0.00	0.40	0.23	0.28	0.00	0.00	0.38	0.26	0.00	0.00
TOTAL	99.91	100.80	99.83	99.90	101.62	101.89	100.23	99.13	98.73	98.66

	C2498	C2498	C2498	C2498	C2498	C2498	C2498	C2498	C2498	C2498
SiO2	51.13	51.97	52.53	51.69	51.99	50.88	50.63	52.39	52.39	51.12
Al2O3	0.53	0.00	0.00	0.00	0.50	0.00	0.00	0.00	0.00	0.00
MnO	0.57	0.41	0.51	0.47	0.57	0.49	0.55	0.53	0.47	0.60
FeO	14.73	12.90	13.15	14.08	13.80	13.59	12.99	13.84	13.04	13.49
MgO	10.29	10.88	11.30	10.03	9.57	9.72	10.56	11.00	11.38	11.24
CaO	20.84	22.88	23.47	23.05	23.78	23.38	24.17	22.54	23.15	22.63
Na2O	1.47	0.00	0.00	0.00	0.00	0.00	0.00	0.88	0.00	0.89
K2O	0.00	0.00	0.00	0.00	0.00	0.00	0.00	0.00	0.00	0.00
TiO2	0.14	0.21	0.00	0.00	0.00	0.00	0.00	0.00	0.00	0.00
TOTAL	100.66	99.26	99.96	99.31	100.21	98.53	99.74	101.18	101.15	101.20

	C2498	C2498	C2498
SiO2	51.51	51.72	51.45
Al2O3	0.00	0.00	0.00
MnO	0.53	0.45	0.53
FeO	12.40	12.97	14.22
MgO	12.11	11.53	10.71
CaO	22.12	22.37	22.50
Na2O	0.63	0.68	0.91
K2O	0.00	0.00	0.00
TiO2	0.31	0.17	0.22
TOTAL	100.25	101.16	100.53

APPENDIX 6 PYROXENE COMPOSITIONS FOR WOLF CAMP LAKE MEGAXENOLITH

	C2531A	C2531A	C2531A	C2531A	C2531A	C2531A	C2531A	C2531A	C2531A	C2531A
SiO2	52.26	52.55	51.49	51.21	53.51	51.48	51.87	52.05	51.86	51.75
Al2O3	0.73	0.00	0.00	0.00	0.72	0.00	0.00	0.78	0.49	0.00
CaO	22.45	23.27	22.42	23.31	22.89	22.85	22.67	23.34	22.91	22.53
MgO	9.36	10.66	10.74	10.38	10.00	10.70	11.30	9.98	10.51	11.56
Na2O	0.00	1.57	0.00	0.00	0.00	0.00	0.00	0.00	0.00	0.00
K2O	0.00	0.00	0.00	0.00	0.00	0.00	0.00	0.00	0.00	0.00
FeO	13.81	12.61	13.25	13.66	13.34	13.20	13.23	13.43	13.14	12.54
MnO	0.39	0.75	0.65	0.47	0.49	0.58	0.63	0.46	0.63	0.59
TiO2	0.11	0.00	0.15	0.00	0.31	0.39	0.00	0.17	0.00	0.14
TOTAL	99.10	101.41	98.70	99.04	101.26	99.10	99.70	100.22	99.54	99.11

	C2531A	C2531A	C2531A	C2531A	C2531A	C2531A	C2531A	C2531A	C2531A	C2531A
SiO2	51.41	52.12	51.78	51.82	51.51	52.38	51.50	52.60	52.03	51.83
Al2O3	0.98	0.00	0.61	0.81	0.00	0.85	0.00	1.13	0.00	0.87
CaO	23.18	21.63	22.77	22.74	22.60	24.00	22.78	22.95	22.83	22.79
MgO	9.84	11.78	11.21	9.41	9.84	10.79	10.80	9.29	10.46	9.85
Na2O	0.00	1.44	1.08	0.00	1.27	0.00	0.00	0.82	0.00	0.00
K2O	0.00	0.00	0.00	0.00	0.00	0.00	0.00	0.00	0.00	0.00
FeO	13.35	13.35	12.88	13.33	13.70	13.83	13.94	13.93	13.45	14.35
MnO	0.44	0.75	0.37	0.43	0.72	0.48	0.51	0.56	0.75	0.53
TiO2	0.00	0.22	0.00	0.00	0.00	0.00	0.21	0.00	0.30	0.25
TOTAL	99.20	101.29	100.70	98.54	99.65	101.32	99.74	101.27	99.82	100.47

	C3120	C3120	C3120	C3120	C3120	C3120	C3120	C3120	C3120	C3120
SiO2	50.99	52.27	52.98	53.99	52.90	52.21	50.52	52.37	51.28	52.11
Al2O3	0.00	0.00	0.00	1.27	0.00	0.00	0.00	0.00	0.00	0.36
CaO	1.59	19.40	1.12	13.61	19.21	1.49	1.23	1.26	1.15	1.38
MgO	15.31	10.99	14.77	9.85	9.89	15.00	15.05	14.95	14.56	14.95
Na2O	0.00	0.00	0.00	0.00	0.00	0.00	1.08	0.00	0.00	0.00
K2O	0.00	0.00	0.00	0.00	0.00	0.00	0.00	0.00	0.00	0.00
FeO	30.70	15.75	30.91	19.47	15.68	30.38	30.68	30.47	30.94	30.05
MnO	1.15	0.62	0.99	0.53	0.52	0.93	1.11	1.09	1.10	1.24
TiO2	0.00	0.00	0.22	0.25	0.00	0.00	0.00	0.22	0.00	0.00
TOTAL	99.74	99.55	100.99	98.96	100.16	100.00	99.68	100.36	99.02	100.08

APPENDIX 6 CONTINUED...

	C3120	C3120	C3120	C3120	C3120	C3120	C3120	C3120	C3120	C3120
SiO2	51.78	51.88	52.61	52.39	53.17	52.96	53.25	53.03	52.86	52.87
Al2O3	0.00	0.00	0.67	0.36	1.06	0.38	0.00	0.00	0.59	0.26
CaO	1.07	1.30	20.00	20.49	19.92	20.74	20.61	20.63	20.87	20.96
MgO	15.15	14.18	11.65	11.00	11.02	11.36	12.62	10.78	11.41	11.55
Na2O	0.00	0.00	0.00	0.00	0.00	0.00	0.00	0.00	0.00	0.00
K2O	0.00	0.07	0.00	0.00	0.00	0.00	0.00	0.00	0.00	0.00
FeO	31.63	30.87	14.86	14.52	14.22	13.87	13.40	14.32	14.40	13.86
MnO	1.13	0.99	0.79	0.59	0.97	0.53	0.73	0.79	0.83	0.65
TiO2	0.30	0.13	0.00	0.00	0.31	0.00	0.27	0.23	0.00	0.24
TOTAL	101.06	99.41	100.58	99.36	100.70	99.84	100.89	99.78	100.96	100.38

	C3120	C3120	C3120	C3120	C3120	C3120	C3120	C3120	C3120	C3120
SiO2	52.89	51.83	52.94	52.79	52.75	52.72	52.69	52.34	54.05	52.48
Al2O3	0.55	0.42	0.26	0.00	0.60	0.00	1.06	0.00	0.43	0.00
CaO	20.80	21.02	21.11	21.32	21.13	21.00	21.12	20.45	20.86	20.92
MgO	10.85	11.33	10.41	11.35	11.27	11.16	11.38	11.70	11.35	10.85
Na2O	0.00	0.00	0.00	0.00	0.00	0.00	0.00	0.00	0.00	0.96
K2O	0.00	0.00	0.00	0.00	0.00	0.00	0.00	0.00	0.00	0.00
FeO	14.01	14.05	13.46	13.72	13.63	14.17	12.89	13.68	13.75	14.44
MnO	0.69	0.68	0.70	0.76	0.73	0.54	0.83	0.50	0.69	0.83
TiO2	0.00	0.28	0.16	0.00	0.24	0.31	0.23	0.28	0.12	0.34
TOTAL	99.79	99.61	99.03	99.95	100.36	99.90	100.19	98.96	101.25	100.82

	C3120	C3120	C3120	C3120	C3122	C3122	C3122	C3122	C3122	C3122
SiO2	52.28	52.17	52.71	52.11	53.23	52.92	52.43	51.90	51.78	51.86
Al2O3	0.35	0.00	0.36	0.00	0.52	0.00	0.72	0.68	0.60	0.00
CaO	20.91	20.64	21.14	20.81	20.62	20.38	20.62	19.98	20.23	20.37
MgO	11.20	11.88	11.14	10.84	11.80	11.96	12.12	11.41	11.55	12.18
Na2O	0.00	1.23	0.00	0.00	0.00	0.00	0.00	0.00	0.00	0.00
K2O	0.00	0.00	0.00	0.00	0.00	0.00	0.00	0.00	0.00	0.00
FeO	13.70	14.13	14.02	14.25	13.65	13.56	13.80	13.97	15.29	13.61
MnO	0.81	0.78	0.85	0.65	0.34	0.52	0.55	0.23	0.46	0.58
TiO2	0.18	0.00	0.23	0.23	0.17	0.17	0.26	0.27	0.43	0.51
TOTAL	99.42	100.84	100.45	98.88	100.32	99.51	100.50	98.45	100.33	99.10

APPENDIX 6 CONTINUED ...

	C3122	C3122	C3122	C3122	C3122	C3122	C3122	C3122	C3122	C3122
SiO2	51.88	51.81	52.35	52.60	52.48	52.07	53.05	51.30	5.00	52.21
Al2O3	0.70	0.00	0.00	0.00	0.80	0.65	0.00	0.64	0.00	0.00
CaO	20.92	20.31	20.43	20.42	19.80	20.59	20.47	20.62	20.07	20.34
MgO	12.54	12.35	12.20	11.57	11.75	11.77	12.44	11.87	12.76	11.78
Na2O	0.00	0.00	0.00	0.00	0.00	0.00	0.00	0.00	0.00	0.00
K2O	0.00	0.00	0.00	0.00	0.00	0.00	0.00	0.00	0.00	0.00
FeO	13.17	13.38	14.28	13.46	14.23	13.74	14.00	13.54	13.98	13.49
MnO	0.61	0.52	0.56	0.53	0.50	0.59	0.55	0.60	0.52	0.65
TiO2	0.22	0.30	0.59	0.00	0.00	0.27	0.58	0.51	0.34	0.17
TOTAL	100.04	98.67	100.42	98.58	99.56	99.69	101.09	99.08	100.67	98.65

	C3122	C3122	C3122	C3122	C3122	C3122	C3122	C3123	C3123	C3123
SiO2	53.15	52.39	52.29	52.64	52.39	51.91	52.37	52.02	50.51	48.50
Al2O3	0.00	0.00	0.00	0.00	0.51	0.00	1.55	0.65	1.31	1.39
CaO	20.51	20.69	20.71	21.19	20.58	20.83	20.76	20.61	19.45	19.58
MgO	10.78	12.48	12.31	12.08	11.44	11.88	11.59	11.27	8.85	12.06
Na2O	0.00	0.00	0.94	0.00	0.00	0.00	0.00	0.62	0.00	0.00
K2O	0.00	0.00	0.00	0.00	0.00	0.00	0.00	0.00	0.00	0.00
FeO	13.36	13.50	12.21	12.09	13.10	13.19	13.04	13.14	16.38	14.94
MnO	0.64	0.46	0.51	0.54	0.62	0.49	0.81	0.44	0.43	0.50
TiO2	0.18	0.26	0.25	0.16	0.32	0.15	0.30	0.80	0.00	3.50
TOTAL	98.61	99.79	99.22	98.70	98.96	98.45	100.42	99.53	98.75	101.31

	C3123	C3123	C3123	C3123	C3123	C3123	C3123	CC3123	C3123	C3123
SiO2	53.44	51.51	52.87	52.21	51.06	52.58	51.72	53.46	51.43	51.43
Al2O3	0.00	1.79	0.00	0.00	1.79	0.00	1.64	0.00	1.47	1.28
CaO	20.50	20.08	20.79	21.34	20.79	21.27	20.53	21.75	20.89	21.00
MgO	12.10	11.56	13.15	12.51	11.94	11.23	11.59	12.36	11.66	12.18
Na2O	0.00	0.00	0.00	0.00	0.00	0.00	0.00	0.00	0.00	0.00
K2O	0.00	0.00	0.00	0.00	0.00	0.00	0.00	0.00	0.00	0.00
FeO	12.58	13.49	12.08	12.64	12.30	12.36	11.96	11.25	12.68	13.49
MnO	0.47	0.64	0.35	0.46	0.49	0.47	0.41	0.49	0.40	0.51
TiO2	0.00	1.36	0.29	0.18	0.79	0.64	0.80	0.00	1.17	1.08
TOTAL	99.10	100.44	99.53	99.34	99.16	99.15	98.65	99.30	99..69	100.97

APPENDIX 6 CONTINUED...

	C3123	C3123	C3123	C3123	C3123
SiO2	53.81	52.94	53.71	53.51	53.40
Al2O3	0.00	0.00	0.00	0.00	0.00
CaO	21.25	21.42	22.67	22.81	21.71
MgO	12.07	10.73	12.13	11.19	11.48
Na2O	0.00	0.00	0.00	0.00	0.00
K2O	0.00	0.00	0.00	0.00	0.00
FeO	12.23	15.39	12.58	12.61	13.50
MnO	0.45	0.58	0.29	0.68	0.70
TiO2	0.17	0.00	0.00	0.00	0.45
TOTAL	99.99	101.06	101.38	100.80	101.24

APPENDIX 7 PYROXENE COMPOSITIONS FOR WOLF CAMP LAKE HOST SYENITES

	C2515	C2515	C2515	C2515	C2515	C2515	C2515	C2515	C2515	C2515
SiO2	49.06	48.90	48.57	48.21	48.65	48.49	47.84	47.93	50.76	47.66
Al2O3	0.76	0.59	0.76	0.43	0.60	0.57	0.62	0.00	0.00	0.46
TiO2	0.37	0.00	0.00	0.33	0.44	0.25	0.39	0.34	0.00	0.19
MnO	0.89	0.53	0.78	0.80	0.85	0.50	0.80	0.88	0.76	0.75
FeO	28.94	28.21	29.17	28.26	28.65	29.45	28.60	28.23	28.91	25.79
MgO	1.22	0.85	1.43	0.73	0.71	0.79	0.61	8.00	0.89	1.98
CaO	18.55	18.68	18.93	18.20	18.44	17.53	17.62	18.49	15.78	19.28
Na2O	0.98	1.61	0.95	1.53	1.08	1.75	2.02	1.50	3.97	2.01
K2O	0.00	0.00	0.00	0.00	0.09	0.00	0.00	0.00	0.00	0.00
TOTAL	100.77	99.38	101.57	98.48	99.52	99.32	99.71	99.04	101.07	99.19

	C2516	C2516	C2516	C2516	C2516	C2516	C2516	C2516	C2531A	C2531A
SiO2	48.10	48.38	48.93	48.95	48.52	47.47	47.58	47.75	49.22	50.20
Al2O3	0.41	0.87	0.64	0.00	0.82	0.36	0.00	0.00	0.55	0.42
TiO2	0.36	0.24	0.18	0.36	0.00	0.40	0.59	0.29	0.23	0.00
MnO	0.76	0.83	0.56	0.81	0.84	0.59	0.85	0.72	1.05	0.91
FeO	29.15	28.24	29.12	28.23	28.46	28.70	28.96	29.10	25.38	25.71
MgO	0.38	0.33	0.73	1.26	0.78	0.48	0.48	0.53	2.30	1.13
CaO	18.13	17.89	17.96	18.07	18.13	17.77	17.51	17.75	18.06	17.23
Na2O	1.61	1.82	1.55	1.58	2.46	1.68	3.25	1.81	2.28	2.58
K2O	0.00	0.00	0.09	0.00	0.00	0.00	0.09	0.00	0.00	0.00
TOTAL	99.54	99.90	100.73	100.36	100.94	98.42	100.19	99.07	100.69	99.31

	C2531A	C2531A	C2531A	C2531A	C2531A	C2531A	C2531A	C2531A	C2531A	C2531A
SiO2	49.78	48.78	49.56	50.30	49.77	49.30	50.15	50.16	50.53	50.89
Al2O3	0.00	0.00	0.00	0.00	0.00	0.82	0.00	0.76	0.45	0.54
TiO2	0.00	0.26	0.00	0.00	0.00	0.27	0.00	0.00	0.00	0.00
MnO	0.88	0.78	0.89	0.89	0.75	0.87	1.09	1.25	0.87	1.03
FeO	25.40	25.49	25.59	25.78	25.09	25.29	25.32	25.78	25.39	25.84
MgO	1.66	2.25	2.31	2.20	1.96	1.69	2.26	1.53	1.71	2.31
CaO	17.17	19.03	18.46	18.09	18.26	17.79	18.28	20.42	18.28	18.56
Na2O	3.94	2.34	2.98	2.61	2.99	1.71	3.91	0.00	2.97	1.97
K2O	0.00	0.00	0.00	0.00	0.00	0.00	0.00	0.00	0.00	0.00
TOTAL	100.65	99.87	99.79	100.90	98.82	98.48	101.02	99.90	100.20	101.14

APPENDIX 7 CONTINUED...

	C2531A	C2531A	C2531A	C2531A	C2531A	C2531A	C2531A	C2531A
SiO2	49.04	49.99	50.23	49.35	48.62	51.03	49.29	49.63
Al2O3	0.44	0.28	0.35	0.00	0.60	0.63	0.64	0.43
TiO2	0.00	0.00	0.00	0.22	0.23	0.00	0.18	0.00
MnO	0.96	0.95	0.80	0.90	1.03	0.91	1.15	0.77
FeO	25.01	25.26	24.94	24.72	25.24	25.47	24.73	25.50
MgO	2.13	2.05	2.63	1.82	1.69	1.60	1.72	2.05
CaO	18.39	17.42	18.16	18.18	18.39	18.14	18.16	17.65
Na2O	3.79	3.44	3.79	4.84	1.77	3.23	1.85	4.16
K2O	0.00	0.00	0.00	0.00	0.00	0.00	0.00	0.00
TOTAL	101.38	99.39	101.16	101.00	98.67	101.03	98.76	101.09

APPENDIX 8 FELDSPAR COMPOSITIONS FOR NEYS/ASHBURTON XENOLITHS

	C2305	C2305	C2305	C2305	C2305	C2305	C2305	C2312	C2312	C2312
SiO2	65.35	65.42	61.96	63.16	64.51	62.95	63.40	63.31	63.55	66.09
Al2O3	23.54	23.71	25.52	19.96	23.05	23.99	24.64	18.88	18.75	21.30
FeO	0.26	0.22	0.25	0.00	0.24	0.24	0.00	0.57	0.43	0.13
CaO	3.49	3.74	6.49	0.96	3.72	4.29	3.89	0.69	0.19	1.86
Na2O	8.98	8.20	7.37	1.35	9.08	8.85	9.25	0.68	0.00	11.53
K2O	0.08	0.21	0.10	12.36	0.24	0.13	0.24	15.77	15.53	0.28
BaO	0.17	0.00	0.00	0.60	0.23	0.00	0.00	0.00	0.00	0.00
TOTAL	101.87	101.50	101.69	98.40	101.07	100.45	101.42	99.92	98.46	101.20

	C2312	C2312	C2312	C2312	C2319A	C2319A	C2319A	C2319A	C2319A	C2319A
SiO2	65.88	62.87	63.07	62.84	63.75	63.36	66.65	63.28	62.93	64.66
Al2O3	20.63	22.76	22.92	22.97	18.12	18.10	20.40	22.40	21.34	21.97
FeO	0.09	0.35	0.36	0.20	0.00	0.23	0.21	0.26	0.23	0.33
CaO	0.87	3.22	3.60	3.59	0.31	0.22	0.70	2.47	2.38	2.30
Na2O	12.42	10.89	9.94	10.27	1.32	3.11	11.93	11.84	12.43	11.60
K2O	0.24	0.21	0.19	0.17	15.55	14.30	0.28	0.40	0.16	0.29
BaO	0.00	0.00	0.00	0.00	0.00	0.00	0.00	0.00	0.00	0.00
TOTAL	100.14	100.29	100.08	100.03	99.04	99.32	100.16	100.65	99.46	101.15

	C2319A	C2319A	C2328A	C2328A	C2328A	C2328A	C2328A	C2328A	C2328A	C2328A
SiO2	65.79	62.94	63.19	65.27	63.77	67.03	67.40	66.32	61.48	61.70
Al2O3	22.06	23.57	19.54	19.00	18.33	21.02	19.49	19.99	21.87	23.80
FeO	0.22	0.25	0.80	0.00	0.16	0.11	0.19	0.30	0.29	0.18
CaO	1.22	4.26	0.83	0.00	0.00	1.02	0.31	1.06	3.34	4.73
Na2O	11.47	10.06	0.83	0.93	1.66	11.70	12.19	12.59	10.89	10.14
K2O	0.18	0.21	15.18	15.75	15.72	0.20	0.14	0.22	0.31	0.17
BaO	0.00	0.00	0.00	0.00	0.00	0.00	0.00	0.00	0.00	0.00
TOTAL	100.95	101.29	100.37	100.95	99.65	101.09	99.73	100.48	98.17	100.74

	C2328A	C2331	C2331	C2331	C2331	C2331	C2331	C2331	C2331	C2331
SiO2	61.42	64.50	64.09	63.50	61.95	62.21	58.86	61.91	60.72	60.43
Al2O3	23.59	24.30	25.03	24.61	25.32	25.77	26.76	25.14	25.25	26.58
FeO	0.33	0.00	0.22	0.27	0.00	0.28	0.37	0.14	0.15	0.35
CaO	4.08	4.89	4.76	5.58	6.19	4.64	7.76	5.37	6.07	7.04
Na2O	9.61	7.89	7.00	7.67	6.49	6.27	6.34	8.08	6.88	7.02
K2O	0.11	0.15	0.00	0.09	0.26	1.35	0.18	0.16	0.13	0.11
BaO	0.00	0.00	0.00	0.00	0.00	0.31	0.18	0.34	0.00	0.15
TOTAL	99.13	101.72	101.11	101.70	100.22	100.82	100.44	101.13	99.20	101.69

	C2331	C2331	C2331	C2331	C2331	C2331	C2331	C2331	C2331	C2331
SiO2	56.32	61.05	65.64	58.58	63.37	58.47	61.84	67.64	66.62	66.53
Al2O3	28.89	25.23	22.74	27.60	24.10	27.28	24.83	21.97	20.89	21.85
FeO	0.27	0.26	0.29	0.25	0.00	0.18	0.00	0.13	0.16	0.00
CaO	10.13	5.82	2.88	7.80	4.50	8.19	5.36	1.10	0.65	1.75
Na2O	5.38	8.19	9.78	6.72	8.71	6.75	7.26	9.37	9.54	9.29
K2O	0.12	0.17	0.12	0.25	0.00	0.16	0.24	0.13	0.39	0.16
BaO	0.28	0.00	0.00	0.29	0.00	0.32	0.00	0.00	0.00	0.00
TOTAL	101.40	100.72	101.46	101.47	100.68	101.36	99.53	100.34	98.26	99.58

	C2331	C2331	C2331	C2331	C2331	C2331	C2331	C2331	C2331	C2331
SiO2	64.92	66.13	63.58	62.69	63.42	63.34	63.53	63.46	60.91	61.77
Al2O3	22.79	21.90	20.05	20.08	20.17	20.26	19.91	20.32	19.45	19.45
FeO	0.23	0.24	0.27	0.00	0.25	0.00	0.40	0.22	0.15	0.00
CaO	3.01	1.49	0.00	0.24	0.10	0.14	0.30	0.11	0.00	0.11
Na2O	9.06	8.60	1.32	1.39	0.83	1.98	1.84	1.21	1.84	0.80
K2O	0.30	0.50	14.28	13.28	14.17	13.34	13.11	13.43	13.23	13.48
BaO	0.00	0.00	1.65	2.75	2.60	1.64	2.72	1.96	2.49	2.83
TOTAL	100.33	98.86	101.15	100.43	101.53	100.70	101.79	100.71	98.07	98.43

	C2331	C2331	C2331	C2331	C2331	C2331	C2331	C2331	C2331	C2331
SiO2	61.99	62.50	60.76	60.04	62.58	60.85	58.47	60.63	61.52	60.99
Al2O3	20.04	19.53	18.90	20.31	19.47	19.91	20.52	19.70	19.69	19.67
FeO	0.48	0.13	0.00	0.43	0.12	0.00	0.00	0.22	0.11	0.19
CaO	0.00	0.14	0.00	1.61	0.23	0.00	0.12	0.28	0.13	0.14
Na2O	1.04	1.39	0.58	1.51	1.12	0.00	0.73	1.23	1.25	1.58
K2O	13.09	13.11	15.04	11.94	12.97	13.91	12.58	13.33	13.19	12.80
BaO	2.67	2.44	2.42	4.01	2.57	4.93	6.45	2.96	3.21	2.75
TOTAL	99.31	99.24	97.70	99.85	99.06	99.60	98.87	98.36	99.10	98.12

	C2331	C2340	C2340	C2340	C2340	C2340	C2340	C2340	C2340	C2340
SiO2	62.69	64.70	67.26	66.11	66.58	67.79	64.54	66.84	65.17	67.14
Al2O3	19.66	19.30	22.26	22.88	22.45	21.24	20.65	22.02	22.23	22.57
FeO	0.38	0.00	0.00	0.00	0.17	0.22	0.14	0.00	0.31	0.10
CaO	0.14	0.28	2.36	2.60	2.75	1.43	1.13	2.12	1.51	2.62
Na2O	1.88	0.83	8.70	8.69	9.84	9.64	4.19	9.54	9.45	8.45
K2O	12.40	12.59	0.18	0.33	0.13	0.41	7.25	0.14	0.57	0.21
BaO	2.30	0.43	0.00	0.00	0.00	0.00	0.50	0.20	0.00	0.00
TOTAL	99.45	98.12	100.76	100.61	101.91	100.73	98.40	100.87	99.24	101.09

	C2340	C2340	C2340	C2340	C2340	C2340	C2340	C2340	C2340	C2340
Si02	65.85	66.37	67.16	67.02	66.30	66.88	65.61	64.59	66.25	65.78
Al203	22.30	22.44	22.41	22.63	21.67	22.97	22.53	22.18	22.39	22.70
Fe0	0.24	0.00	0.23	0.27	0.00	0.27	0.00	0.23	0.20	0.00
Ca0	2.24	2.66	2.33	2.54	2.53	2.34	2.43	2.82	2.77	2.90
Na20	8.77	9.17	9.45	9.33	9.03	9.04	9.22	8.17	9.09	9.06
K20	0.29	0.37	0.17	0.18	0.12	0.16	0.24	0.32	0.09	0.21
Ba0	0.00	0.00	0.00	0.00	0.00	0.00	0.15	0.18	0.00	0.00
TOTAL	99.69	100.99	101.74	101.97	99.65	101.66	100.18	98.49	100.79	100.66

	C2340	C2340	C2340	C2340	C2340	C2340	C2340	C2340	C2340	C2358
Si02	64.62	64.71	65.37	64.34	69.10	65.16	66.34	65.96	65.16	63.48
Al203	21.69	22.42	22.18	22.32	20.00	22.11	22.03	21.68	22.14	23.66
Fe0	0.00	0.25	0.13	0.27	0.34	0.10	0.26	0.16	0.21	0.00
Ca0	2.87	2.52	2.63	2.68	0.24	2.44	2.18	1.92	2.32	3.88
Na20	9.06	8.68	8.98	8.64	9.44	9.31	8.59	9.53	9.78	9.11
K20	0.26	0.26	0.22	0.18	1.45	0.20	0.07	0.10	0.21	0.14
Ba0	0.00	0.00	0.00	0.00	0.33	0.00	0.24	0.19	0.00	0.00
TOTAL	98.50	98.84	99.52	98.41	100.90	99.33	99.71	99.55	99.82	100.27

	C2358	C2358	C2358	C2358	C2358	C2358	C2358	C2358	C2358	C2358
Si02	64.08	63.94	63.40	64.92	62.00	64.81	61.48	64.50	62.01	64.30
Al203	23.46	24.30	24.07	23.38	24.55	22.80	23.60	23.08	25.01	24.09
Fe0	0.00	0.00	0.00	0.12	0.00	0.00	0.15	0.23	0.00	0.10
Ca0	3.62	4.58	4.27	3.43	5.66	3.76	4.72	3.48	5.95	3.83
Na20	7.93	7.82	8.73	8.56	7.67	8.45	8.14	8.40	7.42	8.51
K20	0.23	0.13	0.21	0.28	0.18	0.26	0.21	0.09	0.27	0.00
Ba0	0.00	0.00	0.00	0.00	0.23	0.00	0.23	0.00	0.00	0.00
TOTAL	99.33	100.76	100.67	100.68	100.28	100.08	98.54	99.78	100.66	100.84

	C2358	C2358	C2358	C2358	C2358	C2358	C2358	C2358	C2358	C2358
Si02	64.22	64.43	64.34	63.52	63.14	64.00	63.02	63.44	65.00	64.92
Al203	23.30	19.14	23.88	19.40	19.25	19.79	18.55	18.86	18.84	19.05
Fe0	0.00	0.22	0.23	0.11	0.25	0.29	0.00	0.22	0.17	0.00
Ca0	3.32	0.00	3.81	0.11	0.28	0.15	0.39	0.00	0.00	0.11
Na20	7.70	0.99	8.98	1.35	1.45	1.72	1.13	1.09	1.33	1.94
K20	0.36	14.74	0.28	14.63	15.09	14.31	15.39	14.16	14.21	14.51
Ba0	0.24	0.91	0.30	0.64	0.56	0.71	0.63	0.76	0.89	0.71
TOTAL	99.15	100.43	101.83	99.76	100.01	100.96	99.11	98.54	100.44	101.23

APPENDIX 8 CONTINUED

	C2358	C2358	C2358	C2358	C2358	C2490	C2490	C2490	C2490	C2490
SiO2	64.40	64.85	64.99	64.13	63.81	57.11	56.92	64.57	62.51	57.53
Al2O3	19.99	19.69	19.46	19.22	23.29	26.27	27.75	18.70	22.49	27.02
FeO	0.00	0.00	0.18	0.00	0.00	0.00	0.29	0.14	0.12	0.12
CaO	0.10	0.00	0.00	0.20	3.32	0.47	8.98	0.19	4.26	8.81
Na2O	1.22	1.20	1.32	0.34	8.62	15.33	7.33	1.48	10.58	6.80
K2O	14.29	14.21	13.57	15.43	0.19	0.20	0.00	14.85	19.00	0.58
BaO	0.73	0.76	0.65	0.56	0.00	0.00	0.00	0.64	0.00	0.00
TOTAL	100.73	100.72	100.17	99.88	99.23	99.39	101.26	100.58	100.14	100.87

	C2490	C2490	C2490	C2490	C2490	C2490	C2490	C2490	C2490	C2490
SiO2	55.60	64.44	64.21	65.00	63.17	63.91	62.26	55.39	55.95	60.95
Al2O3	27.36	23.56	22.56	23.08	24.67	24.00	25.75	30.26	29.51	29.15
FeO	0.13	0.31	0.11	0.12	0.30	0.34	0.24	0.34	0.19	0.16
CaO	9.89	4.36	2.93	3.19	5.14	4.57	6.13	10.84	9.78	1.64
Na2O	8.39	8.14	8.07	9.04	8.10	7.64	6.99	4.10	4.98	9.24
K2O	0.10	0.08	0.22	0.00	0.21	0.23	0.07	0.09	0.16	0.18
BaO	0.00	0.00	0.00	0.00	0.00	0.00	0.00	0.29	0.00	0.00
TOTAL	101.48	100.90	98.10	100.42	101.59	100.69	101.44	101.30	100.57	101.32

	C2490	C2490	C2490	C2490	C2490	C2490	C2490	C2490	C2490	C2490
SiO2	59.01	60.93	58.76	60.48	59.81	61.11	60.93	59.96	62.34	60.48
Al2O3	28.45	29.01	28.60	28.29	28.28	28.44	28.18	28.29	28.24	28.82
FeO	0.22	0.25	0.12	0.17	0.22	0.00	0.28	0.25	0.14	0.24
CaO	1.73	1.59	1.42	1.55	1.33	1.55	1.24	1.34	1.38	1.30
Na2O	9.85	8.87	10.12	10.30	9.81	10.66	11.20	11.61	9.75	10.67
K2O	0.15	0.13	0.07	0.00	0.07	0.08	0.00	0.10	0.06	0.00
BaO	0.00	0.00	0.00	0.00	0.00	0.00	0.00	0.00	0.00	0.00
TOTAL	99.40	100.77	99.09	100.80	99.52	101.84	101.82	101.55	101.91	101.50

	C2490	C2490	C2490	C2490	C2490	C2490	C2490	C2490	C2490	C2490
SiO2	60.86	61.34	60.81	56.06	56.11	56.75	56.40	49.17	53.69	55.92
Al2O3	28.20	28.95	27.98	27.46	28.17	28.17	28.21	32.53	30.67	29.05
FeO	0.37	0.00	0.14	0.12	0.32	0.32	0.21	0.51	0.20	0.20
CaO	1.38	1.38	1.25	9.46	9.21	9.66	9.60	13.87	12.48	10.02
Na2O	9.77	9.97	9.49	5.33	4.46	5.86	5.50	2.77	3.94	5.39
K2O	0.21	0.00	0.23	0.17	0.13	0.16	0.08	0.10	0.08	0.00
BaO	0.00	0.00	0.00	0.00	0.00	0.00	0.00	0.00	0.00	0.00
TOTAL	100.79	101.64	99.90	98.59	98.40	100.92	100.00	98.95	101.06	100.58

	C2490	C2490	C2490	C2490	C2490	C2490	C2490	C2490	C2490	C2490
SiO2	55.69	56.75	49.84	50.84	51.23	49.90	55.41	52.66	56.53	56.65
Al2O3	28.22	29.06	32.78	32.54	32.33	32.85	29.47	30.19	27.26	28.13
FeO	0.15	0.31	0.23	0.00	0.27	0.00	0.11	0.39	0.26	0.34
CaO	9.80	9.76	14.96	14.12	13.08	15.06	10.72	10.71	8.70	8.93
Na2O	5.73	5.50	2.97	3.40	2.92	3.31	5.53	4.52	5.69	5.76
K2O	0.06	0.17	0.06	0.00	0.07	0.00	0.11	0.40	0.17	0.28
BaO	0.00	0.19	0.00	0.00	0.00	0.00	0.00	0.00	0.00	0.00
TOTAL	99.66	101.74	100.85	100.90	99.91	101.13	101.34	98.87	99.18	100.10

	C2490	C2490	C2490	C2498	C2498	C2498	C2498	C2498	C2498	C2498
SiO2	50.86	51.04	50.66	61.67	61.43	63.36	62.27	61.67	62.28	63.16
Al2O3	32.97	32.29	32.44	19.73	24.68	23.50	25.16	24.30	23.98	22.26
FeO	0.00	0.28	0.16	0.18	0.15	0.00	0.13	0.00	0.14	0.75
CaO	14.31	14.48	14.13	0.12	5.30	3.62	5.51	5.31	4.43	4.61
Na2O	3.37	3.13	3.27	0.00	7.26	8.59	7.30	7.87	8.65	7.99
K2O	0.00	0.00	0.00	14.61	0.22	0.13	0.22	0.00	0.13	0.35
BaO	0.00	0.00	0.00	1.94	0.00	0.00	0.00	0.00	0.26	0.00
TOTAL	101.51	101.23	100.67	98.25	99.04	99.20	100.59	99.15	99.88	99.11

	C2498	C2498	C2498	C2498	C2498	C2498	C2498	C2498	C2498	C2498
SiO2	58.91	62.01	61.10	61.02	61.25	60.74	60.22	61.49	61.62	62.42
Al2O3	26.69	20.84	20.84	24.64	24.48	25.63	25.49	25.65	24.66	24.22
FeO	0.16	0.11	0.00	0.35	0.24	0.27	0.18	0.27	0.00	0.33
CaO	6.35	0.22	0.23	5.19	5.41	5.11	6.16	5.70	4.98	5.05
Na2O	6.50	0.00	0.58	8.18	7.97	7.21	8.69	7.74	7.89	7.09
K2O	0.74	14.13	14.34	0.33	0.24	0.75	0.00	0.10	0.10	0.21
BaO	0.00	2.84	3.25	0.00	0.00	0.00	0.23	0.00	0.00	0.00
TOTAL	99.34	100.15	99.98	99.71	99.59	99.72	100.98	100.95	99.24	99.31

	C2498	C2510	C2510	C2510	C2510	C2510	C2510	C2510	C2510	C2510
SiO2	63.44	59.85	59.23	59.18	59.90	62.19	59.95	61.92	62.30	59.35
Al2O3	23.12	24.95	26.13	25.55	25.58	22.88	24.83	22.99	22.58	25.66
FeO	0.24	0.16	0.24	0.00	0.26	0.27	0.00	0.14	0.22	0.26
CaO	4.36	7.20	7.33	7.66	7.14	4.54	7.20	4.89	4.49	7.90
Na2O	7.80	8.01	6.99	7.63	7.56	9.20	8.21	9.38	10.24	7.04
K2O	0.16	0.24	0.33	0.10	0.00	0.12	0.10	0.20	0.15	0.11
BaO	0.00	0.00	0.00	0.00	0.00	0.00	0.00	0.00	0.00	0.25
TOTAL	99.12	100.41	100.24	100.28	100.44	99.21	100.27	99.51	99.98	100.56

APPENDIX 8 CONTINUED...

	C2510	C2510	C2510	C2510	C2510	C2510	C2510	C2510	C2510	C2510
SiO2	61.85	60.96	62.65	62.62	63.94	62.84	62.33	63.43	58.46	62.04
Al2O3	24.03	23.52	24.05	23.16	22.17	23.62	22.49	23.04	24.99	22.58
FeO	0.21	0.15	0.11	0.16	0.21	0.37	0.25	0.33	0.29	0.37
CaO	5.57	5.30	5.63	4.45	3.96	4.66	4.49	4.72	7.22	4.36
Na2O	9.02	8.55	8.51	8.75	9.64	8.81	9.52	8.57	7.43	8.97
K2O	0.17	0.14	0.18	0.12	0.16	0.19	0.28	0.25	0.17	0.10
BaO	0.00	0.00	0.00	0.00	0.00	0.00	0.00	0.00	0.00	0.00
TOTAL	100.86	98.35	101.13	99.26	100.07	100.50	99.35	100.35	98.56	98.43

	C2510	C2510	C2510	C2510
SiO2	60.23	59.41	62.01	58.00
Al2O3	24.34	25.16	22.87	25.78
FeO	0.00	0.00	0.32	0.26
CaO	5.94	7.70	4.40	8.14
Na2O	8.23	7.81	9.20	7.25
K2O	0.15	0.10	0.00	0.00
BaO	0.00	0.00	0.13	0.00
TOTAL	98.89	100.34	98.94	99.43

APPENDIX 9 FELDSPAR COMPOSITIONS FOR WOLF CAMP LAKE

	C2531A	C2531A	C2531A	C2531A	C2531A	C2531A	C2531A	C2531A	C2531A	C2531A
SiO2	64.52	63.72	63.88	63.61	63.43	63.77	65.21	62.97	64.30	65.78
Al2O3	23.19	20.34	20.95	20.74	20.43	20.48	23.03	20.04	21.93	21.45
FeO	0.00	0.12	0.26	0.39	0.00	0.00	0.00	0.28	0.20	0.00
CaO	1.54	0.46	0.49	0.00	0.00	0.58	1.90	0.19	1.74	1.21
Na2O	10.35	1.85	1.81	1.65	1.25	2.17	10.85	1.16	9.99	10.96
K2O	0.51	12.23	14.02	13.78	14.82	13.17	0.20	15.26	0.23	0.37
BaO	0.00	0.00	0.00	0.00	0.00	0.00	0.00	0.00	0.00	0.00
TOTAL	100.12	98.57	101.42	100.18	99.94	100.12	101.18	100.48	98.59	99.78

	C2531A	C2531A	C2531A	C2531A	C2531A	C2531A	C2531A	C2531A	C2531A	C2531A
SiO2	63.60	65.61	63.83	64.12	65.24	64.74	66.32	66.34	64.65	63.63
Al2O3	20.69	22.74	20.16	22.76	21.74	21.76	21.37	22.58	21.84	21.27
FeO	0.00	0.00	0.14	0.00	0.00	0.17	0.29	0.00	0.17	0.49
CaO	0.15	1.84	0.30	1.86	1.47	1.51	1.16	1.20	1.70	0.67
Na2O	1.03	10.00	2.38	9.94	10.95	10.75	11.31	11.20	9.96	3.47
K2O	14.95	0.00	12.24	0.15	0.17	0.18	0.29	0.00	0.08	10.19
BaO	0.00	0.00	0.00	0.00	0.00	0.00	0.00	0.00	0.00	0.00
TOTAL	100.44	100.40	99.49	99.07	99.55	99.11	100.75	101.31	98.55	99.95

	C2531A	C2531A	C2531A	C2531A	C2531A	C2531A	C2531A	C3120	C3120	C3120
SiO2	65.00	66.58	64.02	65.39	64.79	66.01	65.10	64.15	57.19	58.48
Al2O3	22.17	22.40	21.71	21.83	22.43	21.95	22.39	24.33	27.48	26.15
FeO	0.00	0.00	0.26	0.30	0.44	0.20	0.22	0.24	0.50	0.46
CaO	1.47	1.44	1.86	1.12	1.75	1.40	1.21	3.38	7.00	5.87
Na2O	10.40	10.84	10.84	10.93	11.07	10.99	10.92	8.82	6.26	7.24
K2O	0.00	0.29	0.09	0.50	0.17	0.22	0.55	0.14	0.44	0.18
BaO	0.00	0.00	0.00	0.00	0.00	0.00	0.00	0.00	0.00	0.00
TOTAL	99.04	101.56	98.92	100.26	100.64	101.12	100.52	100.46	99.33	99.22

	C3120	C3120	C3120	C3120	C3120	C3120	C3120	C3120	C3120	C3120
SiO2	56.65	65.32	65.20	65.81	64.92	65.45	62.78	63.55	64.52	65.66
Al2O3	27.16	22.16	21.68	21.26	22.16	22.40	24.05	23.41	22.22	23.21
FeO	0.48	0.24	0.47	1.10	1.28	1.60	0.36	0.57	0.18	0.56
CaO	7.49	1.96	1.40	1.36	1.44	1.20	3.00	1.76	1.58	2.22
Na2O	6.16	10.03	9.34	9.24	9.47	9.53	8.84	9.49	9.69	9.06
K2O	0.00	0.52	0.49	0.00	0.30	0.26	0.16	0.66	0.06	0.35
BaO	0.00	0.00	0.00	0.00	0.00	0.00	1.28	0.00	0.00	0.00
TOTAL	98.45	100.24	98.58	98.77	99.84	100.44	100.47	99.44	99.08	101.06

APPENDIX 9 CONTINUED...

	C3120	C3120	C3120	C3120	C3120	C3120	C3120	C3120	C3120	C3120
SiO2	63.80	62.59	61.70	65.38	61.57	59.90	57.51	61.10	61.51	64.17
Al2O3	23.95	24.11	24.09	22.33	24.74	26.52	26.57	26.24	24.73	24.56
FeO	0.13	0.29	0.65	0.21	0.29	0.69	1.15	0.53	0.43	0.35
CaO	2.82	3.96	4.31	1.65	4.43	3.46	9.32	5.36	4.48	3.55
Na2O	8.37	9.15	8.34	9.45	7.36	5.11	6.32	6.89	7.52	8.61
K2O	0.00	0.35	0.45	0.00	0.11	3.69	0.36	0.15	0.20	0.07
BaO	0.00	0.00	0.00	0.00	0.00	0.00	0.00	1.20	0.00	0.00
TOTAL	99.07	100.46	99.54	99.03	98.50	99.37	101.23	101.46	98.86	101.32

	C3123	C3123	C3123	C3123	C3123	C3123	C3123	C3123	C3123	C3123
SiO2	58.76	59.62	58.32	58.79	56.73	58.08	59.86	57.89	56.74	56.96
Al2O3	26.34	24.82	26.41	24.26	27.13	27.62	26.42	26.98	27.42	28.61
FeO	1.04	0.62	0.71	0.34	0.50	0.55	0.48	0.50	0.62	0.56
CaO	5.79	5.60	6.35	7.43	7.24	6.54	5.80	6.93	7.50	8.04
Na2O	7.45	8.31	7.90	7.15	6.80	6.55	6.90	6.94	6.18	5.68
K2O	0.14	0.10	0.08	0.16	0.12	0.11	0.33	0.00	0.08	0.00
BaO	0.00	0.00	0.00	0.95	0.00	1.18	0.78	0.00	0.00	0.00
TOTAL	99.51	99.07	99.78	99.08	98.53	100.62	100.56	99.24	98.54	99.84

	C3123	C3123	C3123	C3123	C3123	C3123	C3123	C3123	C3123	C3123
SiO2	63.85	58.89	59.21	59.98	62.33	60.09	61.24	62.32	57.81	57.77
Al2O3	20.52	27.85	26.11	26.26	25.17	25.95	24.68	24.69	26.73	26.29
FeO	0.30	0.20	0.40	0.39	0.34	0.45	1.00	0.36	0.45	1.26
CaO	0.90	6.72	5.85	6.05	4.29	5.89	4.72	4.30	6.40	6.61
Na2O	3.11	6.42	7.58	7.23	7.62	7.31	8.43	8.81	7.31	6.69
K2O	10.78	0.00	0.07	0.10	0.00	0.14	0.39	0.08	0.07	0.16
BaO	0.00	0.00	0.00	0.00	0.00	0.00	0.00	0.00	1.13	0.00
TOTAL	99.46	100.08	99.22	100.00	99.74	99.83	100.46	100.55	99.90	98.78

	C3125	C3125	C3125	C3125	C3125	C3125	C3125	C3125	C3125	C3125
SiO2	57.76	55.44	57.74	58.43	58.59	57.25	58.91	63.31	60.75	60.06
Al2O3	27.10	27.37	26.29	25.63	25.68	26.06	26.56	24.12	24.36	25.61
FeO	0.28	0.74	0.67	0.34	0.25	0.69	0.31	0.42	0.13	0.36
CaO	7.48	5.12	6.64	6.25	6.22	5.80	6.69	3.96	5.39	4.99
Na2O	7.69	6.11	7.42	8.50	7.80	6.63	7.99	8.43	8.66	8.23
K2O	0.00	2.96	0.27	0.11	0.00	1.98	0.10	0.14	0.12	1.63
BaO	1.01	0.66	0.00	0.00	0.00	0.00	0.00	0.00	0.00	0.00
TOTAL	101.33	98.71	99.12	99.44	98.54	98.40	100.66	100.61	99.40	100..88

APPENDIX 9 CONTINUED...

	C3125	C3125	C3125	C3125	C3125	C3125	C3125	C3125	C3125	C3125
SiO2	57.86	62.33	62.59	61.33	60.72	59.25	60.54	61.17	60.95	62.26
Al2O3	21.63	24.04	21.85	24.84	24.35	24.67	25.64	24.65	24.09	24.54
FeO	0.63	0.12	0.19	0.35	0.50	0.34	0.23	0.23	0.55	0.47
CaO	9.31	4.18	1.70	5.38	4.45	4.99	5.36	4.93	4.50	4.77
Na2O	9.04	8.00	10.59	9.04	9.81	9.39	9.24	9.27	8.75	9.09
K2O	1.37	0.29	0.76	0.20	0.12	0.27	0.00	0.00	0.10	0.10
BaO	0.00	0.00	0.94	0.00	0.00	0.62	0.00	0.00	0.00	0.00
TOTAL	100.00	98.95	98.63	101.13	100.06	99.51	101.02	100.45	98.93	101.24

	C3125	C3125	C3125	C3125	C3125	C3125	C3125	C3125	C3125	C3125
SiO2	61.51	61.81	58.73	59.83	60.52	60.18	60.61	60.69	61.08	61.70
Al2O3	24.17	24.28	26.15	24.65	24.55	25.34	24.37	25.02	25.48	24.32
FeO	0.30	0.31	0.17	0.25	0.47	0.30	0.28	0.42	0.28	0.22
CaO	4.70	4.89	7.35	5.08	5.40	5.80	5.14	5.17	4.99	4.75
Na2O	9.88	8.99	7.96	8.75	8.69	7.74	9.41	8.59	9.48	9.61
K2O	0.00	0.11	0.17	0.00	0.00	0.14	0.25	0.09	0.08	0.00
BaO	0.00	0.00	0.00	0.80	0.00	0.00	0.00	0.00	0.00	0.00
TOTAL	100.55	100.39	100.53	99.36	99.62	99.71	100.05	99.98	101.50	100.71

	C3125	C3125	C3125	C3125
SiO2	60.21	60.67	62.13	62.58
Al2O3	25.13	24.85	24.85	24.88
FeO	0.31	0.36	0.51	0.31
CaO	5.36	5.06	4.64	4.55
Na2O	9.02	8.71	8.29	8.84
K2O	0.08	0.21	0.00	0.00
BaO	0.00	0.00	0.00	0.00
TOTAL	100.11	99.86	101.37	101.27